University of Alberta

Aquatic nanotoxicity testing: Insights at the biochemical, cellular, and whole animal levels

by

Kimberly Jessica Ong

A thesis submitted to the Faculty of Graduate Studies and Research
in partial fulfillment of the requirements for the degree of

Doctor of Philosophy

in

Physiology, Cell, and Developmental Biology

Biological Sciences

ABSTRACT

Aquatic organisms are susceptible to waterborne nanoparticles and there is only limited understanding of the mechanisms by which these emerging contaminants affect biological processes. The unique properties of nanomaterials necessitate evaluation of standard toxicity testing techniques to provide a solid foundation for thorough and accurate biological effects testing. I discovered that many biochemical assays used to test toxicity are affected by nanoparticles, thus hindering our ability to properly evaluate nanotoxicity. A meta-analysis showed that ca. 95% of papers from 2010 assessing nanotoxicity did not account for nanoparticle interference, with only minimal improvement in 2012. I then performed a series of biological tests with various nanomaterials. I evaluated the effects of functionalized silicon nanoparticles in cell and zebrafish exposures and determined that they are a less-toxic alternative to cadmium selenide quantum dots. Then, I tested medically relevant hydroxyapatite nanomaterials, and established that nanoparticle shape affects uptake and toxicity *in vivo* and *in vitro*. Using whole animal experiments I determined that nanoparticles could delay or prevent zebrafish hatch, likely due to the inhibition of hatching proteases. Replicating more realistic aquatic environments, I examined whether humic acid, an important component of natural waters, would alter nanoparticle toxicity. The presence of humic acid changed the physicochemical characteristic of nanoparticles, and some biological effects were abrogated, indicating that laboratory toxicity tests might not be representative of effects in the natural environment. Finally, I focused on the physiological and systemic effects of

nanoparticles. I determined that silver nanoparticles affects sodium uptake in juvenile trout, and inhibits ionoregulatory transporter activity. I propose that many of the nanoparticle effects seen in biochemical assays, cellular experiments, and whole animal exposures are often related to nanoparticle interactions with proteins, enzymes, dyes, and other biologically-relevant molecules. Importantly, I found that some biological effects could be attributed to nanoparticle-specific properties, as opposed to the bulk or dissolved components. Determining the potential toxic effects caused by nanoparticle exposure and understanding the mechanism by which nanoparticles cause effects will help properly regulate these materials and allow for their safe development and production.

PREFACE

The majority of the research in this thesis are a result of my individual efforts, however, as with all good science, mentorship and collaboration was essential to performing thorough, rigorous, and interesting experiments throughout my Ph.D. As a representation of these collaborations and contributions, "we" is used throughout this text. Some of the chapters have been published in peer-reviewed journals, and follow their respective journals' format. The appropriate citations are provided at the beginning of these chapters.

ACKNOWLEDGEMENTS

To my supervisor, Greg: I thank you. I am very grateful for all the opportunities you have provided me to grow as a researcher and am lucky to have worked on this exciting project with you as my supervisor. You have always encouraged me to pursue interesting questions and have provided unwavering support. From the moment I joined the Goss lab family I have developed as a scientist, worked with wonderful people, and have had many chances to see and do amazing things. Pillaging flagons of wine in Sweden, an almost calamitous encounter with bioluminescence in Bamfield, convincing you to eat (raw) egg breakfasts in Singapore, savoring stuffed figs in Portland, imbibing warm and flat ESBs in London, devouring lobster in Sackville, and very importantly, celebrating with scotch at the office, are only a few of the memories I will take with me. Your motto will forever be part of my life: "Work hard, play hard".

To Jon V. and the lab: I am exceptionally grateful for your patience with us biologists; my scientific endeavours would not have been possible without you and your lab's collaboration, expertise, and enthusiasm for my projects. Rhett, I'd like to specifically thank you and apologize for making you explain quantum confinement to me so many times.

To Joachim and lab: My short time in your lab was fantastic, thank you for taking the time to train me. Xinxin, thanks for helping me find cheese in Singapore.

To my committee: I am appreciative of your time and insightful comments – you have helped develop my research and I could not be more thankful.

To all the labs, profs, postdocs, students, and others who helped along the way: you were numerous, you were generous, and I am indebted. Thank you.

To all the facilities help, administrative assistance, and support staff in BioSci: you are truly top-notch and have streamlined my research and my academic life. You don't get enough of the recognition you all deserve, and I thank you from the bottom of my heart.

To all my co-authors and collaborators: I thank you for your diligence, perseverance, and enormous contributions. You have made my life easy. Tyson, I especially thank you for your generous support and time contributions.

To those who supported me early in my scientific career and fostered my love for science: Thank you. (Pat W., I'm looking your way.)

To my funding sources: thank you to the Natural Sciences and Engineering Research Council of Canada, Alberta Innovates, and the University of Alberta for supporting me, and further acknowledgements to Vive Crop Protection, BDC Canada, the National Research Council, and Environment Canada for providing materials and funds that allowed me to do my research.

To my lab: you are my colleagues, my friends, my scientific sounding boards, and you made coming to lab fun (even though I had to come in on weekends because sometimes we had too much fun). We have celebrated together, we have cried together, we have whined together. I look forward to continuing these activities in the future. Please feed the fish. I'm rather fond of them.

To all past, present, and future lab managers: Thank you thank you thank you thank you thank you thank you thank you.

To my parents: you have always supported me and encouraged me to take my own path. Thank you for that. Also, thank you for putting so much effort into learning the word "nanoparticle".

To all those who provided moral support, (you know who you are): you are the ones with whom I ate many undercooked venison backstraps, know the feeling of a wolf trap, acquiesce to regular snack room visits, have discovered the most beautiful spots of Alberta with me, share my fascination with the triplets and combat juice, have ordered innumerable 'number 33 with pho noodles', and know why I bring chicken broth with me wherever I go. Thanks to my friends abroad, your support was felt and your open invitations were used (as well as your design skills, thank you Laura). James, I have to especially thank you for always being so game for our adventures – both in science and life. It is rare to have found such a wonderful group of people and I feel incredibly lucky to have met you all.

Finally, for Aaron: You are my inspiration, my rock, and my partner in crime. Nothing fits better than the words of T. Speedman, "You m-m-m-mmm-m-m-make me happy". Thank you.

TABLE OF CONTENTS

CHAPTER 3

EVALUATION OF SILICON AND CADMIUM SELENIDE QUANTUM DOTS:

CHAPTER 4

COMPARISON OF THE TOXICITY OF DIFFERENT-SHAPED HYDROXYAPATITE

CHAPTER 5

MECHANISTIC INSIGHTS INTO THE EFFECT OF NANOPARTICLES ON

CHAPTER 8

LIST OF TABLES

LIST OF FIGURES

LIST OF ABBREVIATIONS

28s.3	catfish T-cell like cell line
3B11	catfish clonal B-cells
Ab	absorbance
Ag	silver
Au	gold
BCA	Bicinchonininc assay
Beas2B	human bronchial epithelial line
BET	Brunauer-Emmett-Teller
BSA	bovine serum albumin
C_{60}	Buckminsterfullerene
CA	carbonic anhydrase
Cd	cadmium
$CdCl_2$	cadmium chloride
CdSe	cadmium selenide
CdSe-11	cadmium selenide nanoparticle functionalized with undecanoic acid
CdSe-3	cadmium selenide nanoparticle functionalized with propionic acid
CdSe-6	cadmium selenide nanoparticle functionalized with hexanoic acid
CdSe/ZnS	zinc sulfide coated cadmium selenide
CEPA	Canadian Environmental Protection Act
Cl^-	chloride
CNT	carbon nanotube
Cu	copper
ddH_20	double distilled water
DFDA	dihydrofluorescein diacetate assay
DLS	dynamic light scattering
DMEM	Dulbecco's modified eagle medium
dTW	dechlorinated tap water
EBSS	Earle's balanced salts
EDX	energy dispersive X-ray
FBS	fetal bovine serum
FITC	fluorescein isothiocyanate
FTIR	Fourier-transformed Infrared Spectroscopy
HA	humic acid
HAP	hydroxyapatite
HAP-ND	needle-shaped HAP
HAP-NDF	FITC-conjugated needle-shaped HAP
HAP-RD	rod-shaped HAP
HAP-RDF	FITC-conjugated rod-shaped HAP
HepG2	human hepatocellular carcinoma cell line
hpf	hours post fertilization

ICP-MS	inductively coupled plasma mass spectrometry
LC50	lethal concentration 50
LDH	lactate dehydrogenase
MEM	modified eagle medium
MTS	3-(4,5-dimethylthiazol-2-yl)-5-(3-carboxymethoxyphenyl)-2-(4-sulfophenyl)-2H-tetrazolium
MTT	3-(4,5-dimethylthiazol-2-yl)-2,5-diphenyltetrazolium bromide
MWCO	molecular weight cut-off
Na^+	sodium
NKA	Na^+/K^+-ATPase
NM	nanomaterial
NOM	natural organic material
NP	nanoparticle
PBS	phosphate buffered saline
PI	propidium iodide
Pt	platinum
QD	quantum dot
RAW264.7	mouse macrophage cell line
RBL 2H3	rat basophilic leukemia cell line
RNT	rosette nanotube
ROS	reactive oxygen species
rpm	rotations per minute
SA	salicic acid
SEM	standard error of the mean
Si	silicon
Si-3	silicon nanoparticle functionalized with propionic acid
Si-5	silicon nanoparticle functionalized with pentanoic acid
Si-7	silicon nanoparticle functionalized with heptanoic acid
Si-11	silicon nanoparticle functionalized with undecanoic acid
SOD	superoxide dismutase
SWCNT	single-walled carbon nanotubes
TEM	transmission electron microscopy
TiO_2	titanium dioxide
tpy	tons per year
vZnO	polymer coated zinc oxide
WST-1	2-(2-methoxy-4-nitrophenyl)-3-(4-nitrophenyl)-5-(2,4-disulfophenyl)-2H-tetrazolium, monosodium salt
XRD	X-ray diffraction
ZHE	zebrafish hatching enzyme
ZnO	zinc oxide
ZnO leaf	leaf-shaped zinc oxide nanoparticles
ZnO sph	spherical zinc oxide nanoparticles
ζ-potential	zeta-potential

Chapter 1

Introduction

1.1. INTRODUCTION

The introduction and rapid expansion of nanotechnologies into the marketplace have resulted in significant advances in medical, environmental, and industrial fields. In response to this fast progression, there has been the formation of nano-focused research groups, increased allocations of academic and research funding, establishment of degree programs based on nano-research, creation of nano-specific journals, and the founding of numerous companies focused on nanotechnologies. This recent focus on nanomaterials (NMs) has been due to the development of cost-effective and relatively straightforward methods of production in large quantities and an increased interest in the use of these materials. Their small size confers unique electronic, physical, and chemical properties as well as increased reactivity due to their higher surface area to volume ratio. This has initiated expansion and exploitation of nano-enabled products in the medical, commercial, industrial, and environmental fields.

Natural NPs exist in the environment; for example, soil, volcanic ash, and freshwater all contain nano-sized particles (Handy *et al.* 2008a; von der Kammer, *et al.* 2008). However, for the purposes of this thesis 'nanoparticle' will refer to only manufactured NPs, as the prime concern is the rapid increase in the volume of production and use of engineered NMs. The current working definition of a NP, as used by Health Canada, outlines a NM as a material that ranges between 1-100 nm in at least one dimension, and/or have an internal or surface structure in the nano-size range, and/or exhibit one or more nanoscale properties/phenomena (Health Canada 2011). There is much debate over the definition of a NP; the exact size range and physicochemical properties that define a NP have been discussed at length since the emergence of this field and still no official definition exists (Shew 2008).

Nanotechnology has a long history that has culminated in fast progression over the past two decades. NPs have been used for thousands of years; the Egyptians and the Chinese took advantage of the surface plasmon properties of gold NPs in ca. 5-4th century B.C. for production of glass and ceramic colorants

2

(Daniel & Astruc 2004). Richard Feynman brought recognition to the significant advances that could be generated by the manipulation of matter at the atomic scale in an inspiring speech, 'There's Plenty of Room at the Bottom', in 1959 (Feynman 1960). In 1974 the term "nanotechnology" was coined by Norio Taniguchi (Shew 2008), and re-introduced into the lexicon in 1986 in Eric Drexler's part sci-fi, part prophetic book: "Engines of Creation: The Coming Era of Nanotechnology". The discovery of a new form of carbon, the "buckyball" (C60) in 1985 by Richard Smalley, in conjunction with his vocal support of nanotechnology development spurred nanoresearch (O'Brien *et al.* 1985). By 2004, enough research and interest had been garnered on the topic of nanotechnology to warrant the first policy conference, entitled "Advanced Nanotechnology".

The rapid advancement of nanotechnology research has resulted in incorporation of NPs into a number of products. The exact number is unknown in Canada, as existing regulations do not require reporting of NM production unless the NPs have unique structural forms or molecular arrangements than their bulk counterparts (CEPA 2007). Voluntary inventories such as the Project on Emerging Technologies suggest that NPs are used in personal care products, clothing, cosmetics, sporting goods, and sunscreens, amongst other consumer products (Project on Emerging Nanotechnologies 2011). A lack of reliable data makes NP production estimates remarkably difficult; best estimates based on largely extrapolated data indicate production as high as 38 000 tons per year (tpy) of nano-TiO_2, 20 tpy of Ag NPs, and 1101 tpy of carbon nanotubes in the U.S. alone (Hendren *et al.* 2011).

The surge in interest in nanotechnology research and development was quickly followed by publications questioning the safety and risk of NP use (*e.g.,* Schultz 2007). Unfortunately, the field of Nanotoxicology, or the study of the biological effects of nanomaterials, has lagged behind the rapid production and development of NMs (Porter and Youtie 2009). Nanoparticle toxicity studies started to emerge in 1979; a search of "nanoparticle toxicity" in Google Scholar (www.googlescholar.com, search performed 1 Mar 2013), limited to only 1979,

yields 4 results. This number stayed below 20 until 1990, then slowly and steadily climbed to 278 in 2001. After 2004, when the number of papers reached 1020, the results very rapidly increase each year, spectacularly hitting 14 200 results for 2012 alone (Figure 1-1). Thorough and extensive research is required to ensure proper regulation and safe development of these materials so that they can continue to improve existing products and spur the creation of new advancements.

Major sites of NP contamination will likely be in aquatic systems through unintentional and intentional inputs. NM-containing products will release individual NPs through the use, disposal, and weathering of such items. Leaching of NPs from paints (Kaegi *et al.* 2008), cosmetics (Müller *et al.* 2002), and clothing (Lo *et al.* 2007) can result in direct input into water. The capacity of NPs to breakdown toxicants is resulting in large volumes of NP solutions to be injected straight into contaminated water sources (Cundy *et al.* 2008; Sanchez *et al.* 2011). Furthermore, runoff from soils, industrial discharges, and accidental spills will further increase aquatic NP burdens (Batley *et al.* 2012).

Given that NPs are expected to end up in various freshwater sources, the main focus of this thesis is on freshwater organisms and the potential for ecotoxicological effects. Some mammalian *in vitro* studies are presented here to elucidate NP effects, with the goal that this data can be related to ecotoxicological effects, and compared to current literature that mainly focuses on mammalian data. To determine what types of NP-specific regulations are necessary, some central questions must be investigated. First we must determine the best methods and approaches to determining NP toxicity. Then, we must gather data on NP-specific biological effects and determine which properties of NPs that can cause these effects. Furthermore, ascertaining the mechanisms by which NPs can cause effects will be of importance to producing NMs that minimize biological effects.

1.2. CHALLENGES AND APPROACHES

Much like the discovery and use of the giant squid axon provided a unique opportunity to study excitable membranes, and propelled the field of

electrophysiology (Keynes 2005), so too must nanotoxicologists forge their way through new territory and determine the models and protocols that best answer their questions. While using established protocols for classical toxicants such as metals, solvents, or pesticides to test for NP toxicity may seem like the best course of action, considerations on appropriate modifications will have to be made due to the unique properties of NPs.

1.2.1. Challenges in nanotoxicity testing

Initial nanotoxicity research was hindered by a myriad of issues associated with the production of new materials. Batch-to-batch inconsistency, unreliable characterization data from manufacturers (Park & Grassian 2010; Klaine *et al.* 2008), and the use of toxic solvents to disperse NPs (Zhu *et al.* 2006; Henry *et al.* 2011), resulted in a number of reports that confounded and slowed research efforts. Early published nanotoxicity results did not include extensive NP characterization data; at the time, only chemical composition, exposure concentration, and production methods were necessary, as was based on the standard for other toxicants. The realization that physicochemical characteristics such as shape, core size, surface coatings, agglomeration, *etc.* could drastically change the behavior and toxicity of NPs lead to a flood of publications emphasizing the importance of characterization (*e.g.,* Burleson *et al.* 2005; Oberdörster *et al.* 2005; Holsapple 2005). Despite these recommendations, nanotoxicologists are often constrained in access or expertise regarding the equipment needed to perform all these characterizations. Indeed, these are issues I encountered throughout my research project, and it highlighted the absolute importance of collaboration, and clear and concise communication between biologists, chemists, physicists, and engineers to fully understand NP behavior and toxicological effects.

1.2.2. Choice of testing methods and materials

There are a considerable number of knowledge gaps regarding the toxicity of NPs. Data regarding how physicochemical characteristics influence NP toxicity

are often published, but there is still a dearth of concrete conclusions (Rivera-Gil *et al.* 2012). Experiments *in vitro* currently dominate the nanotoxicology literature, but it is becoming clear that alterations of NP behavior in aquatic systems will drastically change the availability and toxicity to organisms (Handy *et al.* 2008a; von der Kammer, *et al.* 2008). To test this, more *in vivo* experiments are necessary (Fischer & Chan 2007), and addition of natural abiotic factors will be crucial to ecotoxicity testing (von der Kammer *et al.* 2012). While much research has documented lethal and sublethal endpoints, the physiological and biochemical mechanisms by which NPs can cause toxicity are largely unexplored. The field is further complicated by the inconsistent methodologies and characterization techniques (Hassellöv *et al.* 2008; Stone *et al.* 2009).

Careful choice of NMs and experimental design is crucial to collect valuable data. Due to the exceptional qualities of NPs, there is widespread production and use across a number of fields. As a consequence, considerations during both NP development and toxicity testing can greatly vary. Biomedical NPs intended for delivery or imaging may be designed so that biocompatibility and targeted intracellular localization are desired (Cormode *et al.* 2009), whereas a NP intended for incorporation into personal products may be designed for minimal cell interaction (Cross *et al.* 2007). Predictions on the fate of NPs and establishing where a particular formulation is most likely to accumulate or be deposited will direct toxicologists on the types of exposure that will likely be encountered, and will help dictate the types of tests chosen to study NP exposure.

Nanotoxicologists and regulatory agencies must determine whether conventional toxicity testing protocols and methods are appropriate for the study of NPs. For example, generation of toxicity data in the same manner as classical toxicants (*i.e.,* testing for LC50, LOEC, etc.) may not yield informative results without an understanding of how NPs cause effects. Comparison of LC50s amongst NPs of the same core do not always provide consistent values; LC50s of ZnO NPs are reported as 1.793 mg/L (Zhu *et al.* 2008) and 3.969 mg/L (Yu *et al.* 2011), but extrapolation from other reports suggest that this value reach up to 10 mg/L (Bai *et al.* 2009), and in George *et al.* (2011), mortality was still less than 50

% at 25 mg/L exposure, indicative of even LC50 higher values. Differences in physicochemical NP characteristics and abiotic factors can change these values, therefore focus may be better served on the mechanistic aspects of toxicity so that we can create and modify tests appropriately. Abiotic factors not often included in toxicity tests, such as UV radiation, will influence NP toxicity. For example, exposure to exceptionally high concentrations (>20 g/L) of TiO_2 under normal laboratory lighting did not cause toxicity to Daphnia (Heinlaan *et al.* 2008); however, performance of similar tests with the addition of simulated solar radiation resulted in much higher toxicity, and lethal effects were seen in the μg/L range (Ma *et al.* 2012a). The types of assay used to assess toxicity may need to be re-evaluated for NP use; in the process of performing our own NP toxicity studies, we observed recurring issues with biochemical-based assays producing inconsistent results. To confirm our results, assays that were commonly used for classical toxicity testing were compared to one another, and we determined that the outcomes were often incongruous. For example, in **Chapter 3** we note that assays measuring oxidative stress were providing conflicting results; one assay would indicate an increase in reactive oxygen species (ROS), whereas another, using the same sample, would suggest that no ROS were present. We hypothesized that NPs were interfering with these assays in a manner that classical toxicants would not, and in **Chapter 2** we explore this subject in depth. Nanotoxicologists need to be aware of the potential issues associated with the toxicity tests chosen, and continue to choose and modify tests accordingly.

In the following chapters I attempted to fill some knowledge gaps in the nanotoxicology literature and tackled some issues associated with new toxicant testing. For each set of experiments, I made every effort to choose appropriate NPs based on, 1) the availability of well-characterized and consistently produced materials from trusted sources, and 2) the material and formulation that would best answer the question posed. I used a combination of NPs that were representative of materials that could be used in the market for imaging, such as silicon (Si) and cadmium selenide (CdSe) NPs, and for biomedical purposes, such as nano-hydroxyapatite (HAP) and helical rosette nanotubes (RNT), as well as

NPs that were chosen for their specific properties, such as stable, low dissolving, well capped polymer coated zinc oxide (ZnO) and titanium dioxide (TiO_2) NPs, and different shaped materials, such as hydrophilic single walled carbon nanotubes (SWCNT), and leaf-shaped ZnO. Furthermore, I attempted to design my experiments to best suit the NP(s) being tested or the question being asked.

1.3. NP CHARACTERISTICS AFFECTING TOXICITY

The study of NP toxicity is often focused on determining whether nano-specific effects exist. In general, the dissolved substituent is of concern in classical toxicants; NP toxicity testing is particularly complex due to the need to test for the toxicity caused by the dissolution of ions from the NP core, and the need to test for any effects caused by the NP form itself. NPs differ than classical toxicants in that they are colloidal and stay suspended in the water column, they have a very high surface area to volume ratio and thus are very reactive, and they have a high propensity to bind to small molecules. Individually studying the toxicity of each NP-formulation is unfeasible; the ability to alter a multitude of physicochemical properties will result in thousands of unique types of NPs. Many reviews group NPs based on core materials to discuss toxicity (*e.g.,* Farré *et al.* 2008; Scown *et al.* 2010). For example, quantum dots, carbonaceous, zero valent iron, and metal oxide core materials are typically grouped, and NPs within each group were initially suspected to have similar toxicological profiles. However, it was quickly established that many physicochemical properties such as size, charge, surface coating, and shape, amongst other characteristics, could alter the toxicity of a NP, even amongst NPs composed of the same core material (Rivera-Gil *et al.* 2012; Zhu *et al.* 2012b). One of the objectives throughout my research was to determine the influence of NP physicochemical characteristics and their relation to biological effects.

1.3.1. Core composition

An important aspect of NP production will be the choice of materials to form the NP core and the coatings and functionalizations selected to coat the NPs. The composition of a NP itself can enhance its toxicity via the breakdown of its core. Many studies show that metal NPs cause toxic effects *via* dissociation of free metal ions from the core. Free metals are known to cause a myriad of negative effects in aquatic organisms, and can affect almost every physiological process and induce oxidative stress (Jezierska *et al.* 2008; Wood 2011). On the contrary, low release of metals may have positive effects in aquatic organisms. For example, if essential micronutrients such as iron, selenium, nickel or zinc NP are used as core materials in well-capped NPs, they could slowly release small concentrations of free metal and provide beneficial effects, especially in nutrient-depleted environments (Chapman & Wang 2000). However, even if NPs are initially stable in solution, breakdown of the core may occur with exposure to pH, UV, oxidation, and time (Lévy *et al.* 2010; Gorham *et al.* 2012). Furthermore, uptake of NPs and localization of NPs in acidic lysosome and endosomes (pH 4.5 – 6.5) could lead to degradation of the core inside a cell (Zhu *et al.* 2012b). Many physicochemical studies demonstrate effects of acidic pH; for example, dissolution rates are higher in acidic environments for bare Ag (Elzey & Grassian 2009), platinum (Tang *et al.* 2010), and ZnO (Bian *et al.* 2011; Cho *et al.* 2011), and organic coated superparamagnetic (Lévy *et al.* 2010) NPs. Therefore, lysosomal and endosomal localization of NPs (Shiohara *et al.* 2011) and decreases in lysosomal stability (Cho *et al.* 2011) could result in cellular death during exposure to metal NPs *via* free metal effects.

While production and development of NPs with the most ideal material and properties for commercial or industrial use is appealing, considerations of the potential biological effects and ecotoxicity will need to be taken into account. For example, Cd-based NPs are currently the prevailing quantum dot investigated for production for medical and imaging use. Various semiconductor materials exhibit unique optical properties in the nanometer range, and will fluoresce intensely

when excited with light (Wang *et al.* 2013). These NPs are superior to classic dyes in many circumstances, and Cd based NPs in particular have very high quantum yield (*i.e.,* have the brightest fluorescence), therefore a vast amount of research effort has been expended on these NPs (Zhong 2009; Wang *et al.* 2013). Given that numerous reports conclude that these NPs can be toxic (Shiohara *et al.* 2004; Kirchner *et al.* 2005; Ryman-Rasmussen *et al.* 2006; Cho *et al.* 2007), research into alternate and more biocompatible NPs should be investigated. The influence of the core composition of materials is explored more in depth in **Chapter 3**, where I compare the toxicity of Si and CdSe NPs, **Chapter 5**, where I determine the effects of different materials on zebrafish hatch, and **Chapter 6**, where I elucidate the effects of different materials on zebrafish development, in the presence of natural organic materials (NOM).

1.3.2. Surface coating

Continued development of NPs will likely lead to innumerable types surface functionalizations and coatings to allow for specific targeting of NPs, and to tune NPs for specialized uses. Capping agents and functionalization of the NP core can reduce the oxidation and dissolution of the core, and also serve to stabilize NPs in aquatic systems (Clark *et al.* 2010), but these may break down under oxidative conditions or in the presence of UV light (Gorham *et al.* 2012). Coatings provide both electrostatic (charge-charge effects) and steric (physical) repulsion (Figure 1-2), and thus affect agglomeration of the NPs, stability in a water column, and inter-molecule interactions. Functionalization of Si NPs with varying carboxylic acid chain lengths has been shown to alter oxidation state, hydrodynamic radius, and polydispersity (Clark *et al.* 2010). It is still unclear which circumstances will enhance the protective or harmful effect of surface coatings. Coated NPs have been reported as both more toxic (*e.g.,* Suresh *et al.* 2012; Perreault *et al.* 2012) and less toxic (*e.g.,* Bae *et al.* 2011) than their bare counterparts. In **Chapter 3** I compare the toxicity of Si NPs with different carboxylic acid chain-length functionalizations both *in vitro* and *in vivo*.

1.3.3. Agglomeration

Agglomeration is influenced by a number of factors; surface functionalization, charge, abiotic factors, and the presence of other small molecules can strongly influence the agglomeration of the NPs. The size of these NP clusters can affect their toxicity and uptake. For example, cerium oxide NP agglomerates larger than 100 nm appeared to be more likely to be taken up by human lung fibroblast cells than smaller agglomerates (Limbach *et al.* 2005). Settling of agglomerated NPs on the cell surface, effectively concentrating the NPs at the site of uptake (Kühnel *et al.* 2009; Laurent *et al.* 2012), and can result in increased toxicity. Similarly, NP agglomerates in aquatic systems can sink and come in contact with benthic organisms (Ward & Kach 2009), and immobile embryonic organisms still within their chorion (Zhu *et al.* 2009a), effectively increasing exposure concentration. In contrast, large agglomerates of NPs may also prevent bioavailability; NPs may not penetrate the zebrafish chorion if they form agglomerates larger than 0.5-0.7 μm, the size of the chorionic pores (Rawson *et al.* 2000).

Difficulties in reliably linking hydrodynamic size and effects exist due to the limited techniques available to measure hydrodynamic size. The standard for hydrodynamic diameter measurement is dynamic light scattering (DLS), a technique based on the Brownian motion of NPs. However, these data tend to be skewed to overrepresent larger agglomerates and complexities still lie in interpreting heterogeneous populations of NPs (Hoo *et al.* 2008). Improved methods have been developed to measure agglomerate size and distribution, such as NP tracking analysis (Montes-Burgos *et al.* 2009), and atomic force microscopy (Hoo *et al.* 2008), but these techniques still have inherent issues, such as limited concentration range detection, lowered sensitivity to smaller particles, an inability to measure in media, complex procedures, and they are not yet as readily available as DLS (Hassellöv *et al.* 2008; Filipe *et al.* 2010). Relating hydrodynamic size to biological effects are explored in this thesis in regards to HAP cytotoxicity and *in vivo* toxicity (**Chapter 4**), effects on zebrafish hatch

(**Chapter 5**), and the interactions of NPs with humic acid (HA) and their effect on zebrafish development (**Chapter 6**).

1.3.4. Charge

There is considerable conflicting data regarding how charge (often measured as ζ-potential) alters the toxicity of NPs. NP charge can affect both the stability and the degree of interaction with other molecules and surfaces. It is generally accepted that NPs below -25 mV and above +25 mV are considered stable (*i.e.,* repulse one another so that they resist agglomeration and stay suspended in solution).

One of the main uncertainties concerning differently charged particles is determining whether charge will affect the interaction with biological membranes. The cell membrane carries a net negative charge, and is dominated by the head groups of phosphatidylserine and phosphatidylinositol. Based on this, the general hypothesis is that positively charged NPs would be more likely to bind to plasma membranes and result in higher translocation into the cell than negatively charged NPs. A number of experimental studies comparing positive and negative uptake of NPs of the same core, shape, and size support this theory (Harush-Frenkel *et al.* 2008; Park *et al.* 2011), but a seeming equal number of results for the opposite outcome challenge this notion (Ryman-Rasmussen *et al.* 2006; Zhang & Monteiro-Riviere 2009). Though negative charge may not prevent uptake, it may influence the rate and/or mechanism of uptake (Ryman-Rasmussen *et al.* 2006; Park *et al.* 2011). Both negatively and positively charged NPs can be toxic (Clift *et al.* 2010; George *et al.* 2011), and it is clear that measurement of initial ζ-potential may not be adequate for predicting toxicity, particularly given the propensity for charge characteristics to change in different media and in the presence of other molecules (Fabrega *et al.* 2009; Bian *et al.* 2011). Throughout my research (**Chapter 1-6**) I concentrated on negatively charged NPs to establish whether these NPs would cause effects at the biochemical, cellular, and whole animal levels.

1.3.5. Shape

Shape may play an important role in the toxicity of NPs and its interaction with other small molecules and surfaces. While spherical and cylindrical NP forms are highly studied, it is likely that other shapes will be produced for specific applications with desirable characteristics. For example, silver nanoprisms, cubes, and truncated tetrahedrons exhibit unique optical, magnetic, and catalytic properties (Jin *et al.* 2001; Wiley *et al.* 2004) and could be tuned for use in catalysis, sensing, and imaging. Changing the shape of a particle changes the surface area, affecting the probability of adsorption to other molecules and altering the exposure of reactive groups. Uptake has been shown to be affected by shape; for example, spherical gold NPs have higher uptake than rod-shaped NPs in HeLa cells (Chithrani & Chan 2007). Not only do different shapes alter uptake, but aspect ratio of tubular materials strongly influence uptake and toxicity (Chithrani & Chan 2007; Meng *et al.* 2011). In **Chapter 4**, I determine if there are differences in *in vitro* and *in vivo* toxicity between rod and needle shaped HAP NPs, and in **Chapter 5 and 6** I elucidate if there are differences between differently shaped ZnO NPs.

1.3.6. Dissolution

Distinguishing NP-specific toxicity from the effects cause by the dissolution products of NPs will help determine whether NP-specific regulations are necessary. Dissolution, simply defined here as the dissociation of free ions from the core, likely plays a key role in NP toxicity (Shaw & Handy 2011). The release of free metals from the core will be dependent on all the characteristics discussed above, as well as the medium in which the NP exists (Borm 2005). This necessitates the need to perform experiments designed to determine dissolution effects. Early studies recognized the importance of running pair-wise ionic metal controls, however few measurements were performed to determine the actual concentration of dissolved metal in exposure media. Due to the use of artificially high concentrations of free metal (the assumption was often 100% breakdown of

NP), not many valuable conclusions could be made on the significance of dissolution. Recent development and use of relatively simple ultracentrifugation or ultrafiltration protocols has allowed for more realistic testing of dissolution effects. Based on the current data, results suggest that there may be effects specific to NPs that are independent of their dissolved counterparts, as observed *in vitro* (Beer *et al.* 2012), in fish survival and morphological measurements (Bai *et al.* 2009), histological observations (Ispas *et al.* 2009), and in gene expression studies (Griffitt *et al.* 2011). To distinguish NP-specific effects from free ion effects, I perform dialysis experiments in **Chapters 4-7** and run pair-wise free metal exposures.

1.3.7. Aquatic exposure medium and natural environmental variables

Upon addition to media, NPs adsorb molecules, effectively changing the surface structure and altering their physicochemical properties (Nel *et al.* 2009; Laurent *et al.* 2012). These interactions change the behavior of NPs in different aquatic conditions, and can alter the toxicity of NPs. Therefore, it is crucial to measure the NP physicochemical characteristics in the media used for exposures to get an accurate representation of what the cell or organism encounters. The presence of serum can affect the uptake and toxicity of NPs, and some authors have even removed this 'confounding' factor in their studies (Jones and Grainger 2009). As a consequence, these types of studies may be even less representative of realistic scenarios. Furthermore, Guo *et al.* (2008) found that SWCNT could adsorb to amino acids and vitamins, depleting the serum of essential nutrients, and resulting in decreased cell health.

A large amount of data has been generated in pristine waters in laboratory conditions regarding NP toxicity. Ultimately, these data will be needed to predict the probability of NPs to cause effects in natural aquatic environments, but these experiments do not accurately represent real conditions. A relatively recent push for testing of NPs in media representing more realistic abiotic conditions (Handy *et al.* 2008b; Klaine *et al.* 2008) has led to an increase in published material regarding these factors. Agglomeration and dissolution of NPs are affected by

ionic strength, pH, and presence of divalent ions and can alter aquatic toxicity (Truong *et al.* 2012; Li *et al.* 2013; Kim *et al.* 2013). Notably, NOM appears to interact with NPs and was of particular interest due to their apparent ability to coat, or replace the coating, of NPs (Diegoli *et al.* 2008). Since the composition and organization of the surface of a NP strongly influences its behavior and potential for biological interaction (Lynch *et al.* 2009), I performed a study to determine the influence of NOM on NP toxicity in zebrafish embryos (**Chapter 6**).

1.3.8. Other NP characteristics

Many additional characteristics not extensively investigated in this thesis can affect NP behavior and toxicity. Core size of a NP can alter uptake and distribution within cells (Chithrani & Chan 2007) or an organism (Kashiwada 2006), can change dissolution rate (Tang *et al.* 2010), and dictate the affinity for a surface (as opposed to aggregate size) (Lin & Wiesner 2012). The hydrophobicity of a NP may affect its interaction with membranes (Nel *et al.* 2009). Different photochemical conditions have been shown to induce higher oxidative stress in organisms and cells due to the photoactivity of NPs (Ma *et al.* 2012b). It is clear that no single physicochemical characteristic of a NP can be used to predict toxicity. Linking NP-characteristics to their effects is a complex issue, as many parameters are related to one another and can change drastically in different aquatic environments.

1.4. BIOLOGICAL NANOTOXICITY ASSESSMENT

To thoroughly study the potential of NPs to cause biological damage, experiments must be performed at the biochemical, cellular and whole animal levels. While *in vivo* experiments are the gold standard for biological toxicity testing, *in vitro* experiments may represent *in vivo* outcomes, and biochemical testing can provide more insight into the mechanisms of a toxicants' effect. Use of cells and biochemical assays is often more cost-effective and allows for higher

throughput than *in vitro* studies, however, aquatic *in vivo* models are absolutely essential (Fischer & Chan 2007) to properly predict ecotoxicity. A summary of the advantages and disadvantages of performing experiments at each of these levels, as in relation to this thesis are shown in Figure 1-3.

1.4.1. Aquatic effects – *in vitro*

Cell studies give insight as to the route of uptake and processing of NPs, as well as the mechanism by which NPs can cause oxidative stress, produce cytokines, affect gene regulation and DNA, and how they can ultimately result in apoptosis or necrosis. Particular cell lines are often chosen to represent the predicted mode of exposure; for example, epidermal cells are often used in TiO_2 studies, as a predicted mode of uptake will be through application of sunscreens on the skin, and many studies employ the use of lung cells to represent inhalation of NPs as an occupational hazard (Love *et al.* 2012).

Uptake

Data showing NPs taken up into cells has been presented using a number of techniques (Iversen *et al.* 2011; Tantra & Knight 2011). The mechanism for uptake is still not completely understood. Passive diffusion through ionic channels is not expected; estimates of maximum pore radius, ca. 8Å, or 0.8 nm (Tieleman *et al.* 2002) fall well below the size of individual NPs. The mode of uptake into a cell is likely *via* endocytosis, and cell-type and physicochemical characteristics of a NP will influence its mode of uptake (Iversen *et al.* 2011; Rivolta *et al.* 2012). For example, it has been suggested that both negatively and positively charged NPs are taken up by ATP-dependent endocytosis but only cationic NPs use energy-independent pathways, such as lipid-raft mediated micropinocytosis (Singh *et al.* 2012). It should be noted that many mechanistic studies use 'specific' inhibitors of endocytosis to determine the mechanism of uptake; however, it has been suggested that many of these inhibitors can have effects on multiple endocytic pathways (Iversen *et al.* 2011), and care must be used in

interpreting these studies. Using fluorescent-tagged HAP, we determine whether NPs could associate or be taken up by different cell lines in **Chapter 4**.

Intracellular localization

NPs have been shown to accumulate in essentially every area of the cell; the lysosomes and endosomes (Shiohara *et al.* 2011; Park *et al.* 2011), the mitochondria (Wang *et al.* 2011), the perinuclear region (Zhang & Monteiro-Riviere 2009; Meng *et al.* 2011), in the cytosol (Asharani *et al.* 2008; Park *et al.* 2011). Localization within different intracellular compartments can result in different toxicological consequences; dissolution within lysosomes resulting in increased oxidative stress, interference with mitochondrial function and integrity (Wang *et al.* 2011), and effects on DNA (An & Jin 2012) are some possible consequences of internalized NPs. The exact fate of NPs once inside a cell is still not completely understood – techniques used to determine the localization can be hindered by poor resolution (*e.g.*, fluorescence and confocal microscopy), artifacts introduced by processing (*e.g.,* transmission electron microscopy, TEM), and difficulties in identifying the NP itself, especially if it undergoes intracellular dissolution or is composed of low atomic contrast materials (Elsaesser *et al.* 2010).

Oxidative stress

Many studies report increased oxidative stress induced by NP exposure, and the presence of ROS can disrupt a number of cellular processes that affect proliferation and growth. NPs can induce ROS production through a number of routes. Release of metal (Cho *et al.* 2011), disturbance of mitochondria or endoplasmic reticulum (Xia *et al.* 2006), and NPs themselves can directly catalyze the production of ROS (Xia *et al.* 2006; Ma & Lin 2012). ROS-caused damage can be countered by generation of antioxidative molecules, such as catalase, superoxide dismutase, and glutathione. Addition of antioxidants during aquatic NP exposure often decreases or completely abolishes cytotoxicity (*e.g.,* Clift *et al.* 2010). On the opposite end, NPs may inhibit the production or impede the actual

action of antioxidant molecules; however, this is difficult to identify. Other cellular effects induced by NP exposure can include genomic DNA damage, effects on replication and transcription, leading to apoptosis, suppression or stimulation of immune function (Zolnik *et al.* 2010), or protein denaturation or inhibition (MacCormack *et al.* 2012), as discussed further below. All of these can manifest as either a cause of, or a result of, oxidative stress, therefore is used as a marker for general disturbance caused by a toxicant. I use measurements of oxidative stress in **Chapter 3** to determine whether Si NPs are a safer alternative to CdSe NPs**.**

Shortcomings of in vitro testing

Unfortunately, *in vitro* experiments are often not representative of exposures *in vivo* (Jones & Grainger 2009). Laboratory cell cultures may not accurately represent native cell lines; inherent issues associated with long-term passage of cell lines, misidentification of cells, and even contamination may decrease the value of *in vitro* studies (Hughes *et al.* 2007). The complex composition of tissues and effect of physiological processes are not represented by *in vitro* systems. Additionally, the behavior of NPs the surrounding media before encountering an organism will play an essential role in *in vivo* experiments.

1.4.2. Aquatic effects *- in vivo*

Aquatic organisms will be very sensitive to exposure to NPs; the stability of NPs in the water column mean that they will certainly come in contact with aquatic organisms, and the chance for uptake may occur over multiple surfaces. Effects have been shown in all levels of aquatic biota; microbes, algae, and invertebrates are not immune to the negative effects of aquatic exposure to NPs (Scown *et al.* 2010). However, this thesis focuses on the effects on fish, and discussion of other biota is limited. Fish are commonly used as a model for aquatic toxicity, as they are sentinels of water quality, have complex physiological systems that are not represented by other groups, and are the primary freshwater aquatic vertebrate (Spitsbergen & Kent 2003; Hill 2005). Furthermore, negative

effects of toxicants on fish often has an impact on the public and thus, from a non-scientific point of view, augments the importance of studying these species (Braunbeck & Lammer 2006).

Uptake

A number of routes of possible NP uptake, including the skin, gills, or gut epithelia are available during NP exposure in fish (Handy *et al.* 2008a; von der Kammer *et al.* 2008). Difficulties in distinguishing NP and free metal in techniques such as ICP-MS have so far resulted in few studies definitely demonstrating localization of NPs within aquatic organisms. With the use of transparent fish, uptake of fluorescent latex NPs has been seen in the medaka (Kashiwada 2006). Use of dark-field single NP optical microscopy and spectroscopy Ag NPs can become embedded in the tissues of embryonic zebrafish (Lee *et al.* 2007). Embryonic fish may be partially protected by their chorion; large agglomerates will likely not penetrate the 0.4-0.6 μm pores (Rawson *et al.* 2000). Some evidence suggests that some NP formulations will not cross the chorion (Cheng *et al.* 2007; Osborne *et al.* 2012). In adult fish, NPs can bind to potential sites of uptake, such as the gills, stomach, and gut (Sun *et al.* 2006; Smith *et al.* 2007; Johnston *et al.* 2010), but it is not clear whether these NPs are taken up or by what mechanism. Recent advances in detection techniques, such as dark-field optical microscopy and spectroscopy (Lee *et al.* 2007), coherent anti-Stokes Raman scattering microscopy (Volkmer 2005), and synchrotron-based techniques (Wang *et al.* 2010) have improved the ability to detect single or small agglomerates of NPs within an organism.

Survival

A number of NPs, such as ZnO, CdSe, C_{60}, Au, and Ag (Zhu *et al.* 2008; Yu *et al.* 2011; George *et al.* 2011; Osborne *et al.* 2012), can decrease embryo survival rates. Mortality is not often reported as a main effect of NP exposure in fish, particularly in adult fish (Federici *et al.* 2007). Adult fish have mechanisms that may prevent NP effects; for example, mucus secretion on the skin and gills

may trap NPs and eventually slough off (Federici *et al.* 2007; Johnston *et al.* 2010), or compensatory mechanisms against sublethal damage. The mechanisms by which NPs cause death are likely through a combination of developmental and morphological effects, oxidative stress, and physiological effects, as discussed below. Some of the NPs used in our experiments could affect embryonic zebrafish survival; these effects are documented in **Chapter 3, 4, and 6**.

Developmental and morphological effects

NPs are well documented to cause morphological effects in both embryonic and adult fish. Early stage embryos are sensitive to toxicants (McKim 1977), and are a commonly used model for toxicity testing. Exposure to Ag, ZnO, CdSe/ZnS, and Pt NPs can result in edemas, axial curvatures, slowed growth, and tail defects in developing fish (Zhu *et al.* 2008; Bai *et al.* 2009; Asharani *et al.* 2011; George *et al.* 2011). Muscle development in fish can be strongly affected, leading to defects in movement and swim ability (Asharani *et al.* 2011). Adult NP exposures result in changes in gill morphology, such as increased filament width and thickening of secondary lamellae (Smith *et al.* 2007; Griffitt *et al.* 2008; 2011). Irritation of the skin, tissue ulceration, and increased mucus production has been observed (Zhu *et al.* 2008). Erosion of gut epithelia and fusion of the villi has been seen upon exposure to NPs (Smith *et al.* 2007; Federici *et al.* 2007). Due to a number of studies reporting morphological effects in the absence of lethal effects, developmental and morphological changes in NP-exposed embryonic zebrafish are determined in **Chapter 4**, **Chapter 5** and **Chapter 6**.

Oxidative stress

As in *in vitro* studies, production of ROS *in vivo* is used as a general indication of sublethal toxicity. In many cases increased oxidative stress has been linked to tissue damage (Smith *et al.* 2007; Federici *et al.* 2007), in which case the subsequent immune response could result in increased ROS. There appears to be much lower and fewer incidences of oxidative stress in *in vivo* studies compared to *in vitro* studies; this is likely due to the ability of organisms to counter

increased oxidative stress (Fischer & Chan 2007). For example, exposure to either 1 g/L Ag or 1 g/L TiO_2 NPs in zebrafish did not yield any signs of oxidative stress (Griffitt *et al.* 2008), but cell exposures to Ag and TiO_2 NPs at concentrations 100x lower caused marked increases in oxidative stress (*e.g.,* Okuda-Shimazaki *et al.* 2010; Farkas *et al.* 2011a). Furthermore, it is possible an even higher number of studies have determined that there are no NP-induced effects in *in vivo* exposures, but do not publish these data (Hankin *et al.* 2011). Quantum dots are often reported to cause an increase in oxidative stress (Clift *et al.* 2010; George *et al.* 2011) and I explore this topic in **Chapter 3.**

Physiological effects at the gill

Documentation of survival, and morphological endpoints are commonly recorded, but few reports to date have studied the physiological effects of NPs. The gill is site of NP accumulation, and may be a target organ during NP exposure (Sun *et al.* 2006; Johnston *et al.* 2010). The gill has many functions; it acts as a site of ion regulation, respiration, excretion, and acid-base regulation (Evans 2005). Therefore, a number of processes may be affected by NP-adsorption and uptake. Ventilation rates can increase in response to NP-exposure (Smith *et al.* 2007), thus exacerbating the effect and conceivably increasing the rate of adsorption or uptake of NPs. NP-induced changes in Na^+/K^+-ATPase (NKA) in the gill could create ionoregulatory imbalances that could lead to mortality. NKA levels have been shown to be downregulated in response to Cu NPs (Griffitt *et al.* 2008; Shaw *et al.* 2012) and upregulated in response to SWCNT exposure (Smith *et al.* 2007). Since free-metal exposure can affect ion regulation, and NKA levels (Morgan 2004), then it is imperative to determine whether this is a NP-effect. In **Chapter 7** we explore this topic in depth and use a juvenile trout model to assess physiological effects of Ag NPs on ionoregulatory balance.

1.5. BIOCHEMICAL INTERACTIONS

The high affinity for NPs to adsorb to other surfaces and molecules has been well documented, in aquatic matrices NPs will adsorb molecules and form a "protein corona" (Lundqvist *et al.* 2008). NP-interactions have been developed a great deal for use in detection, remediation, and targeted delivery (Asuri *et al.* 2006b; Sanchez *et al.* 2011), however, the potential for NPs to bind physiologically relevant molecules has been largely overlooked. The distinction between traditional toxicant effects and NP effects may be due to their affinity for small molecules. If NPs are capable of translocating into organisms, the function of a myriad of proteins and enzymes essential for proper biological function may be disrupted.

Incubation of NPs with plasma results in interactions between both polystyrene and metal oxide NPs and a number of blood proteins (Lundqvist *et al.* 2008; Deng *et al.* 2009). Notably, NPs had strong affinities for immunoglobins and fibrinogen, which could hinder immune function. Given that *in vivo* effects on immune function as has been seen in TiO_2-exposed fathead minnow (Jovanović *et al.* 2010), it would be valuable to determine if these NP-protein interactions could play a role. Exploration into high affinity adsorption and subsequent inhibition of acetylcholinesterase by copper and carbon nanotubes (Wang *et al.* 2009) may help explain effects in the brain (Oberdörster *et al.* 2005) or reduced response to touch (Asharani *et al.* 2011). Interaction and inhibition of membrane transporters may contribute to ionoregulatory imbalances (Zhao & Wang 2013). Preliminary studies show that NP-interactions can result in protein deformation (Zhao *et al.* 2009; MacCormack *et al.* 2012), but it unknown whether these will lead to dysfunction or effects on survival in whole organisms. Given the paucity of data regarding the potential for these biochemical interactions to cause real, *in vivo* effects, I evaluate the potential for NPs to interact with proteases essential for zebrafish hatch (**Chapter 5** and **6**), and elucidate whether effects on transporters may result in imbalances in ion regulation in rainbow trout (**Chapter 7**).

1.6. THESIS GOALS

This thesis is organized into six discrete data chapters; however, the themes and goals of each overlap. To be able to create relevant data that will be of use to the nanotoxicity community, each chapter contains information that suits multiple objectives. The overall goals of this thesis were to: 1) Determine appropriate biochemical, *in vitro*, and *in vivo* assays for NP toxicity testing, 2) Link physicochemical characteristics with NP-toxicity, 3) Ascertain whether there is NP-specific toxicity, and 4) Elucidate mechanisms by which NP-interactions can affect biological function, with a focus on environmentally and physiologically relevant molecules.
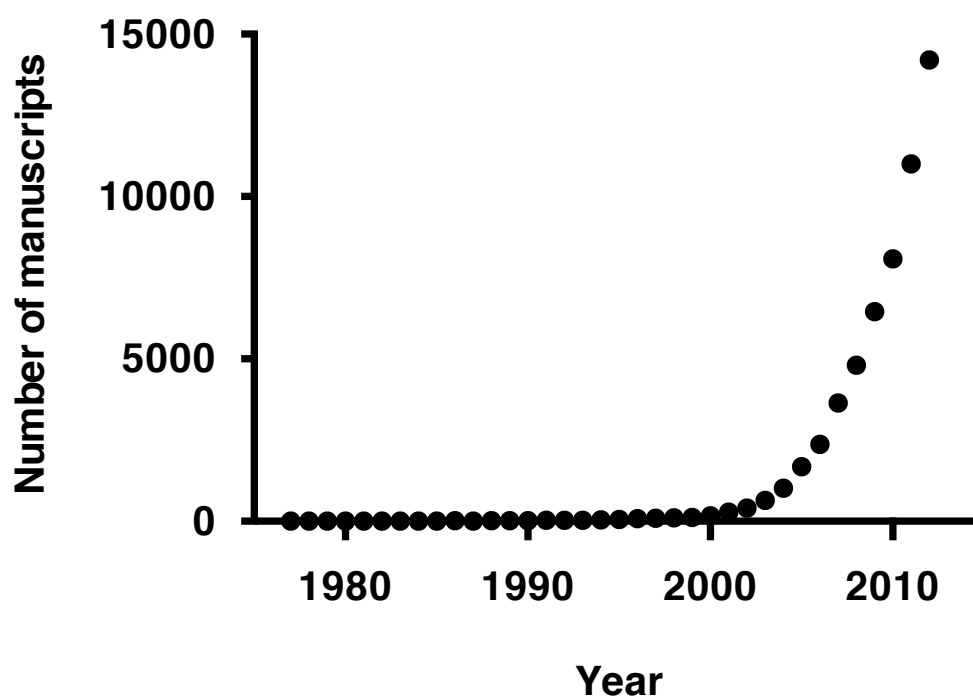
Figure 1-1. Number of manuscripts per individual year as a result of a Google Scholar search for "nanoparticle toxicity'.
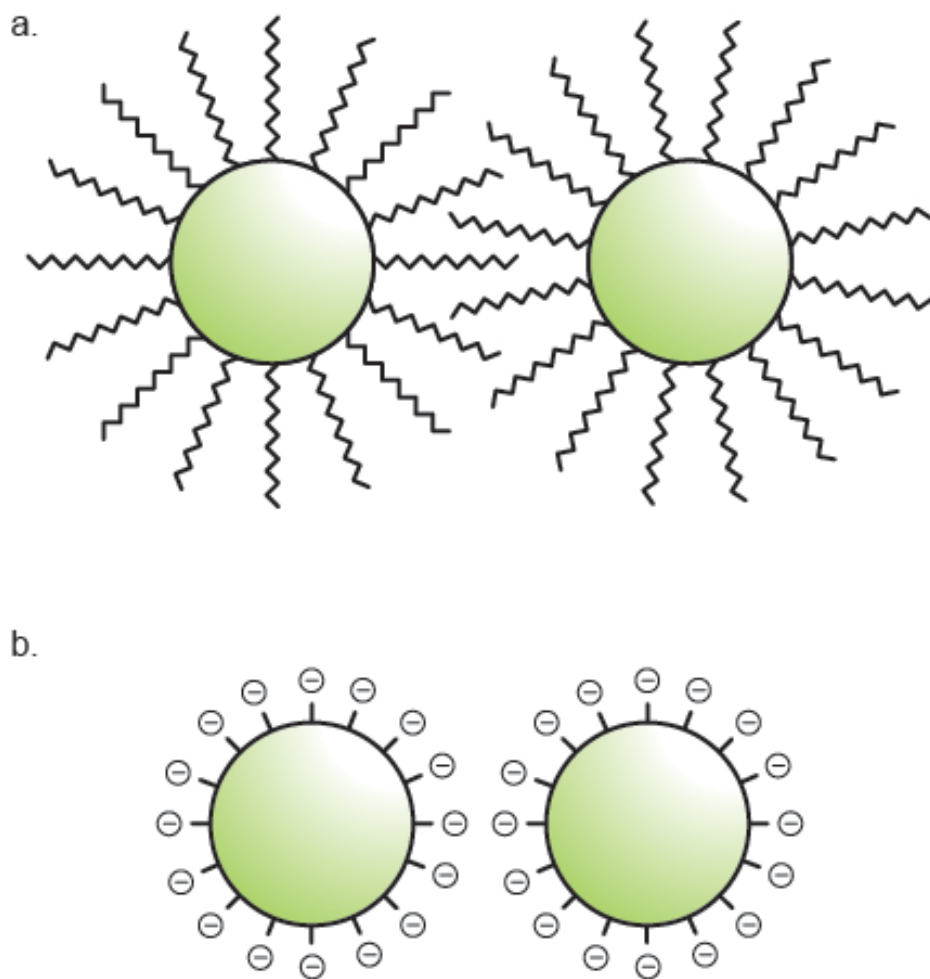
Figure 1-2. Schematic showing a) steric, or b) electrostatic interactions between nanoparticles with different surface functionalizations.
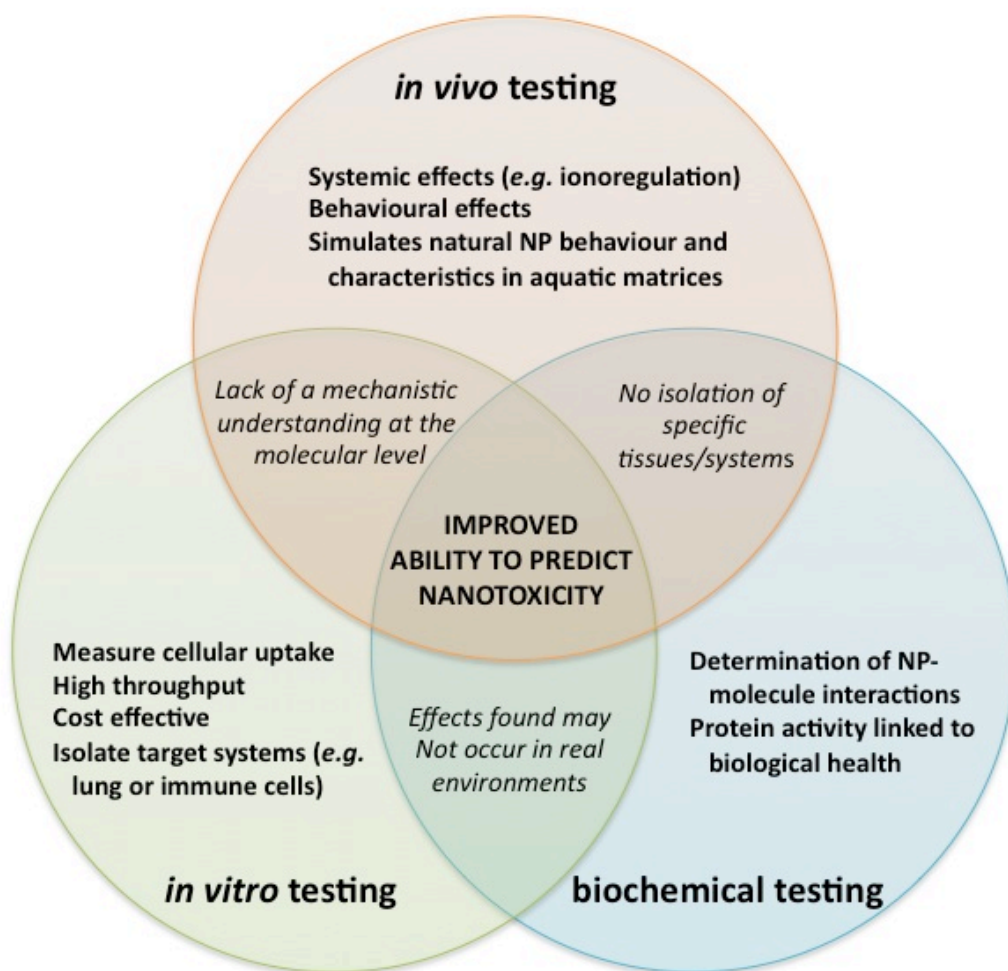
Figure 1-3. The foundations for this thesis were based on the performance of experiments at the biochemical, cellular, and whole animal levels. The advantages as it pertained to my work for each type of testing are noted, as well as the disadvantages of only performing two of these categories of experiments. A combination of data from all levels will provide a solid basis for the understanding of the potential biological effects of nanoparticles and an improved ability to predict nanotoxicity.

CHAPTER 2

Widespread nanoparticle-assay interference: Implications for nanotoxicity testing

2.1. INTRODUCTION

As nanomaterial (NM) production and use continues to become more prevalent, consistent and accurate NM toxicity testing is crucial for the ability to properly regulate these materials. Many conflicting reports on the toxicity of NMs have made it difficult to predict their biological effects (Wörle-Knirsch *et al.* 2006; Monteiro-Riviere *et al.* 2009). One of the primary issues afflicting consistent toxicity testing may be the use of biochemical assays that can be affected by NMs themselves, leading to data artefacts and subsequent incongruent estimations of toxicity. Such inconsistent and/or inaccurate data will make it difficult for regulators to establish guidelines and procedures for NM production and use, ultimately hindering our ability to predict how NMs will affect organisms in the environment.

Due to the unique physicochemical properties and increased reactivity of nanoparticles (NPs), there is a high potential for these materials to interfere with spectrophotometric and spectrofluorometric assays. Commonly used tests such as the lactate dehydrogenase (LDH) cytotoxicity assay, alamar blue, and tetrazolium based assays (*e.g.,* MTS and MTT) are frequently reported to be affected by a range of different NPs (Han *et al.* 2011; Kroll *et al.* 2012; MacCormack *et al.* 2012; Holder *et al.* 2012). A large number of *in vivo* and *in vitro* nanotoxicology experiments include these or similar assays which are designed to quickly and efficiently assess toxicity. Many of these protocols rely on multi-step biochemical reactions resulting in changes in absorbance or fluorescence, which are then quantified to provide information on physiological or biochemical endpoints. A comprehensive review of assays used for nanotoxicity testing is beyond the scope of this discussion and can be found elsewhere (Marquis *et al.* 2009; Stone *et al.* 2009; Love *et al.* 2012).

Most assays contain dyes or proteins with significant potential to interact with NPs. NPs can bind to proteins and dyes and alter their structure and/or function, and it is probable that this process is occurring in common toxicity assays (Asuri *et al.* 2006a; Kane & Stroock 2007; Fei & Perrett 2009; Lord *et al.* 2010). The presence of NPs may adversely influence these reactions and cause

significant changes in enzyme activity (Asuri *et al.* 2006a; Kane & Stroock 2007; Fei & Perrett 2009), fluorescence, and/or the absorbance characteristics of indicator molecules (Ramakrishna & Ghosh 2001; Hedderman *et al.* 2004). Carbon-based NMs have been shown to consistently affect a number of toxicity assays and are documented to bind to dyes (Monteiro-Riviere & Inman 2006; Casey *et al.* 2007). Carbonaceous NPs bind to alamar blue (Casey *et al.* 2007), coomassie blue (Casey *et al.* 2007), neutral red (Monteiro-Riviere & Inman 2006; Casey *et al.* 2007), MTT dye (Monteiro-Riviere & Inman 2006; Wörle-Knirsch *et al.* 2006; Casey *et al.* 2007; Holder *et al.* 2012), and WST-1 dye (Casey *et al.* 2007), and can therefore interfere with assays using these indicators (Singh *et al.* 2010).

To assess the extent of NP interference with toxicity assays and to determine if effects are predictable based on the physicochemical properties of the NP, we performed a systematic investigation of the accuracy of commonly used toxicity assays. First we tested assay reliability with only NPs and assay components, and then tested several of the procedures under more realistic conditions (*i.e.,* with cellular debris or protein present). Since a number of papers have already reported interference of assays by carbonaceous materials, we chose to investigate a broader suite of other commonly used NPs; silicon (Si), cadmium selenide (CdSe), zinc oxide (ZnO), titanium oxide (TiO$_2$) NPs, and helical rosette nanotubes (RNTs). An additional goal was to review existing nanotoxicology literature to assess whether appropriate assay controls were performed. In this regard, we also analyze a subset of peer-reviewed papers from both 2010 and 2012 to determine what proportion employ a colorimetric or fluorometric biochemical assay, and to evaluate whether there has been improvement in the performance and reporting of controls for these assays.

2.2. MATERIALS AND METHODS

2.2.1. Optical measurements

To determine the intrinsic fluorescence and absorbance of each NP an absorbance and fluorescence spectrum were plotted. NPs were diluted to 100 mg/L in ddH$_2$O and 2 mL were pipetted into a cuvette. An absorbance spectrum from 300-600 nm (Hewlett Packard 8452A diode array spectrophotometer) and a fluorescence spectrum (excitation 535 nm, Cary Eclipse photoluminescence spectrometer) were recorded.

2.2.2. Assay treatments

All assay validations, with the exception of the LDH cytotoxicity assay, were performed with the same protocol. A standard curve using appropriate samples was calculated for each 96-well microplate assay and microplates were only used if the standard curve had an R^2>0.99. In each experiment we first determined if NPs were interfering with the assay's reagents. NPs in ddH$_2$O were added to kit reagents and the assay was run according to manufacturer's instructions. In separate experiments simulating a more realistic assay scenario, 40 μg/mL bovine serum albumin (BSA) for the Bradford assay, 250 μg/mL BSA for the Bicinchoninic (BCA) assay, or 250 U/mL catalase for the Amplex Red Catalase assay was added to the microplate wells in addition to the NPs and kit reagents. This manipulation was not possible with the MTS or alamar blue assay since they are dependent on cellular metabolic activity, which is difficult to replicate experimentally. Results are reported as 'difference in reported protein/catalase activity/number of cells', which was calculated by subtracting the actual value of protein/catalase activity/number of cells added to the microplate well from the value reported by the assay. For example, if an assay reported 130 μg/mL of BSA and 40 μg/mL BSA was actually added, then the 'difference in reported protein' would be 90 μg/mL.

2.2.3. Protein quantification assays (BCA and Bradford Assays)

Protein quantification assays were performed using BCA (Pierce Biotechnology, Rockford, IL, USA) and Bradford methods (BioRad Laboratories, Hercules, CA, USA). Microplate assays for both methods were performed according to manufacturer's recommendations and absorbance was measured on a Molecular Devices (Sunnyvale, CA, USA) Spectramax microplate reader. Briefly, for the BCA assay, protein reduces Cu^{2+} to Cu^+ under alkaline conditions, and this cupric ion binds 2 molecules of BCA dye, which absorbs at 562 nm and is sensitive from 20-2000 μg/mL protein. The Bradford assay is a more direct method for protein quantification; Coomassie Brilliant Blue G-250 dye binds to aromatic and basic amino acid residues in proteins and the resulting complex absorbs at 595 nm and is sensitive from 8-80 μg/mL protein. In both cases, standard curves were prepared using BSA in ddH_2O. Test samples consisted of ddH_2O containing only NPs (0.1, 1, or 10 mg/L final concentration) or ddH_2O with NPs and BSA.

2.2.4. MTS cell proliferation/viability assay

MTS [3-(4,5-dimethylthiazol-2-yl)-5-(3-carboxymethoxyphenyl)-2-(4-sulfophenyl)-2H-tetrazolium] is a tetrazolium compound that can be bioreduced by metabolically active cells to a soluble formazan product. The quantity of formazan produced is indicative of the number of viable cells in culture and can be determined colorimetrically by recording the change in absorbance at 490 nm. This assay was performed according to manufacturer's recommendations for the Cell Titer 96 Aqueous Non-Radioactive Cell Proliferation Assay Kit (Promega, WI, USA). Briefly, Complete Minimal Essential Media (Hyclone) with 10% heat inactivated fetal bovine serum (Hyclone) and 2 mM L-glutamine (Gibco), 100 U/mL penicillin (Gibco), and 100 μg/mL streptomycin (Gibco) and was dispensed into a 96-well plate. NPs were added to each well to achieve final concentrations of 1, 10 or 100 mg/L. The kit reagents were then prepared, added to the plate, and incubated for 2 h (37°C, 5% CO_2). Absorbance (490 nm) was recorded using a microplate reader (WALLAC 1420, PerkinElmer, MA, USA). A standard curve

with a rat basophilic leukemia cell line, RBL 2H3, was run in parallel. RBL cells (5, 10, 20, 40, and 80×10^3 cells/well) were used to determine changes in reported cell number indicating NP interference.

2.2.5. Alamar Blue cell viability assay

AlamarBlue Cell Viability Reagent (Invitrogen, DAL1025) is commonly used to assess cell health. Simply, the metabolic activity of cells converts soluble resazurin dye into fluorescent resorufin, and fluorescence (excitation 535 nm, emission 590 nm) of this dye was recorded. For the standard curve, RBL 2H3 cells were seeded from $0-60 \times 10^3$ cells/well, and incubated for 2 h (37°C, 5% CO_2), after which the assay was run according to manufacturer's instructions. Final well concentrations of 1, 10, and 100 mg/L of each NP were used with the exception of Si, which were only measured at 1 and 10 mg/L due to low NP stock concentration.

2.2.6. Catalase assay

Catalase is an enzyme important in the reduction of harmful hydrogen peroxide into water and oxygen. Catalase activity was assessed with Molecular Probes' Amplex Red Catalase Assay Kit (A22180) and the assay was performed according to manufacturer's instructions. Briefly, Amplex Red reagent reacts in a 1:1 ratio with hydrogen peroxide in the presence of horseradish peroxidase to produce the fluorescent molecule resorufin. When catalase is active, it decreases the concentration of hydrogen peroxide and thus the amount of resorufin. Absorbance (560 nm) and fluorescence (excitation 535 nm, emission 595 nm) were recorded using a microplate reader (Wallac 1420, Perkin Elmer). A standard curve of 0-1000 U/mL catalase was used to extrapolate the catalase activity levels, ("reported catalase levels") and 1, 10, and 100 mg/L NP were used with the exception of Si, which were tested only at 1 and 10 mg/L due to low stock concentration.

2.2.7. LDH cytotoxicity assay

Many commercially available cytotoxicity assay kits measure the activity of the intracellular enzyme lactate dehydrogenase (LDH), which can be released to the extracellular media by damaged cells. It has been previously shown that NPs can inhibit or even abolish the activity of purified LDH (MacCormack *et al.* 2012) but it is not clear if this phenomenon will occur in more complex sample mixtures. LDH activity was assessed in RBL cells. The culture media contained substantial LDH enzyme activity (data not shown), and as such cells were washed to remove excess media. A known quantity of cells was centrifuged at 2100 rpm for 7 min, the supernatant was removed, and the cells were resuspended in phosphate buffered saline. This process was repeated 3 times. Cells were lysed using a wand type sonicator (model SLPe, Branson Ultrasonics, Danbury, CT, USA) to release the LDH enzyme. The lysed mixture was centrifuged briefly at 2100 rpm to remove cell debris and the final mixture was subsequently assayed for LDH activity by following the oxidation of β-NADH to β-NAD at 340 nm in a 96-well spectrophotometer (SoftMax Pro, Molecular Devices, Sunnyvale, CA, USA).

The cuvette-based protocol, described previously by MacCormack *et al.* (2012) was modified for a 96-well plate. A seven-point standard curve was generated for each plate that ranged from 0 to 20×10^6 cells/mL and run in parallel with LDH-containing test samples. Test samples were added to wells at a cell concentration of 12.5×10^6 cells/mL and exposed to either a NP treatment or vehicle (ddH$_2$O) in triplicate, and immediately assayed for β-NADH oxidation. Background oxidation was determined in the absence of pyruvate and was negligible for each plate assayed. The number of cells reported for each sample was calculated using the linear equation of the standard curve. Due to low stock concentration, only 1 mg/L of Si, 1 and 10 mg/L of CdSe and RNT, and 1, 10, and 100 mg/L of TiO$_2$ and ZnO were measured.

2.2.8. Statistical analysis

Protein, enzyme, or cell concentrations were established using absorbance or fluorescence values from treatment wells and calculated using the equation determined from the standard curve on the same plate. Values are reported as differences between this calculated concentration and the actual concentration of protein, enzyme, or cell added to the plate. All statistics were calculated using Prism 4 using one-way analyses of variance (ANOVA) followed by post-hoc Dunnett's test. Statistical significance was set at $p \leq 0.05$. Each treatment was repeated in triplicate per plate and each experiment replicated 3-6 times. Data are reported as the mean ± SEM.

2.2.9. Meta-analysis of nanotoxicological papers

A meta-analysis on current papers published in the area of nanotoxicology was performed to determine the percentage of studies running and reporting controls for colorimetric or fluorescent-based assays. On 28 September 2010, a search for "nanoparticle toxicity assay" in Google Scholar was performed and the top 200 papers were reviewed. The number of papers using a colorimetric or fluorescent assay were recorded, and of those, the number performing the following controls: 1) Measurement of the intrinsic fluorescence and absorbance of the NPs; 2) Assessment of the interference of NPs with the assay components and dyes; 3) Assessment of the interference of NPs with the assay components and dyes together with a test sample. On 14 November 2012, this search and analysis was repeated to determine whether there was a change in the reporting of controls in the literature.

2.3. RESULTS AND DISCUSSION

2.3.1. Nanoparticle characterization

To determine whether basic physicochemical NP characteristics could be used to predict interference with assays, hydrodynamic diameter, ζ-potential, and NP core size measurements were performed (as described in Appendix I and II).

Functionalization, hydrodynamic size, and ζ-potential information for all NPs are provided in Table 2-1. Other physicochemical parameters of some of the NPs used here have also been reported previously (Si: Hessel *et al*. 2007; RNTs:Fenniri *et al*. 2002). NP core diameters ranged from 3-9 nm (Appendix IV). TEM confirmed the spherical shape of each particle with the exception of tubular RNT (Appendix IV). Hydrodynamic diameter of NPs in ddH$_2$O ranged from 20-700 nm as determined by dynamic light scattering (DLS), and NPs tended to agglomerate as concentration increased (Table 2-1). RNTs were too highly agglomerated (>1μm) to allow for a reading at 100 mg/L on the DLS. NPs with similar functionalizations did not always follow the same pattern of hydrated diameter and agglomeration; for example, Si and CdSe NPs were of similar size at 1 mg/L (151±2 nm and 181± 12nm, respectively), but CdSe NPs agglomerated at 10 mg/L (240±8 nm) and 100 mg/L (703±13 nm) whereas the hydrodynamic diameter of Si NPs did not significantly change. The more labile binding of the surface coating of the mercaptoundecylenic acid functionalizations to CdSe NPs likely results in greater variations in hydrodynamic diameter at different concentrations than the covalently capped Si NPs. Steric stabilization by polymer coating of TiO$_2$ and ZnO generally resulted in smaller agglomerations than CdSe and Si. At 100 mg/L, TiO$_2$ and ZnO had similar hydrated diameters (150±1 nm and 153±12 nm, respectively), but varied at 1 mg/L (20±2 nm and 118±13 nm) and 10 mg/L (25±1 nm and 109±1 nm). CdSe NPs had the most negative ζ-potential (-52±2 mV) while other particles ranged from -26 to -52 mV, with the exception of RNTs, which were strongly positive (+77 mV) (Table 2-1). These variations in hydrated diameter and charge were predicted to alter interactions with charged dyes and proteins in the assays.

2.3.2. Optical measurements

The optical properties of a NP can interfere with the endpoint measurement of absorbance or fluorescence in a biochemical assay. For example, the absorbance spectrum of gold NPs overlaps with the absorbance range measured in a hemolysis assay, leading to erroneous results (Dobrovolskaia *et al.*

2008). Possible interference effects (such as surface plasmon resonance and quantum confinement) that can originate from varying size, shape, composition, surface modality and inter-particle interaction (Kelly *et al.* 2003; Bailey & Nie 2003) make optical characterization of each NP species essential. Of the tested NPs, Si were the only ones to absorb (0.28 a.u. at 340 nm, Figure 2-1). Si NPs do interfere with the LDH assay which is measured at 340 nm (Figure 2-2c); however, this assay is based on the rate of absorbance change as opposed to final absolute absorbance, therefore in this case the effect of the absorbance of the NPs is negated. It is likely that in this case interference is the result of direct interaction between Si and the enzyme (MacCormack *et al.* 2012), as discussed below, rather than via the intrinsic absorbance of the Si. The other NPs used in our study did not fluoresce or absorb at wavelengths monitored in the presented assays but they still affected the results, indicating other sources of assay interference.

2.3.3. Spectroscopic assays

Many spectroscopic protocols may not be appropriate for use in NP toxicity testing; every assay in the current study was affected by at least one NP formulation and each NP formulation tested, with the exception of ZnO, affected at least one assay (Figure 2-2, 2-3). There does not appear to be any obvious link between measured NP physicochemical properties and the observed interference with spectroscopic assays tested within.

Solely adding NPs to the assay components and performing the assay as suggested by the manufacturer led to substantially erroneous results. In many cases a substantial underestimation of toxicity occurs in the presence of NPs. Both the MTS and alamar blue assays were affected by exposure to NPs (Figure 2-2c,d). 100 mg/L CdSe and 100 mg/L RNT interfered with the MTS assay, calculating 547±224 and 1118±89 cells respectively (Figure 2-2c), and 100 mg/L CdSe and 100 mg/L TiO$_2$ affected the alamar blue assay (Figure 2-2d), reporting 1297±50 and 593±173 cells respectively, despite no presence of cells in the assay. These assays are often used as proxies of cytotoxicity, viability, or proliferation *via* cell counts; this type of data artefact could lead researchers to overlook a toxic

NP effect. Reports of protein concentration, as in the BCA assay, are often used to normalize values of enzyme activity and inaccurately high values can lead to an underestimation of damage. At relatively low concentrations, 1 mg/L Si (12±2 µg/mL), 10 mg/L Si (98±6 µg/mL) and 10 mg/L CdSe (13±2 µg/mL) interfere with the BCA protein assay (Figure 2-2a). An artefact in this assay would further exacerbate the problem if it was used in conjunction with other assays that are similarly affected by the presence of NPs. In other cases, we found that the presence of NPs in assays commonly used to test for oxidative stress caused effects. The activity of catalase in the presence of TiO_2 was inaccurately reported in both the fluorescence-measured assay (120±44 U/mL) and the absorbance-measured assay (110±22 U/mL) (Figure 2-2e,f). This finding is of substantial significance as oxidative stress is often reported as the main cause of *in vitro* toxicity associated with NP exposure (Nel *et al.* 2006). This leads to critical difficulties in differentiating between true oxidative stress and artefacts caused by NP-assay interference. It is clear from these data that NPs can interfere with the components of the assays themselves; however, these assays measure activity in an actual biological sample. Therefore, we assessed the validity of some of the assays under more realistic test conditions by addition of biological samples.

Identifying NP interference with assay reagents alone cannot always be used to predict interference under the final working conditions of the assay. We found that in some cases, addition of a protein (*i.e.,* BSA in the protein assays and catalase in the catalase activity assay), could either eliminate or enhance the interference observed when only assay reagents and NPs were mixed (Figure 2-3). The interference caused by 1 mg/L Si and 10 mg/L CdSe in the BCA assay (Figure 2-2a) is abolished by the addition of BSA (Figure 2-3a), and similarly, 100 mg/L TiO_2 effects in the catalase assay (Figure 2-2e,f) are abrogated in the presence of catalase (Figure 2-3d,e). Therefore, the use of these assays may be acceptable under these more realistic conditions. However, of concern is the incidence of erroneous results with the addition of sample. While NPs did not affect the Bradford assay with no protein present (Figure 2-2b), addition of 40 µg/mL of BSA with 10 mg/L CdSe over-estimated by 7±1 µg/mL BSA

concentration (Figure 2-3b). Similarly, RNT did not affect the catalase activity assay components themselves (Figure 2-2 f), but in the presence of catalase, an overestimation of 120±96 U/mL is observed (Figure 2-3e). The only case where NP interference with assay components alone was an accurate indicator of compatibility with the assay during practical use was the addition of 10 mg/L Si in the BCA assay (Figure 2-2a, 2-3a); NP incubated with assay components yielded a value of 98±6 µg/mL, and with the addition of BSA this value was 99±14 µg/mL. This suggests that simply performing controls with assay components and NPs alone may not be enough to confirm whether an assay is appropriate for use with NPs. Furthermore, there are many assays where running controls by the addition of sample is not possible due to the complex nature of the assay itself. Many assays used for cytotoxicity testing (*e.g.,* MTS and alamar blue) rely on live cells to metabolically convert dyes. It is experimentally difficult to reproduce these situations in order to perform accurate controls. In the case of the LDH cytotoxicity assay, we performed an analogous control by lysing cells to measure LDH activity (Figure 2-3c). We found that the presence of 1 mg/L Si resulted in a reported number of 7.4×10^6 cells, which was significantly lower than the actual 12.5×10^6 cells present (Figure 2-3c). In an experimental situation, this would have resulted in significant overestimates of cell death in NP-treated cells. Other studies suggest that this assay is susceptible to a number of different NPs (*e.g.s,* CdSe: MacCormack *et al*. 2007, soot, carbon, TiO_2 :Holder *et al.* 2012). However, we found that neither CdSe nor TiO_2 affected the assay in this instance. This may be attributed to differences in NP physicochemical characteristics between studies as well as our use of lysed cell preparations instead of purified LDH. Lysed cell preparations will contain a myriad of proteins and macromolecules that may bind the NPs and prevent interactions with LDH, a mechanism that will not be present in purified LDH samples.

NPs readily bind to various macromolecules and such interactions have been exploited in applications such as environmental remediation, imaging, and detection. It is clear from our data that these interactions may also affect the outcome of spectrophotometric assays. LDH assays have been shown to be

affected by NPs through the interaction of NPs with the LDH enzyme itself, causing adsorption and/or inactivation of the protein and an associated loss of activity (MacCormack *et al.* 2012; Holder *et al.* 2012). Electrostatic interactions between NPs and the components of the assays and biological samples are likely to occur (Lim & Zhong 2009; Manokaran *et al.* 2010). If electrostatic interactions were the main predictor of interference, we would expect to observe differences in interference between positively and negatively charged NPs. RNTs affect the final measurement of the negatively charged tetrazolium dye of the MTS assay (Berridge *et al.* 2005). We observed a false count of 1118±89 cells (Figure 2-2c) despite an absence of cells in the presence of these positively charged NPs. However, CdSe, a negatively charged NP, also affected the results significantly (547±224 cells) (Figure 2-2c). Further, RNTs do not always affect negatively charged dyes, as no interference was apparent with resorufin in the alamar blue assay (Figure 2-2d). These data suggest that interference cannot easily be predicted solely using the basic characteristics of the NPs (Holder *et al.* 2012).

Interestingly, we observed an increase in final absorbance or fluorescence in almost every assay when NPs were present. This suggests that NPs are interacting with the final form of the dyes in such a way as to enhance their absorbance or fluorescence, and/or that the NPs themselves are causing reduction of the dyes, leading to a higher concentration of the final form of the dye. Quenching of fluorescent dyes has been observed for alamar blue (Casey *et al.* 2007) and DCF dye, the final product of the oxidative stress marker dichlorodihydrofluorescein diacetate (H_2DCF-DA) (Kroll *et al.* 2012). On the contrary, incubation of either 100 mg/L CdSe or TiO_2 with alamar blue reagent resulted in much higher fluorescence than expected in the current study, reporting 1297±50 cells and 593±173 cells, respectively (Figure 2-2d), and was also observed with TiO_2 in the catalase assay (Figure 2-2e,f). Pfaller *et al.* (2010) observed a similar enhancement of DCFH-DA dye fluorescence in the presence of gold or iron oxide NPs. Free electron transfer from excited CdSe or TiO_2 semiconductor NPs may contribute to this phenomenon (Zhong 2009). Many assays are dependent on redox reactions to generate a colorimetric or fluorometric

signal, and the small size of metal NPs can enhance the reduction potential of these materials, which may allow NPs to reduce dyes in the absence of cellular activity (Mallick *et al.* 2006; Yang *et al.* 2009). For example, the BCA protein assay is dependent on the reduction of Cu^{2+} to Cu^+ by a protein. In the absence of protein, we hypothesize that NPs may drive this reduction, causing Cu^+-mediated dye interaction and resulting in erroneous protein concentration measurements. Metal NPs can catalyze redox reactions (Huang *et al.* 2005; Hikosaka *et al.* 2008), and this may account for some of the results presented here.

Differences in the nature and magnitude of NP-assay interference with and without protein present suggests strong interactions are occurring between NPs and proteins in the assay (Lundqvist *et al.* 2008). These interactions appear to alter the effects of NPs on assays and may further complicate the task of predicting and controlling for interference. NPs can change the conformation of proteins and decrease or even stabilize enzyme activity under denaturing conditions (Karajanagi *et al.* 2004; MacCormack *et al.* 2012). In addition, the presence of proteins can affect the stability and agglomeration state of the NPs themselves (Casals *et al.* 2010), which may influence the characteristics of NP exposure. Circular dichroism spectroscopy reveals that 100 mg/L Si binds to LDH and changes its native structure, subsequently altering the activity of the enzyme (MacCormack *et al.* 2012). However, this interaction is abolished with the addition of BSA, which likely binds the NPs and reduces associations with LDH (MacCormack *et al.* 2012). CNTs bind to phenol red, but in the presence of serum this association decreases significantly (Zhu *et al.* 2009b). In the current study, addition of protein and enzyme to the BCA and catalase assays may have decreased the availability of NPs to catalyze reduction of the dyes. However, in the case of the Bradford assay, none of the NPs tested affected the Bradford protein assay in the absence of protein (Figure 2-2b), but when 40 μg/mL BSA was added, the CdSe treatment falsely reported 46±1 μg/mL protein (Figure 2-3b). The CdSe were highly agglomerated (Table 2-1), and addition of protein may have led to dispersal and stabilization of the NPs in suspension, which could have increased NP binding to assay components (Kühnel *et al.* 2009; MacCormack *et*

al. 2012). Regardless of the mechanism at work, it is clear that NPs impact all of the assays investigated here and care must be exercised when using these methods for nanotoxicity testing.

2.3.4. Meta-analysis

Clearly, toxicological/biological studies require controls to validate whether a particular assay is appropriate for each NP formulation. Our analysis of the literature in 2010 demonstrates that ~84% of papers in the nanotoxicology field used at least one type of colorimetric or fluorescence assay and of these, ~95% were published without reporting controls for NP interference (Figure 2-4a). Even with an ever increasing number of published reports on NP-assay interference, this number has only marginally improved; a re-analysis of the literature in 2012 shows that ~90% of papers were published without some type of assay control (Figure 2-4a). Reporting in all areas monitored in this study was slightly improved in 2012 (Figure 2-4b). The common control performed was the addition of NPs to the assay components alone (2010: 5%, 2012: 8%), followed by measurement of the intrinsic fluorescence or absorbance of the NPs (2010: 2%, 2012: 5%), then with NPs and a biological sample (2010: 1%, 2012: 4%). The results of this study highlight the critical need for more stringent requirements for the use of these types of assays in nanotoxicity testing. The misinformation resulting from NP-assay interference has substantial implications for our understanding of, and confidence in the reported bioactivity of NPs. We believe that such problems have contributed significantly to the conflicting reports of NP toxicity in the literature.

2.3.5. Recommendations for future nanotoxicology studies

We suggest that more stringent controls be required for nanotoxicological studies and provide the following recommendations to minimize the potential for NP-assay interactions and associated aberrant results. Higher concentrations of NPs (>10 mg/L) have greater probability of interfering with assay function, and the use of such concentrations is not uncommon in toxicological studies. Therefore, NP concentration should be limited in the final sample, recognizing

41

that even with multiple washes and/or centrifugations NPs could remain within cells or bound to membranes. Furthermore, centrifugation can be counterproductive if NPs have bound to the assay components, inadvertently removing dyes and/or proteins essential for accurate readings (Holder *et al.* 2012). For all assays, controls should be measured with NPs and the assay reagents, and if possible, with the protein in question to determine if interactions will occur with these components. Given that we are currently unable to accurately predict how each NP will interact, it is imperative that each individual formulation be tested for compatibility with all assays used. Such quality control practices will allow for the appropriate interpretation and evaluation of published results and provide accurate scientific data for the establishment of regulations related to NP production, utilization, and disposal.

	Functionalization	Source	Hydrodynamic diameter (nm)[a]			Zeta potential (mV)[b]	
			1 mg/L	10 mg/L	100 mg/L	10 mg/L	100 mg/L
Si	undecylenic acid	Veinot[29]	151±2	150±1	147±2	-28±3	-43±6
CdSe	undecylenic acid	Veinot	181±12	240±8	703±13	-47±0	-52±2
TiO₂	polyacrylic acid	Vive Nano	118±13	109±1	150±1	-26±2	-31±1
ZnO	polyacrylic acid	Vive Nano	20±2	25±1	153±12	-30±5	-35±3
RNT	lysine	Fenniri[12]	344±200	544±334	N/A	77±4	73±4

Table 2-1. Physicochemical characterization of nanoparticles. [a] Hydrodynamic diameter as measured by DLS and reported as mean±standard error. [b] Zeta potential as measured by Zetasizer and reported as mean±standard error
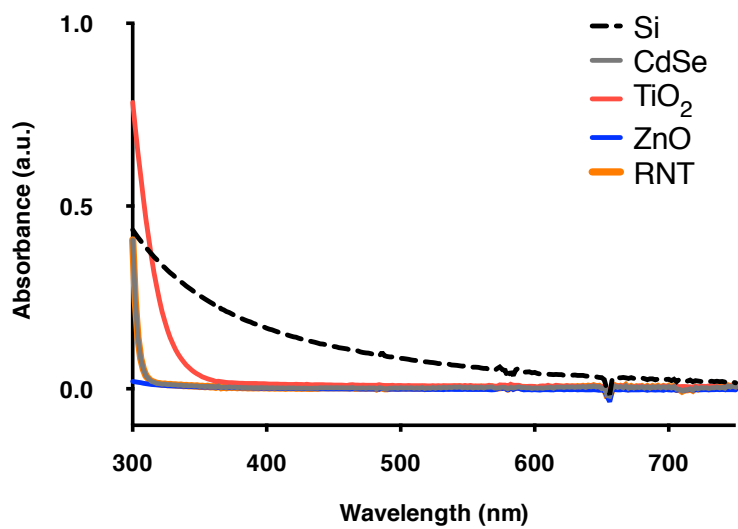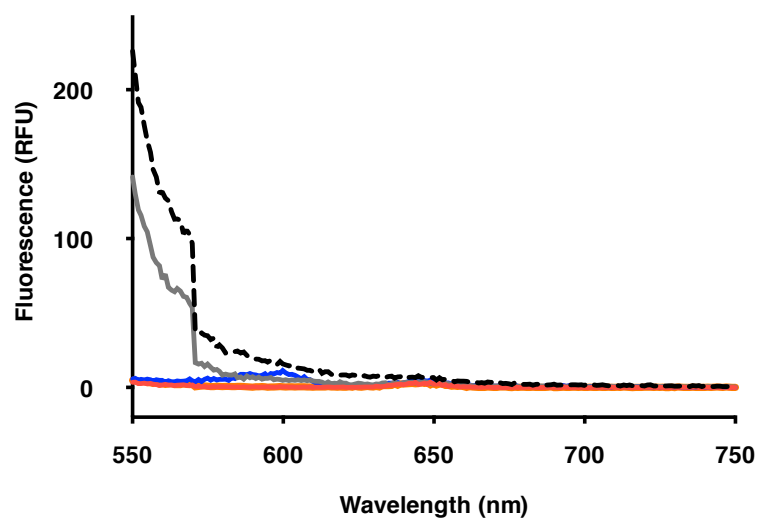
Figure 2-1. Spectroscopic measurement of the optical characteristics of nanoparticles. (a) Absorbance of nanoparticles; (b) Fluorescence (RFU) of nanoparticles (excitation, 531 nm).
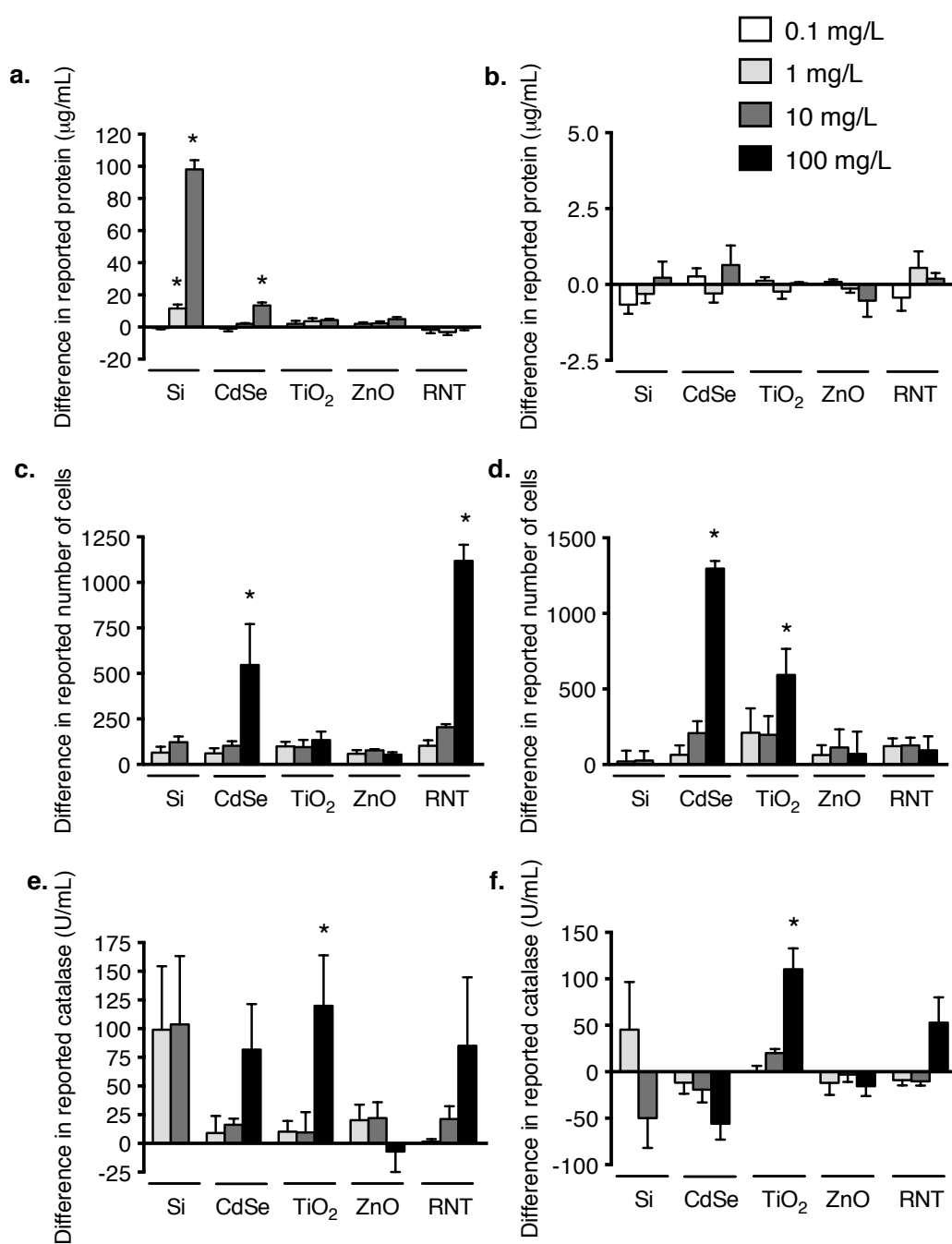
Figure 2-2. Nanoparticles interfere with the components of common biological assays. Assessment of nanoparticle interference with the dyes and molecules used in biological assays: (a) BCA (bicinchoninic) protein assay; (b) Bradford protein assay, (c) MTS (3-(4,5-dimethylthiazol-2-yl)-5-(3-carboxymethoxyphenyl)-2-(4-

sulfophenyl)-2H-tetrazolium) assay; (d) Alamar blue assay (excitation 531 nm, emission 595 nm); (e) Amplex red catalase assay (excitation 531 nm, emission 595 nm); (f) Amplex red catalase assay (emission 560 nm). * indicates significantly different than control ($p < 0.05$, ANOVA followed by Dunnett's post-hoc comparison).
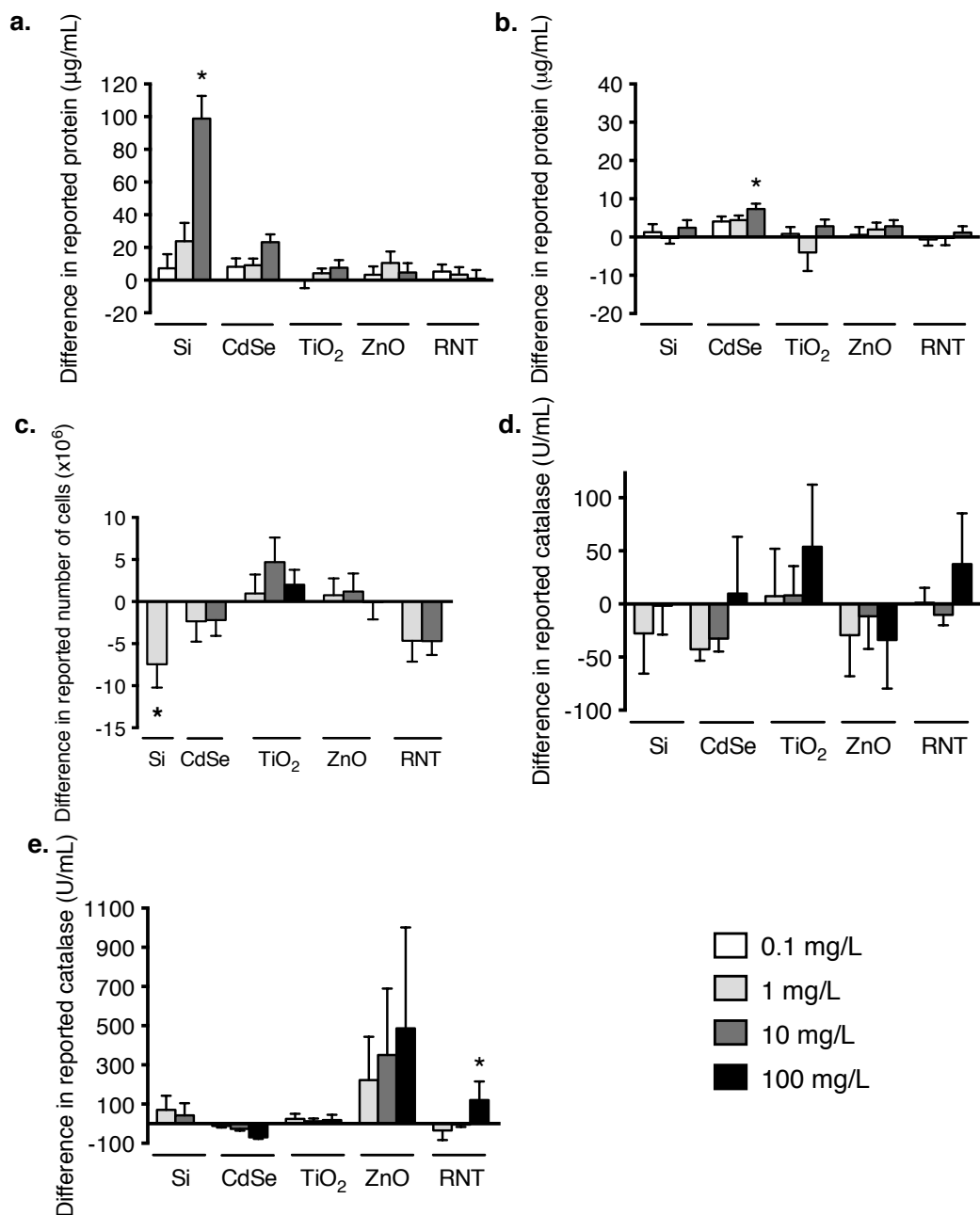
Figure 2-3. Nanoparticle interference can be influenced by addition of test sample. Assessment of nanoparticle interference with the addition of sample to a biological assay. (a) BCA protein assay with 250 μg/mL BSA addition; (b) Bradford protein assay with 40 μg/mL BSA addition; (c) LDH assay with 12.5x10^6 cells; (d) Catalase assay with 250 U/mL catalase addition (excitation 531 nm, emission 595 nm); (e) Catalase assay with 250 U/mL catalase addition

(absorbance 560 nm). * indicates significantly different than control (p<0.05, ANOVA followed by Dunnett's post-hoc comparison).
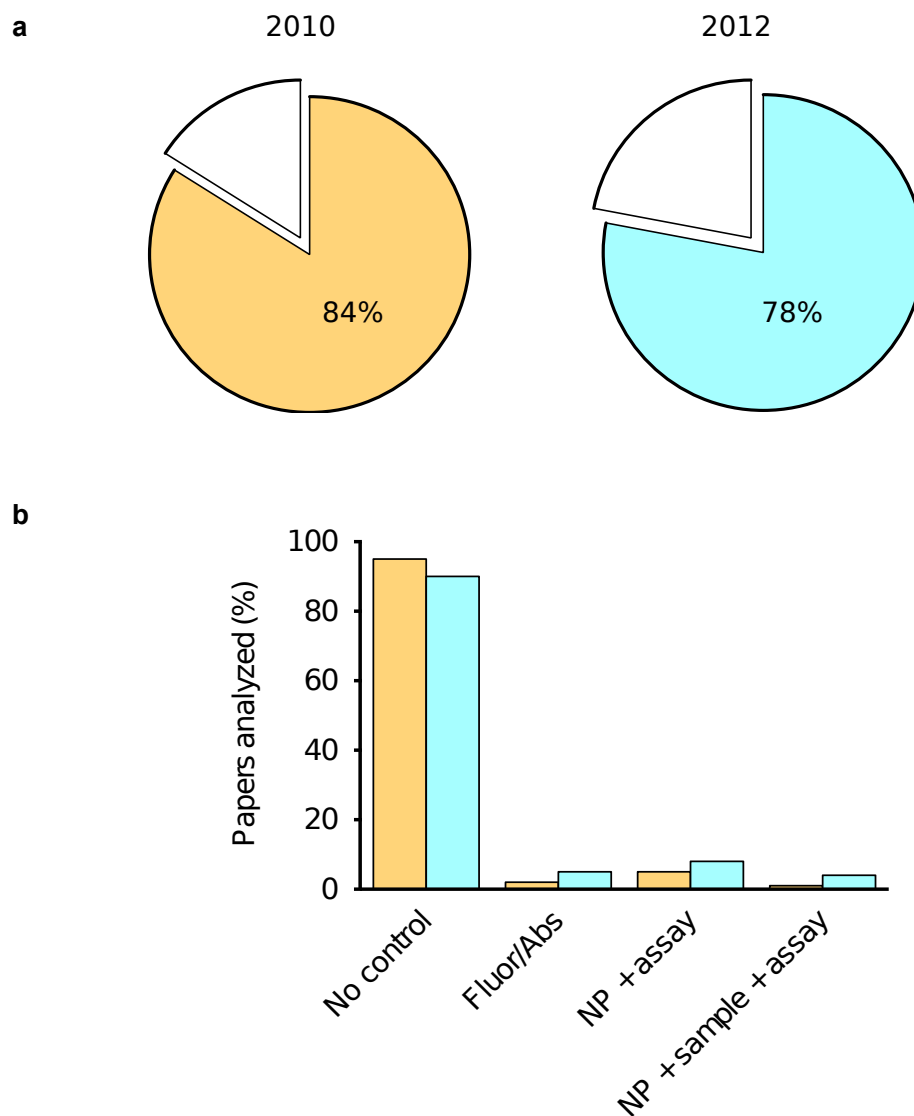
Figure 2-4. Meta-analysis of literature reveals that most published papers do not test for nanoparticle interference in absorbance- or fluorescence-based toxicity assays. (a) Percentage of papers that use a toxicity assay based on measurement of colorimetric or fluorescent change in 2010 and 2012; (b) Breakdown of controls performed in papers using one of these assays. (note: Percentages do not add up to 100% due to overlap in papers performing more than one control).

CHAPTER 3

Evaluation of silicon and cadmium selenide quantum dots: Biological effects *in vitro* and *in vivo*

3.1. INTRODUCTION

Quantum dot (QD) nanomaterials have great potential for use in biology and medicine in a number of applications. These semiconductor nanoparticles (NPs) are likely to replace traditional dyes and fluorescent proteins due to their broad adsorption and narrow emission bands, resistance to photobleaching, size-tunability to fluoresce in a range colours, straightforward production and functionalization techniques, and high luminescence output (Walling *et al.* 2009). Their unique electronic and optical qualities will result in extensive use for imaging, detection, and therapeutics (Li & Rothberg 2004; Clark *et al.* 2010; Wang *et al.* 2013). While QD cores can be composed of a number of different semiconductor materials, most studies have focused on QDs that incorporate cadmium (Cd) (Walling *et al.* 2009), a heavy metal known for its biological toxicity (Wright & Welbourn 1994). Many cadmium-core nanomaterial formulations have been shown to be cytotoxic (Shiohara *et al.* 2004; Kirchner *et al.* 2005; Ryman-Rasmussen *et al.* 2006; Cho *et al.* 2007) and have negative effects *in vivo* (King-Heiden *et al.* 2009). Cytotoxic effects of Cd NPs may be related to oxidative stress, endocrine disruption, mitochondrial effects, and DNA damage (Winnik & Maysinger 2012; Wang *et al.* 2013). In light of this hazard, alternative QD materials with lower potential for toxicity should be studied.

Silicon (Si) materials have been suggested to be a non-toxic alternative to Cd based materials. These nanomaterials possess advantageous qualities over conventional dyes and imaging agents and could theoretically replace CdSe NPs (Zhong 2009; Erogbogbo *et al.* 2011). A few studies have looked at crystalline Si NP toxicity *in vitro*, but it has not been studied in depth, likely due to the assumption that Si is inert. In general, little cytotoxicity has been reported at exposures to low concentrations (<50 mg/L) of Si NP; polyacrylic functionalized (Wang *et al.* 2013), unfunctionalized (Fujioka *et al.* 2008; Choi *et al.* 2009; Hanada *et al.* 2013), and drug conjugated (Hanada *et al.* 2013) Si NP exposures have not yielded cytotoxic effects.

Non-agglomerated, stable, and water soluble NPs have been produced by the Veinot group at the University of Alberta, and have the potential for use as a

replacement for Cd-based NPs (Clark *et al.* 2010). These NPs can be covalently bonded to different acid functionalizations, creating a range of different NPs with varied physicochemical properties (Clark *et al.* 2010). Surface modifications can alter properties such as size and aggregation characteristics (Clark *et al.* 2010), and differences in surface chemistries can alter uptake and toxicity (Hoshino *et al.* 2004; Verma & Stellacci 2010). We test the toxicity of Si NPs using zebrafish embryos and a range of vertebrate cell lines as some reports suggest that different cell lines may have different susceptibilities to NP exposures (Shiohara *et al.* 2004; Fernández-Cruz *et al.* 2012). We also tested the NPs in an *in vivo* aquatic model to explore how toxicity would be altered with increased biological complexity. Human Beas2B lung cells, human HepG2 liver cells, and catfish clonal 3B11 cells (an immunological model) were used for comparative *in vitro* tests. These represent a range of possible exposure conditions, such as *via* occupational inhalation, medical administration, and aquatic exposure (Erogbogbo *et al.* 2011; Clift 2012). Zebrafish embryos are used as sentinels for toxicants, and a well studied vertebrate model for developmental toxicity. Advantages of their use include high fecundity, relatively fast development, translucency during development, and ease of husbandry (Hill 2005). Very few studies have looked at *in vivo* toxicity of Si NPs (Yong *et al.* 2013), and no studies have been published regarding the toxicity of Si NPs to embryonic fish. These data will help fill in literature gaps regarding the biocompatibility and toxicity of Si NPs as a replacement of CdSe NPs.

3.2. MATERIALS AND METHODS

3.2.1. Cell maintenance and exposures

Catfish clonal B-cells (3B11) were maintained in AL-3 medium (equal parts AIM-V and/L5 Invitrogen Life Technologies), and supplemented with 1 μg/ml NaHCO$_3$, 50 U/ml penicillin, 50 μg/ml streptomycin, 20 μg/ml gentamicin, 50 μM 2-ME and 3% heat-inactivated catfish serum (Miller et al. 1994) and grown at 27°C. The human bronchial epithelial cell line (Beas-2B) and

the human hepatocellular carcinoma cell line (HepG2) were obtained from the American Type Culture Collection (ATCC). Cells were cultured in Dulbecco's Modified Eagle Medium (DMEM, Invitrogen Life Technologies) supplemented with 5% FBS, and maintained in an incubator at 37°C, 5% CO_2. Prior to use, all culture media was filter sterilized using 0.22 μm filters (Corning). 3B11 cells were seeded into 96-well plates at a density of 2.0×10^4 cells per well in 180 μL complete AL-3 media and incubated for 24 or 48 h with 20 μL 10x NP exposures before measurement. Beas-2B and HepG2 cells were plated into 96-well plates at a density of 5.0×10^3 cells per well in 100 μL of complete DMEM and incubated for 24 or 48 h at 37°C with 11 μL 10x NP treatments before assay measurements. All plates contained internal controls including no NP exposure well (only cells and media) and control wells (only media, no cells or NPs). Due to observations of media evaporation within the wells around the perimeter of the plates (particularly during 48 h exposures), the outside wells (*i.e.,* A 1-12, B-G 1&12, and H 1-12) were filled with 200 μL PBS and not used for any treatments or controls to avoid confounding effects.

3.2.2. Flow cytometry

After exposures, cells were rinsed 3 times in PBS and 0.5 μL of 100 μg/mL propidium iodide (PI) (prepared in PBS) was added to each well. PI is a fluorescent dye that intercalates with DNA, and is used as a marker of viability as it is not permeant in live cells. Cells were counted and measured for fluorescence staining in the FL-2 gate and viable cells were calculated as the number of alive cells (*i.e.,* those not stained with PI) in relation to the total number of cells. Cell counting was performed on a Cell Lab Quanta SC Flow Cytometer (Beckman Coulter) equipped with a single 488 nm argon laser.

3.2.3. CCK assay

A CCK-8 kit (Dojindo Molecular Laboratories, Kumamoto, Japan) was used according the manufacturer's instructions to measure metabolic activity. This kit uses 2-(2-methoxy-4-nitrophenyl)-3-(4-nitrophenyl)-5-(2,4-disulfophenyl)-2H-tetrazolium, monosodium salt (WST-8) dye that can permeate the cell wall. Once

inside metabolically active cells, WST-8 is reduced by dehydrogenases into orange coloured, water soluble formazan, and absorbance of the final form of the dye is measured. In brief, 10 μL of CCK-8 solution was added to the plate and incubated for 1 h at 37°C and measured at 450 nm in a microplate reader (Infinite M200, Tecan Inc., Switzerland). WST-8 does not affect the viability of cells, therefore wells were then measured using a PicoGreen Quant-iT counting kit (Invitrogen, CA, USA) to determine total DNA for standardization of metabolic activity to the number of cells. Media was removed and cells were rinsed three times with PBS, and 0.1% (v/v) Triton in deionized water was added to lyse the cells. Plates were shaken for 30 seconds, and after 30 min at 37°C, 50 μL of the lysed cells were transferred to a new 96-well plate and 50 μL of PicoGreen working solution was added. Plates were incubated for 5 min in the dark, and fluorescence was measured (435 nm excitation, 535 nm emission) on an Infinite M200 (Tecan Inc, Switzerland.). The cell metabolic rate was measured as a ratio of the absorbance readings between treated and control wells, after correction for blank absorbance readings of the control mixtures that were processed in the same manner as treatment wells. 10 mg/L of each side chain (acrylic acid, propionic acid, heptanoic acid, and decanoic acid) were tested for effects in Beas2B and HepG2 cells and not found to have any effects (Appendix V)

3.2.4. DFDA assay

Intracellular reactive oxygen species (ROS) was measured using the dihydrofluorescein diacetate assay (DFDA) (97%, Sigma-Aldrich, MO, USA). Non-fluorescent DFDA permeates live cells, is deacetylated by cellular esterases to a non-fluorescent compound, and then is oxidized by ROS present in the cell, transforming the dye into fluorescent dihydrofluorecein (DF). 1 mM DFDA stock was stored in 1x PBS at -80°C, then working stocks of 5 μM DFDA in PBS were made fresh for each experiment. 5 μL of 5 μM DFDA working solution was added to wells and plates were incubated (37°C, 5% CO_2) for 30 min in the dark. Cells were washed 3 times with PBS, and then fluorescence was immediately measured (excitation 492 nm, emission 517 nm) on an Infinite M200 spectrometer.

Fluorescence from control wells with only media and no cells were subtracted from treatments wells, and values were normalized to control wells (cells with no NP treatment) and expressed as fold increase.

3.2.5. Embryo toxicity study

Embryos were collected in petri dishes within 30 minutes of spawn from wildtype AB strain zebrafish. Eggs were rinsed three times with dechlorinated tap water (pH 7.5±0.5, 168±10 μS/cm, 28.5°C, general water hardness 180±8 ppm, and carbonate water hardness 103±5 ppm). Embryos were pipetted into 6-well plates, 30 embryos per well, and 5 mL of treatment solution was added to each well. Every plate contained one control well, and plates were only used if survival > 80%. Survival and hatch were evaluated at 24, 48, 72, and 96 hpf and dead embryos were immediately removed.

3.2.6. Zebrafish oxidative stress assays

For oxidative stress testing five embryos were collected at each time point (24 hpf, 48 hpf, and 72 hpf), rinsed 3 times in distilled water and homogenized in Tris EDTA. Homogenized solutions were spun at 10 000 rpm at 4°C for 15 minutes and supernatant was immediately frozen at -80°C. Catalase was indirectly measured with Molecular Probe's Amplex Red Catalase Kit (Molecular Probes, A22180) according to manufacturer's directions. In short, Amplex Red reagent reacts with H_2O_2 in a sample in the presence of horseradish peroxidase to produce a fluorescent product, resorufin. Catalase catalyzes the breakdown of H_2O_2 to water and oxygen, therefore an increase in catalase results in less fluorescence. Fluorescence was detected (excitation 535 nm, emission 595 nm) using a microplate reader (Wallac 1420, Perkin Elmer). The superoxide dismutase (SOD) determination kit (Fluka, 19160) was used to calculate SOD activity. SOD activity is indirectly measured by use of (2-(4-Iodophenyl)- 3-(4-nitrophenyl)-5-(2,4-disulfophenyl)- 2H-tetrazolium, monosodium salt (WST-1), whose reduction into a coloured formazan product is inhibited by the presence of SOD due to its catalysis of the reduction of the superoxide anion. The absorbance of the formazan

product therefore decreases with an increase in SOD, and this absorbance was measured at 450 nm in a microplate reader (Wallac 1420, Perkin Elmer).

3.2.7. Statistical analysis

All results are presented as mean ± standard error of the mean. All *in vitro* experiments were repeated three times, with three replicates per plate. *In vivo* experiments were repeated five times per treatment. Data was analyzed using ANOVA followed by a Tukey's multiple comparison test. Results were considered significant if $p \leq 0.05$. Data are reported as the mean ± SEM.

3.3. RESULTS AND DISCUSSION

We investigated the basic toxicity of various Si and CdSe NPs, and found that Si NPs may be a practical alternative to CdSe NPs, as they do not demonstrate appreciable responses associated with toxicity at the same dose as CdSe NPs. None of the Si formulations affected cell viability in either the fish or mammalian cells (Figure 3-1, 3-2, 3-3), in agreement with literature (Wang *et al.* 2012; Hanada *et al.* 2013). Unfunctionalized hydride-terminated Si NPs are cytotoxic at higher concentrations (≥ 50 mg/L) (Fujioka *et al.* 2008; Choi *et al.* 2009; Hanada *et al.* 2013), however, these NPs were more likely to be oxidized, and do not closely resemble the stable acid-functionalized NPs used in this study (Clark *et al.* 2010). In contrast, 10 mg/L CdSe NPs were acutely toxic to the fish cells, reducing the number of viable cells to 26.1 ± 9.9 (x10^3), compared to 49.9 ± 6.3 (x10^3) cells in controls (Figure 3-1). However, this trend was not found for the mammalian cells (Figure 3-2, 3-3). Contrary data regarding the comparable sensitivity of fish and mammalian cells lines exist; heightened (Raisuddin & Jha 2004), reduced (Fernández-Cruz *et al.* 2012), and comparable (Castaño & Gómez-Lechón 2005) sensitivity have been reported. Differences in metabolic rate, DNA repair, and ability to counter oxidative stress can account for different sensitivities between cell lines (Raisuddin & Jha 2004). Furthermore, the agglomeration and dissolution of the NPs can affect piscine and mammalian cells lines by different

mechanisms (Fernández-Cruz *et al.* 2012), and likely played a role in this study, as the media composition was unique to each cell line.

At present, there is no consensus as to whether Cd-based QDs are safe to use; reports of QD cytotoxicity indicate that effects are altered in a number of conditions and also by the physicochemical characteristics of the NPs themselves. For example, oxidative conditions alter CdSe toxicity in hepatocytes (Derfus *et al.* 2004), different surface chemistries can change toxicity in murine macrophage-like cells (Clift *et al.* 2011) and rat kidney fibroblasts (Kirchner *et al.* 2005). Similarly, size can change subcellular distribution and subsequent metabolic activity of CdTe NPs in rat pheochromocytoma cells and microglial cells (Lovrić *et al.* 2005). The dissociation of free metal from the NP core is often suggested as the main cause of CdSe NP toxicity (Kirchner *et al.* 2005; Chen *et al.* 2012; Wang *et al.* 2013). Oxidation of the surface or exposure to UV may lead to release of free Cd and result in higher toxicity (Derfus *et al.* 2004). We ruled out that the likelihood that the CdSe NPs used in this study were substantially dissolving due to the incongruent results between CdSe NP exposures and the significant effect of all 10 mg/L CdCl$_2$ exposures. In later experiments, we tested the dissolution rates of the CdSe and Si NPs by dialysis, and found that the materials we use are quite stable and release very low levels of free metal (see Chapter 5). To reduce aging and oxidation of the NPs, these NPs were stored in the dark, and under argon. Passivation of the surface and alterations of free metal dissociation may have also occurred; NPs have strong affinities for serum and other small molecules present in exposure medium. These interactions can change the surface structure of the NPs, alter molecular and biological interactions, and reduce dissolution, thus affecting their toxic potential (Kirchner *et al.* 2005; Zhu *et al.* 2009b; Jones & Grainger 2009; Lynch *et al.* 2009).

Exposure to QDs can lead to the onset of oxidative stress, leading to harmful effects on cellular function (Clift *et al.* 2010; Yong *et al.* 2013; Wang *et al.* 2013). The DFDA assay did not detect any ROS differences in cells exposed to Si NPs (Figure 3-4). In Beas2B cells, 10 mg/L of both CdSe-3 and CdSe-6 decreased ROS to 72±9% and 69±10% of control fluorescence, and 1 mg/L and

10 mg/L CdCl$_2$ also resulted in 64±13% and 40±18% decrease (Figure 3-4), indicating effects on cellular oxidative balance. This finding is in contrast to the majority of studies reporting an increase of ROS upon exposure to NPs in the same time period and measured with similar methods (Lovrić *et al.* 2005; Chan *et al.* 2006; Cho *et al.* 2007; George *et al.* 2011). Exposure to ionic Cd^{2+} can inhibit cellular respiration and destabilize mitochondrial membrane potential, leading to a decreased ROS production (Belyaeva *et al.* 2008). Perturbations in mitochondrial membrane potential (George *et al.* 2011) and alterations in mitochondrial morphology (Lovrić *et al.* 2005) can result from exposure to Cd-based NPs, and they may affect ROS production in a similar manner to ionic Cd^{2+}. However, if this were the case, then mitochondrial activity as measured by the CCK assay (Figure 3-2), should be affected. No significant effects were observed during exposure to CdSe NPs at 24 or 48 h (Figure 3-2), indicating conflicting data. It is possible that the assays used to test toxicity may be significantly affected by the NPs themselves, as is discussed further below, and in Chapter 2.

Studies on the toxicity of Si NPs *in vivo* have so far been limited to mammalian studies. In these studies, injected Si NPs were not overtly toxic, nor do they induce pathological changes in mice (Park *et al.* 2009; Erogbogbo *et al.* 2011). We determined if Si NPs were toxic to zebrafish embryos upon aquatic exposure, which could occur, for example, at point source production or in the case of an accidental spill. All formulations of Si NPs were not acutely toxic in zebrafish, and in fact were less toxic than the silicic acid control (Figure 3-5). Zebrafish hatch may be affected by NP exposure (Zhu *et al.* 2009a), but we did not observe any delay in hatching rate (Figure 3-6). While we do not present data for CdSe exposure here, later experiments showed that CdSe does delay hatch, leading to toxicity within the chorion (Chapter 3-5). Other studies have shown that exposure to CdSe NPs induce morphological abnormalities and increased mortality in zebrafish (King-Heiden *et al.* 2009; George *et al.* 2011).

While Si NPs did not result in acute toxicity, exposure to 1 mg/L Si-11 did increase levels of SOD at 24 h (Figure 3-6) to 2.8±0.3 fold over control fish, indicating elevated oxidative stress. Elevated SOD is commonly reported as a sign

of sublethal toxicity in NP-exposed fish (Zhu *et al.* 2008; Ramesh *et al.* 2012). Of the four Si NPs tested here, Si-11 were the most stable and disaggregated, with a hydrodynamic diameter of 18.2 nm while Si-3, Si-5, and Si-7 measured 116.4, 130.8, and 103.7 nm respectively (Clark *et al.* 2010). This may result in the Si-11 NPs being the most bioavailable to the zebrafish embryos, and the most likely to interfere with physiological function, although this remains to be demonstrated. An increase of SOD activity is often associated with an increase of catalase activity, as SOD catalyzes the transformation of superoxides into oxygen and hydrogen peroxide, which is then converted into oxygen and water by catalase. However, in our exposures, there was no significant increase in catalase activity over the 72 h exposure (Figure 3-7). A possible explanation for this finding could be due to an artifact of the assay itself. After this series of experiments were completed, we discovered that many commonly used assays used to assess toxicity could be affected by NPs. Oxidative stress assays and other fluorescence- or absorbance-based assays appear to be affected by NP-interference, and this topic is explored in detail in Chapter 2. Neither Si nor CdSe NPs affected the catalase assay (Chapter 2), but the SOD assay was not tested with these NPs, and we no longer have these QD formulations on hand to run these controls. Even Si NPs did not cause acute toxicity, further study of the sublethal effects of Si NP is warranted.

In general, the Si and CdSe NPs did not result in acute toxicity both *in vitro* and *in vivo*, and it is still unclear whether these QDs can cause sublethal effects. Further studies on the mechanisms by which QDs can affect aquatic organisms need to be further explored. Negatively charged NPs such as those used in this experiment may be less likely to adsorb to negatively charged biological membranes due to electrostatic repulsion (Ruizendaal *et al.* 2009). Despite this, negatively charged NPs still can get endocytosed by cells (Ryman-Rasmussen *et al.* 2006; Zhang & Monteiro-Riviere 2009; Park *et al.* 2011; Wang *et al.* 2012), and may localize within lysosomes and endosomes, near the nucleus, or in the cytoplasm ((Ryman-Rasmussen *et al.* 2006; Zhang & Monteiro-Riviere 2009; Park *et al.* 2011). The stability of the NPs may differ once endocytosed (Zhang &

Monteiro-Riviere 2009; Shiohara *et al.* 2011) and NPs could dissolve and release metal ions. My attempts to visualize and measure fluorescent QDs within zebrafish embryos and cells failed due to high intrinsic autofluorescence masking the potential QD signal (Appendix VI), and limited resolution compared to the small size core size of these NPs (Appendix IV). Other attempts using techniques such as 14C-radiotracer labeling, ICP-MS, Raman spectroscopy, 2-photon microscopy to measure of adsorbed and/or translocated NPs were unsuccessful (not shown). Further experiments determining whether these QDs can translocate across membranes *in vivo*, and whether negative charge prevents uptake are needed.

Some indications that aquatic animals may be more susceptible to NPs than those reported in mammalian literature were observed. Although these NPs are primarily proposed for mammalian use, aquatic contamination must be considered. Few specific conclusions can be made regarding the toxicity of QDs in *in vitro* and *in vivo* systems, especially given that physicochemical properties of NPs can change drastically in different aquatic media. The minimal lethality of both the Si and CdSe nanomaterials used in this study suggests that any stable QDs may be suitable for acute use in certain conditions. However, despite this fact, the release of Cd ions, a known toxicant, will be a concern where direct human contact occurs (*e.g.,* medical diagnostic imaging), and in cases where aging and weathering may lead to the release of Cd ions over time. Therefore, the study and development of Cd-free materials such as Si nanomaterials is worthwhile and should be explored in greater depth, especially in *in vivo* systems once the detection systems for Si NPs become more advanced and refined.
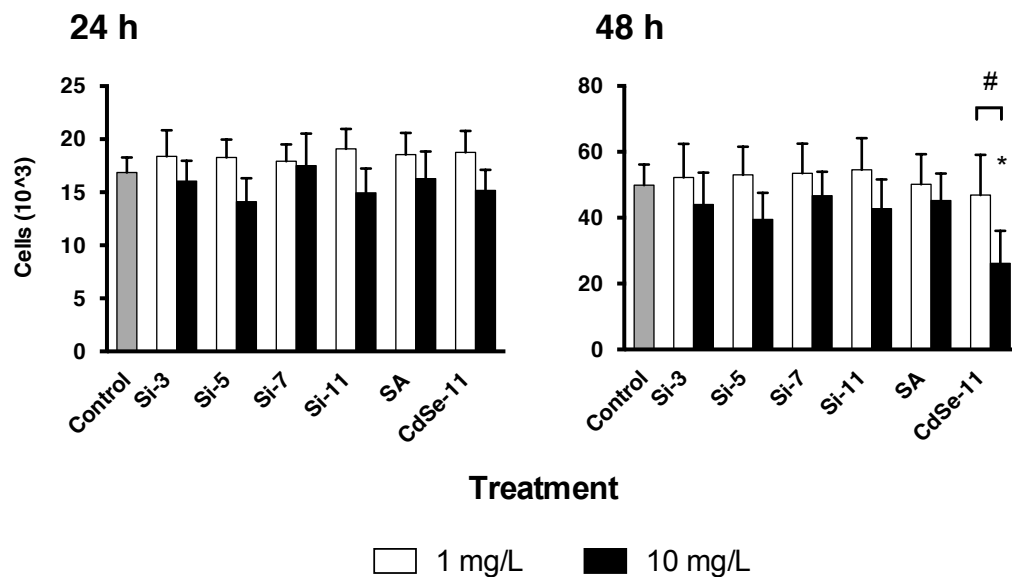
Figure 3-1. Effect of carboxylic acid functionalized silicon NPs (Si-#), silicic acid (SA), and mercapto-undecylenic acid functionalized cadmium selenide NPs (CdSe-11) on catfish B-cell (3B11) growth, as quantified by propidium iodide staining and measured with a flow cytometer after 24 and 48 h exposures. * denotes significantly different ($p<0.05$) than control, and # denotes difference between concentrations of the same nanoparticle.
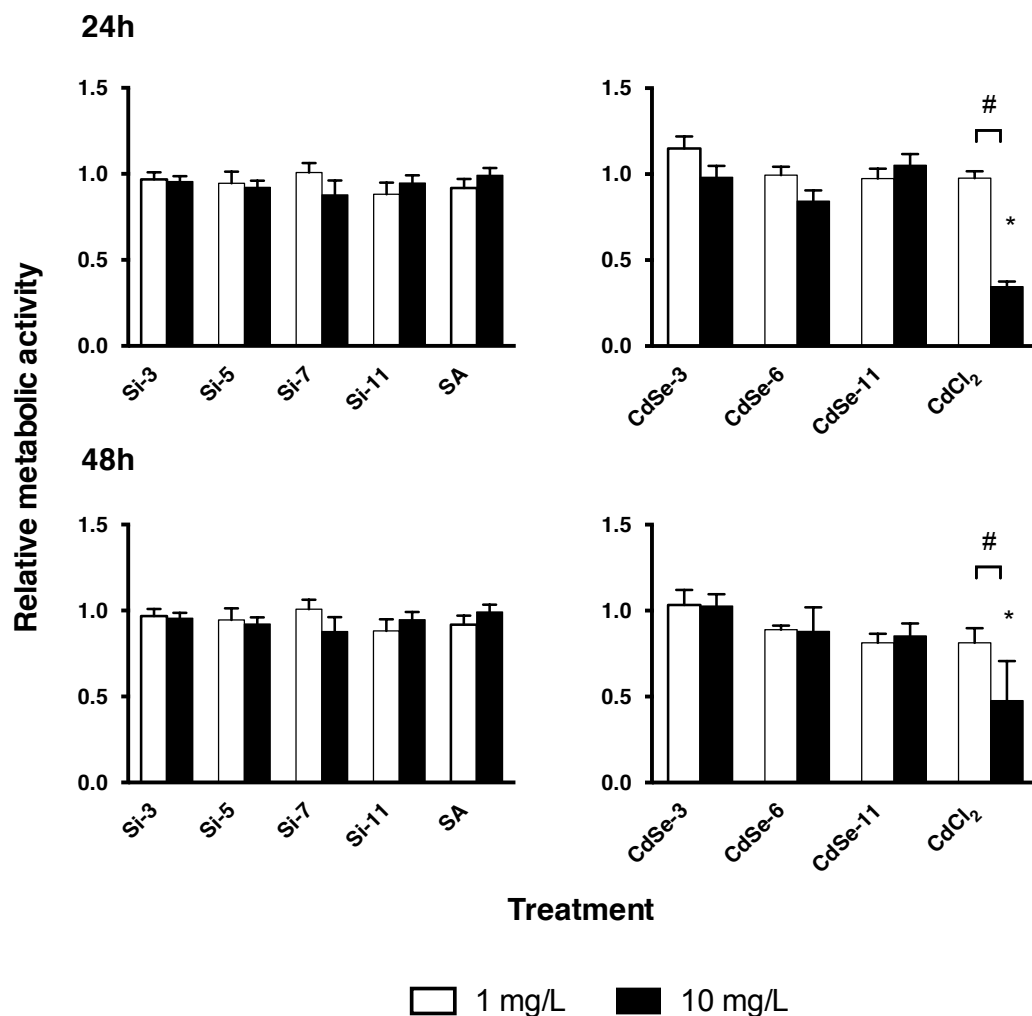
Figure 3-2. Effect of carboxylic acid functionalized silicon (Si-#) and cadmium selenide (CdSe-#) NP on metabolic activity of human lung epithelial cells (Beas2B) after 24 and 48 h as measured by the CCK assay as compared to non-exposed cells. * denotes significantly different ($p<0.05$) than control, and # denotes a significant difference between concentrations of the same nanoparticle.
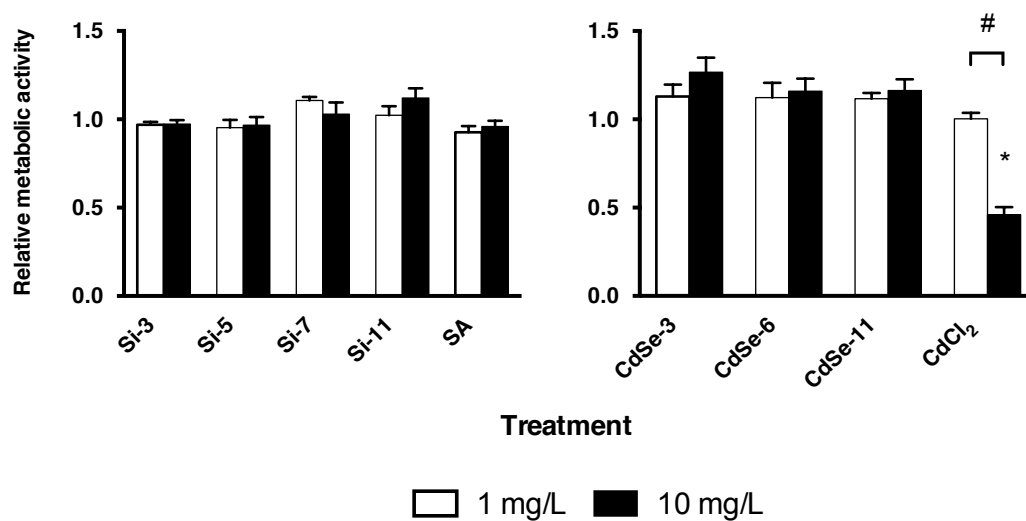
Figure 3-3. Effect of carboxylic acid functionalized silicon (Si-#) and cadmium selenide (CdSe-#) NP on metabolic activity of human liver cells (HepG2) after 24 as measured by the CCK assay and normalized to non-exposed cells. * denotes significantly different ($p<0.05$) than control, and # denotes a significant difference between concentrations of the same nanoparticle.

a. Beas2B

b. HepG2

☐ 1 mg/L   ■ 10 mg/L
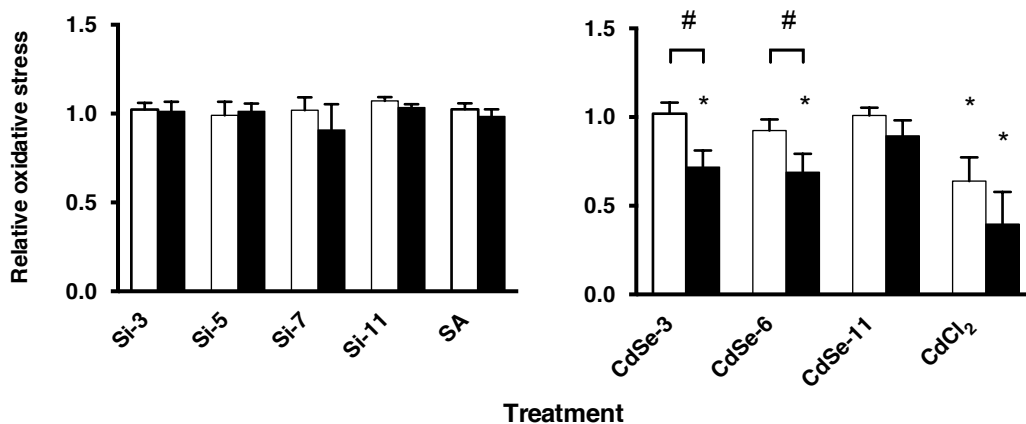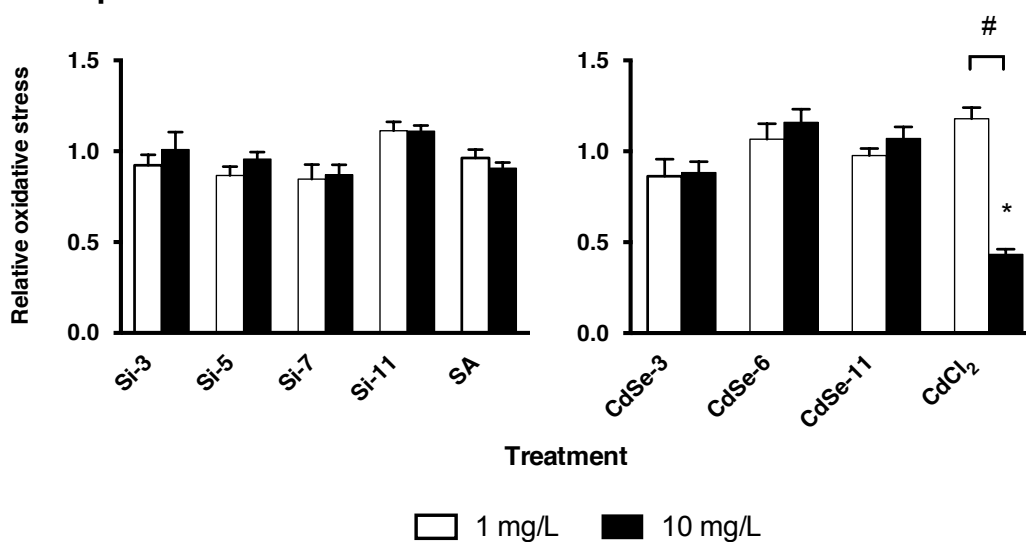
Figure 3-4. Effect of carboxylic acid functionalized silicon (Si-#) and cadmium selenide (CdSe-#) NP on reactive oxygen species' production on (a) Beas2B and (b) HepG2 cells after 24 has measured by the DFDA assay and normalized to non-exposed cells. * denotes significantly different ($p<0.05$) than control, and # denotes a significant difference between concentrations of the same nanoparticle.
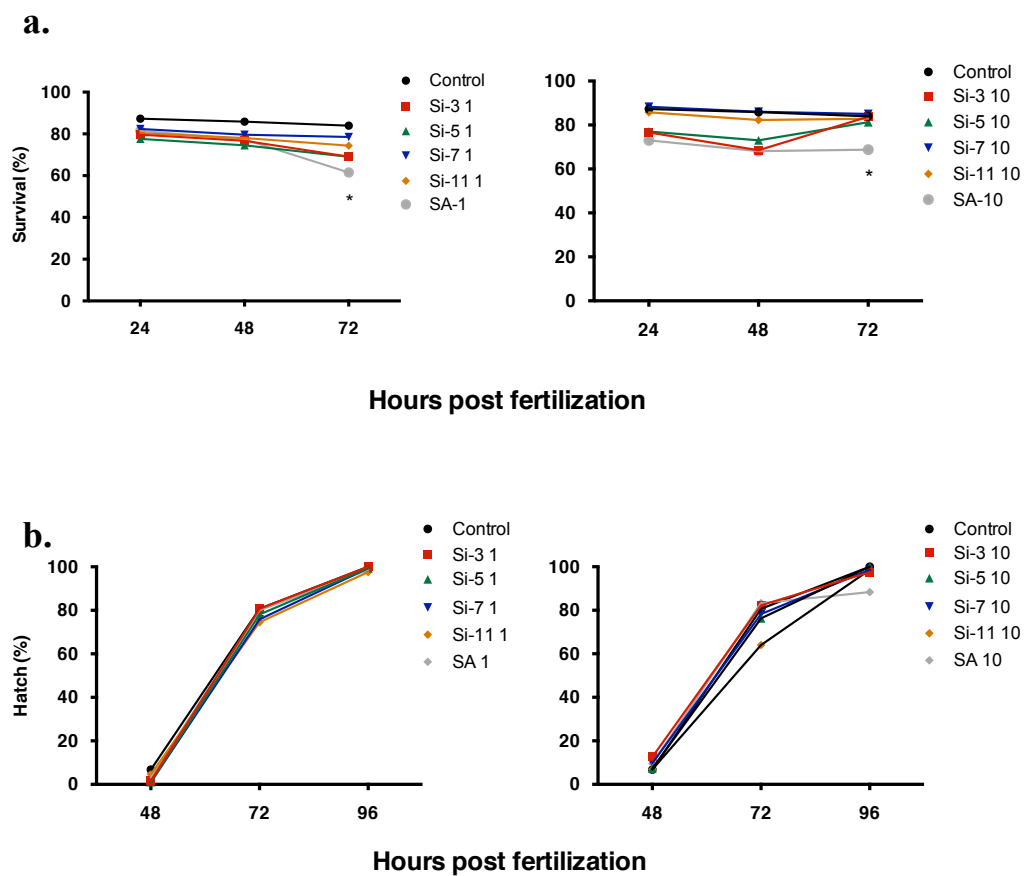
Figure 3-5. Effect of carboxylic acid functionalized 1 mg/L (Si-# 1) and 10 mg/L (Si-# 10) silicon nanoparticles on (a) zebrafish survival over 72 h and (b) zebrafish hatch over 96 h. * denotes significantly different ($p < 0.05$) than control.
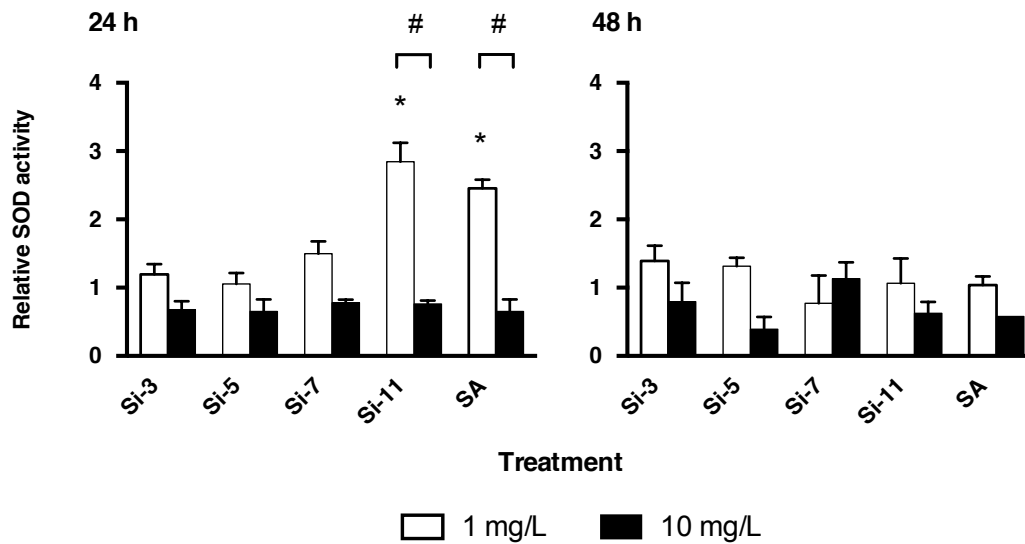
Figure 3-6. Effect of carboxylic acid functionalized silicon NPs on superoxide dismutase activity in whole zebrafish embryos at 24 and 48 h, as normalized to non-exposed embryos. * denotes significantly different ($p<0.05$) than control, and # denotes a significant difference between concentrations of the same nanoparticle.
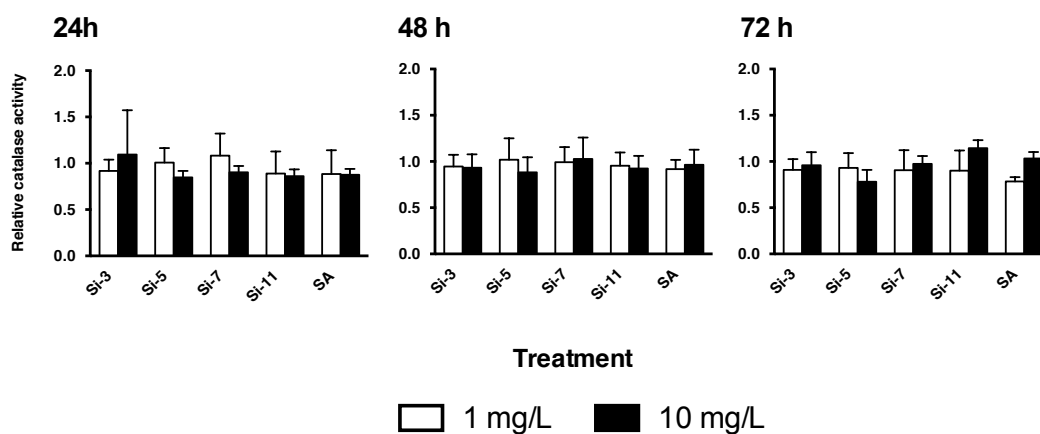
Figure 3-7. Effect of carboxylic acid functionalized silicon on catalase activity in whole zebrafish embryos at 24, 48 and 72 h, as normalized to non-exposed embryos. No significant differences were detected.

CHAPTER 4

Comparison of the toxicity of different-shaped hydroxyapatite nanoparticles *in vitro* and *in vivo*

4.1. INTRODUCTION

Hydroxyapatite has been widely used as a bone substitute due to its bioactivity, mechanical properties and similar composition to bone mineral (Paul & Sharma 1999; Takeda *et al.* 2002; Kim & Park 2005; Li *et al.* 2007). In recent years, its biomedical applications have expanded to the field of drug delivery, where hydroxyapatite nanoparticles (HAP NPs) are used as carriers for pharmaceutical molecules (Ong *et al.* 2007), bio-imaging moieties (Wang *et al.* 2006; Han *et al.* 2008; Yang *et al.* 2008), and other therapeutic agents (Paul & Sharma 1999; Lin *et al.* 2006). Such particulate systems for drug delivery have enhanced bioavailability, predictable therapeutic responses, greater efficacy and safety, and can provide controlled release (Palazzo *et al.* 2005). Although the employment of HAP in the biomedical field is showing great promise, rigorous assessment of its toxicity is still critical before it can be a suitable candidate for biomedical applications.

There are some reports that evaluate the *in vitro* toxicity of HAP, with a particular focus on mammalian cells (Harada *et al.* 1998; Albrecht *et al.* 2009; Motskin *et al.* 2009). In a recent study, particle size of HAP was found to induce different toxic effects to lung epithelial BEAS-2B cells (Zhao *et al.* 2011b). Mouse macrophage RAW264.7 cells incubated with needle-shaped HAP were found to express the highest level of TNF-α compared with rod- or plate-shaped HAP (Scheel *et al.* 2009). Furthermore, Li *et al*. (2008) reported that the proliferation of malignant melanoma cells was affected by HAP.

While *in vitro* studies on HAP toxicity have been reported in the literature, *in vivo* models remain the gold standard for toxicological evaluations. However, few reports currently exist in the literature. This creates a gap regarding how *in vitro* toxicity results of HAP can reliably be translated into *in vivo* outcomes to determine the safety of HAP. Although toxicological evaluation of higher order organisms is desirable, such models are expensive, difficult to handle, and economically unjustifiable for the number of NPs that require investigation. The ability to mimic higher order organisms through *in vitro* models is also difficult

due to the complex nature of the biological interactions that are involved (Hertog 2005; Hall *et al.* 2007; Teraoka *et al.* 2008). A rapid, high-throughput, cost effective, readily accessible and reliable *in vivo* model that has a good correlation with *in vitro* models would be advantageous for comprehensive toxicological assessment of NPs. The use of zebrafish has been suggested as an alternate model for mammalian studies (Zon & Peterson 2005).

Zebrafish have proven to be a prospective vertebrate model in exploring human disease, development, and physiology (Parng 2005) due to their high degree of homology to the human genome and comparable human tissue types (Zon & Peterson 2005; Pyati *et al.* 2007). Zebrafish embryos are transparent, thereby allowing for direct optical observation of their internal organs (Hill 2005). Their synchronous and rapid post-fertilization development of the embryos makes this model ideal for developmental assessments over a short period of time (Hill 2005). In addition, their sensitivity to chemical exposure and ability to absorb molecules through their skin and gills make zebrafish embryos a viable model for evaluating the toxicity of NPs (Parng 2005; Hill 2005). The applicability of such models in evaluating nanotoxicity has recently been validated by Xia *et al.* (2006), who reported correlations between findings on the toxicity of Fe-doped ZnO NPs in rodent lungs and zebrafish gills.

The objective of this study was to evaluate the toxicity of different shapes of HAP using both *in vitro* and *in vivo* models of fish origin and to compare the effects to mammalian cell response. Two different shapes (rod and needle) of HAP were evaluated *in vitro* on catfish B-cells (3B11) and catfish T-cells (28s.3), and *in vivo* in zebrafish embryos. Cytotoxicity tests were conducted using a metabolic activity assay (MTS) and a viability-staining assay (PI staining). In addition, fluorescein isothiocyanate (FITC) was tagged to HAP for *in vitro* cellular uptake studies. For *in vivo* studies, zebrafish embryos were monitored for death, deformation and hatch rates.

4.2. MATERIALS AND METHODS

4.2.1. Characterization of HAP materials

Information on the synthesis of HAP materials can be found in Appendix I. All HAP samples were characterized using X-ray diffraction (XRD) and Fourier-transformed Infrared Spectroscopy (FTIR). Particle size, shape and hydrodynamic sizes were evaluated using TEM and DLS, respectively. Specific surface areas were determined by the Brunauer-Emmett-Teller (BET) method. All characterization tools and parameters were similar to that reported previously.

4.2.2. Cell maintenance

Catfish 3B11 (B-cell like) and 28s.3 (T-cell like) cells were maintained in 25 cm^2 cell culture flasks and passaged whenever 70-80% confluence was attained, approximately every 2–4 days. Cells were cultured in AL-3 media containing 225 mL AIM V medium, 225 mL/L5 medium, 3 % (v/v) catfish serum, 0.5 g sodium bicarbonate, 0.5 ml 2-ME (0.05 M), 2.5 ml penicillin:streptomycin (Pen/strep) solution and topped up to 500 ml with DI water before incubating within a humidified incubator (37 ºC, 5 % CO$_2$).

4.2.3. Cytotoxicity assays

The effects of HAP on cell viability were determined using both the MTS assay (Cell Titer 96 Aqueous Non-Radioactive Cell Proliferation Assay [Promega, WI, USA]) and propidium iodide (PI) staining. The MTS assay is based on cellular metabolic activity, which involves reduction of the stable tetrazolium salt MTS to a soluble yellow formazan product by viable, respiring cells. Cells were seeded in 96-well plates at a density of 20,000 cells/well in 180 µl cell culture medium and 10-300 mg/L 10x HAP was added. The same concentration of HAP particles in cell culture medium was used as a control to account for background absorption caused by HAP particles. After a 24 h exposure, 40 µl MTS working solution was added to each well and incubated for 3 h (37 °C, 5% CO$_2$). Subsequently, absorbance (Ab) readings were measured at 490 nm using a microplate reader (Wallac 1420, Perkin Elmer). The absorbance of wells

containing only cell culture medium was used as background control, while cells without nHA were used as negative control. The metabolic activity (%) of cells was calculated based on the following formula:

Viability % = 100% x (Ab of nHA treated cells – Ab of particle control)/(Ab of negative control – Ab of background control).

PI is a DNA binding dye that intercalates double stranded DNA. The fluorescence intensity of DNA bound by PI is proportional to the quantity of DNA. Cells were stained with 3.5 mg/L and 2.0 mg/L PI diluted in AL-3 media for 3B11 and 28s.3 cells respectively. Flow cytometry was performed on Cell Lab Quanta SC Flow Cytometer (Beckman Coulter) equipped with a single 488 nm argon laser. PI fluorescence intensity was measured in the FL-2 gate.

4.2.4. Nanoparticle-cell interaction

Particle-cell interaction was investigated using flow cytometry (Cell Lab Quanta SC Flow Cytometer (Beckman Coulter). Cells were seeded at 20,000 cells/well in a 96-well plate and incubated with HAP-NDF and HAP-RDF (100 mg/L) for 1 h, 4 h, 6 h and 24 h respectively. Phosphate buffered saline (PBS) was added (200 μl) to wash the cells three times. Subsequently, cells were centrifuged and the medium was aspirated. Flow cytometric data was analyzed with Cell Lab Quanta SC MPL Analysis (Beckman Coulter). The content of the fluorescent dye FITC was quantified for NDF and RDF based on the fluorescent spectra. The fluorescence intensities obtained from flow cytometry were normalized based on the calculated FITC content per unit mass, so that fluorescent measurements can be directly correlated to cellular association with the particles.

4.2.5. Zebrafish embryo exposures

For *in vivo* studies, fertilized sphere stage embryos (4-6 hours post fertilization, hpf) were distributed into 96-well cell culture plates (one embryo/well). The water was removed and different concentrations of nanoparticles (3, 10, 30, 100 and 300 mg/L) in dTW were added to the wells and incubated for 120 h at 28.5 ℃. Embryos were checked daily for survival,

morphology abnormalities and hatch. Tests were repeated twelve times (36 embryos per concentration). Zebrafish embryos incubated in dTW (without nHA) served as control. Mortality was recorded after 24, 48, 72 and 120 hpf. Hatching rate was expressed as the number of embryos that hatched after 72, 80 and 96 hpf, in comparison to the total embryo number. Morphological changes were imaged by a stereomicroscope (Discovery V8, Zeiss) and photographed with a DFC 420C camera (Leica).

4.2.6. Measurement of particle dissolution

Dialysis tests were carried out to ascertain particle dissolution from *in vitro* and *in vivo* test solutions. Depending on the tests (i.e., *in vitro* or *in vivo*), HAP was incubated in either AL-3 at a concentration of 100 mg/L for 24 h, or in dTW of same concentration for 120 h before dialysis. 0.5 ml of incubated solution was then injected into a 7000 MWCO dialysis cassette (Slide-A-Lyzer, Thermo Scientific). This cassette was spun slowly in 50 mL DI water for 2 h, and the solution sent for inductively coupled plasma mass spectrometry analysis (ICP-MS) (Elan 6000 ICP-MS, Perkin Elmer) to measure for calcium and phosphate.

4.2.7. Statistical analysis

All experiments were conducted in triplicate and the data are expressed as mean ± standard deviation. Statistical analysis of the data was carried out using ANOVA, followed by Tukey's multiple-comparison post hoc test. These tests were performed using SPSS software, version 11.5. Differences were considered statistically significant when the $p \leq 0.05$. Data are reported as the mean ± SEM.

4.3. RESULTS AND DISCUSSION

4.3.1. HAP synthesis, characterization and stability in media

In this study, rod (RD) and needle-shaped (ND) HAP (with and without FITC) were synthesized. TEM micrographs showed HAP with homogeneous shapes and with a narrow size distribution (Figure 4-1a). Successful tagging of

FITC on HAP was shown using FTIR and fluorescent spectra (Figure 4-1b). The hydrodynamic size of HAP was determined using DLS at the highest and lowest study concentrations. HAP was found to be relatively stable in AL-3 (10 and 300 mg/L HAP-RD were 161±3 and 150±6 nm, and HAP-ND were 201±2 and 256±6 nm, respectively) likely due to stable steric repulsion, provided by the adsorption of serum protein (Wassell *et al.* 1995; Nghiem *et al.* 2010; Zhang *et al.* 2011) (Table 4-1). Severe agglomeration of HAP was observed in dechlorinated tap water, and hydrodynamic diameter of 300 mg/L HAP-RD and HAP-ND reached 3766±147 and 4957±236 nm, respectively. This agglomeration was moderated at lower concentrations, and at 3 mg/L HAP-RD and HAP-ND decreased to 316±19 and 394±45 nm. The difference in particle shape resulted in different specific surface area measurements, of which a lower specific surface area was obtained for HAP-RD (23.3 cm^2/g) as compared to HAP-ND (74.9 cm^2/g). The ζ-potentials of HAP samples were all slightly negative in DI water, with negligible difference between HAP-RD and HAP-ND. FITC-tagged HAP samples (termed HAP-RDF and HAP-NDF) were slightly more negatively charged due to surface adsorption of the anionic FITC. All particle characterization results are summarized in Table 4-1.

Reports suggest that the dissolution of HAP increases the concentrations of calcium and phosphate ions in the culture medium and result in toxic effects.[14] Therefore, dissolution of calcium and phosphorus from HAP in both AL-3 and dTW was measured by ICP-MS and compared to concentrations from AL-3 or dTW without HAP. Interestingly, regardless of media, the concentrations of calcium and phosphate were consistently lower for media that contained colloidal HAP over control (media without HAP) (Table 4-2). This decrease in Ca and P content in AL-3 and dTW suggests the physisorption of Ca^{2+} and PO_4^{3-} ions on HAP, rather than the dissolution of HAP as previously expected. Any toxicity could therefore be directly related to the NP *per se*, rather than their dissolution products. This physisorption of Ca^{2+} and PO_4^{3-} is intriguing as it raises the possibility that other micronutrients could be adsorbed onto the nanomaterials in solution. This sorption phenomenon has been reported to both impair enzyme

function (MacCormack *et al.* 2012) and also remove folic acid as a micronutrient from cell media (Guo *et al.* 2008).

4.3.2. Effects *in vitro*

In vitro studies were conducted on cells of teleost origin, the channel catfish (*Ictalarus punctatus*). After 24 h exposure at varying doses, cell viability was measured and the results obtained from PI staining assay are shown in Figure 4-2a (3B11) and 2c (28s.3). As a non-permeate dye that can only penetrate the membranes of dying/dead cells, the DNA content measured by PI staining is directly correlated to the number of dead cells within the culture and compared with negative controls (Figure 4-2a,c). Cellular metabolic activity (MTS assay) was also measured and the results were normalized against cell viability and expressed as specific metabolic activity, as shown in Figure 2b (3B11) and Figure 2d (28s.3). Both cell- and particle shape-dependent cytotoxicity were observed. HAP did not significantly affect the viability of catfish B cells (3B11) and T cells (28s.3) after 24 h incubation for concentrations from 10 to 300 mg/L (Figure 4-2a,c). This is comparable to mammalian cell HAP exposure studies, in which BEAS-2B, RAW264.7, and HepG2 (Zhao *et al.* 2011b), microvascular endothelial cells (CVECs) (Pezzatini *et al.* 2005), and rat macrophages (Albrecht *et al.* 2009) did not undergo loss of cell viability. HAP-ND was consistently found to exhibit higher inhibition to the specific metabolic activity compared with HAP-RD in both 3B11 and 28s.3 cells (Figure 4-2b,d). These results mirror the results as shown in mammalian BEAS-2B cell, but are contrary to the lack of NP effects on metabolic activity in RAW264.7 exposure to needle-shaped HAP (Zhao *et al.* 2011b). Such varied sensitivity of cell lines has been reported in heavy metal toxicity studies (Tan *et al.* 2008). Gülden *et al.* (2005) found that cell lines derived from either fish or mammals were equally sensitive in gauging cytotoxic effects using certain metrics. However, measurement of activity using MTS may be strongly affected by both the metabolic rate and the increased doubling time of the fish cells, therefore comparisons may be skewed (Raisuddin & Jha 2004; Gülden *et al.* 2005).

Cell-particle interactions were investigated using flow cytometry. It is not known whether these interactions occurred on the surface of the cell or due to intracellular uptake. These NPs are likely not strongly bound to the membrane due to their almost neutral charge (Verma & Stellacci 2010), and washes performed during this experiment presumably removed adsorbed NPs. A rapid decrease in fluorescent intensity in HAP-RDF exposed cells compared to HAP-NDF exposed cells, especially in 3B11s between 4 and 6 h of incubation time and between 1 and 4 h in 28s.3 cells (Figure 4-3) was seen. This decrease in fluorescent intensity of HAP-RDF suggests either a fast intracellular dissolution or prompt exocytosis. After uptake, HAP can be sequestered in the lysosome and the acidic pH may cause the NPs to dissolve (Motskin *et al.* 2009). The dissolution of HAP in the lysosome would increase intracellular calcium concentration, and affect cellular metabolism. Inhibition of metabolism was seen in HAP-ND exposures (Figure 4-2b,d), indicating that these NPs may have dissolved within the cell. However, HAP-RD did not affect metabolic rate, and instead may have been exocytosed.

Particle size and shape could affect uptake, exocytosis, and influence membrane interaction (Chithrani & Chan 2007; Aaron *et al.* 2010). Aspect ratio, or the ratio of maximum to minimum diameter of the NPs, can govern the speed of uptake of a NP in a cell (Aaron *et al.* 2010; Meng *et al.* 2011). Rod shaped quantum dots (QD) with aspect ratio of 2.0 diffused slower in the plasma membrane than spherical QD with aspect ratio of 1.2 and 1.6 (Aaron *et al.* 2010). Mesoporous silica NPs (MSNP) with an aspect ratio of 2.1 to 2.5 were found to be uptaken in larger quantities compared to shorter or longer length MSNP rods (Meng *et al.* 2011). Rod shaped HAP (lower aspect ratio) have higher uptake rates than needle shaped HAP (higher aspect ratio) by mammalian BEAS-2B and RAW264.7 cells (Zhu *et al.* 2012a). In this study, the observation that significantly more rod shaped NPs were internalized by the cell at 4h (Figure 4-3a) suggests that the uptake of HAP is influenced by aspect ratio. Also, the higher specific surface area of the needle shaped NPs (Table 4-1) may lead to higher blockage of receptor sites and reduce the chance of internalization (Chithrani &

Chan 2007; Aaron *et al.* 2010). These results demonstrated a shape-dependent effect of uptake and toxicity *in vitro*.

4.3.3. Effects *in vivo*

The toxicity of HAP to zebrafish embryos was studied by observing toxicological endpoints up to a period of 120 hpf. A concentration range of 3 to 300 mg/L was used to allow for comparison of *in vivo* results with *in vitro* studies, despite the fact that this would be an unlikely concentration encountered by fish in the natural environment. At 24 and 120 hpf, the embryonic mortalities induced by exposure to HAP were recorded and it was found that HAP exposure did not lead to embryo death, in concurrence with the *in vitro* results.

Hatching rate was also recorded and hatching delay was observed at 72 hpf (Figure 4-4). Interestingly, this hatching delay was concentration- and shape-dependent. When incubated at normalized 28.5 ºC freshwater condition, control zebrafish embryos hatched from their chorion between 48 and 72 hpf. However, zebrafish embryos exposed to HAP had a significant delay in hatching compared to the control groups at 72 hpf (Figure 4-4a). Normal hatching rate was restored by 80 hpf (Figure 4-4b) and all embryos hatched out at 96 hpf (Figure 4c). For example, at 72 hpf, 75±11% of control embryos had hatched, whereas only 30±8% of embryos exposed to HAP-RD at 3 mg/L hatched. Subsequently (80 hpf and beyond), the hatching rate for embryos exposed to HAP finally reached 100% hatch at 96 hpf. It has previously been reported that zebrafish embryos show delayed hatching when exposed to single wall carbon nanotubes and ZnO NPs (Cheng *et al.* 2007; Bai *et al.* 2009). While most studies show increased effects with higher NP concentration, the lowest concentration (3 mg/L HAP-ND) caused the highest hatching inhibition (17±0%) at 72 hpf (Figure 4-4), and no significant hatching delay was observed at other concentrations. Comparatively, HAP-RD inhibited hatch at all tested concentrations (Figure 4-4), and the lowest hatching rate (30±8% and 29±6%) was still found at the lowest particle concentrations, 3 and 10 mg/L respectively. At 3 mg/L the HA NPs are much less agglomerated in dTW (Table 4-1), increasing the likelihood of translocation through the 0.5-0.7

μm chorionic pores, and getting trapped in the chorionic space (Lee *et al.* 2007), whereas at higher concentrations the NPs may not be able to pass through the chorion (Rawson *et al.* 2000). Protein-NP interaction studies have shown that NPs can have high adsorption affinity for proteins (Fei & Perrett 2009; MacCormack *et al.* 2012). There is potential for NPs to interact with the zebrafish hatching enzyme, a metalloprotease released from the hatching gland and crucial to the digestion and weakening of the chorion at hatch, and is explored more in depth in Chapter 5. Adsorption of HAP to the hatching enzyme could result in conformational changes, leading to hindered function of the enzymes (MacCormack *et al.* 2012). The high specific surface area of HAP-ND (74.88 cm^2/g) might increase the chance of enzyme adsorption (Lynch & Dawson 2008) and thereby could result in a lower hatching rate as compared to HAP-RD (23.33 cm^2/g). The hatching delay effect did not influence the hatching success rate and survival of the exposed embryos, and all HAP-exposed embryos eventually hatched out at 96 hpf (Figure 4-4c). While a delay in zebrafish hatch may not be immediately comparable to mammalian studies, this is an interesting result as it highlights the need to consider NP-specific effects, namely the ability of NPs to bind to proteins and affect their function.

The hatched embryos from the control group appeared normal throughout the study period. However, there was an obvious developmental delay for larvae whose embryos were incubated with HAP-ND. This is in good agreement with the hatching results (Figure 4-4), as 3 mg/L HAP-ND caused the most significant developmental delay, as observed at 72 hpf. The developmental delay was also observed with embryos incubated with 3 mg/L HAP-RD. The highest concentration exposures did not display significant inhibition on the larvae development compared with controls. At 120 hpf, ca. 75% of the embryos incubated with 300 mg/L HAP-ND had a bent spine (Figure 4-5). Exposure to various metals and NPs have been shown to cause axial curvature (*e.g.,* heavy metals (Jezierska *et al.* 2008), cadmium selenide NPs (King-Heiden *et al.* 2009), platinum, and silver NPs (Bar-Ilan *et al.* 2009; Asharani *et al.* 2011)). Impairment of cardiac function, interference with somite formation, and oxidative stress have

all been hypothesized to contribute to axial deformation (Chow & Cheng 2003; King-Heiden *et al.* 2009; Liu *et al.* 2010). The high incidence of morphological malformation caused by HAP-ND at 300 mg/L may be related to the depression in cell metabolic activity seen *in vitro* in catfish cells under the same exposure concentration.

4.3.4. Conclusion

We conclude that there is a shape-dependent influence on HAP toxicity. Needle-shaped HAP was found to inhibit metabolic activity of catfish B cells (3B11) and T cells (28s.3), especially at the highest concentration of 300 mg/L. The time-dependent HAP/cell interaction revealed that the cytotoxicity may be caused by dissolution or slow exocytosis. Interestingly, both needle-shaped and rod-shaped HAP delayed zebrafish embryo hatching. Approximately 75 % of embryos had malformed spines when exposed to HAP-ND at 120 hpf, which could indicate sublethal toxicity specific to this shape. The consistent sublethal toxic effects observed from *in vitro* and *in vivo* models showed a general correlation between these two studies. Exposure to the lowest concentration of HAP (3 mg/L) induced the highest inhibition to zebrafish embryo hatch at 72 hpf and most obvious effects on embryo development. The results suggest that the smaller agglomerates of HA NPs may cross the chorion and interact with the embryo.

Table 4-1. Hydrodynamic size, polydispersity index (PDI), ζ-potential, and specific surface area of the rod and needle-shaped hydroxyapatite (HAP-RD and HAP-ND) and FITC-conjugated HAPs (HAP-RDF and HAP-NDF) in AL-3 media and dechlorinated tap water (dTW).

NP	Hydrodynamic size (nm)				Polydispersity index				ζ-potential (mV)	Surface area (cm^2/g)
	AL-3		dTW		AL-3		dTW			
	10 mg/L	300 mg/L	3 mg/L	300 mg/L	10 mg/L	300 mg/L	3 mg/L	300 mg/L		
HAP-RD	161±3	150±6	316±19	3766±147	0.29±0.004	0.27±0.02	0.22±0.03	0.26±0.07	-5.7±0.6	23.3
HAP-ND	201±2	256±6	394±45	4957±236	0.27±0.02	0.25±0.03	0.41±0.08	0.24±0.15	-4.8±0.3	74.9
HAP-RDF	175±5	187±2	327±12	4388±151	0.26±0.003	0.17±0.01	0.25±0.08	0.29±0.04	-9.7±0.3	
HAP-NDF	199±7	237±2	355±24	6012±124	0.34±0.001	0.24±0.09	0.37±0.05	0.05±0.08	-14.2±0.4	

Table 4-2. Calcium and phosphate content determined by ICP-MS after 24 h dispersion in AL-3 and after 120 h dispersion in dTW.

NP	AL-3 (mg/L)		dTW (mg/L)	
	Ca	P	Ca	P
Control	0.418	0.108	0.146	<DL
HAP-RD	0.366	0.024	0.115	<DL
HAP-ND	0.391	<DL	0.112	<DL
HAP-RDF	0.367	0.011	0.151	<DL
HAP-NDF	0.356	0.050	0.126	<DL
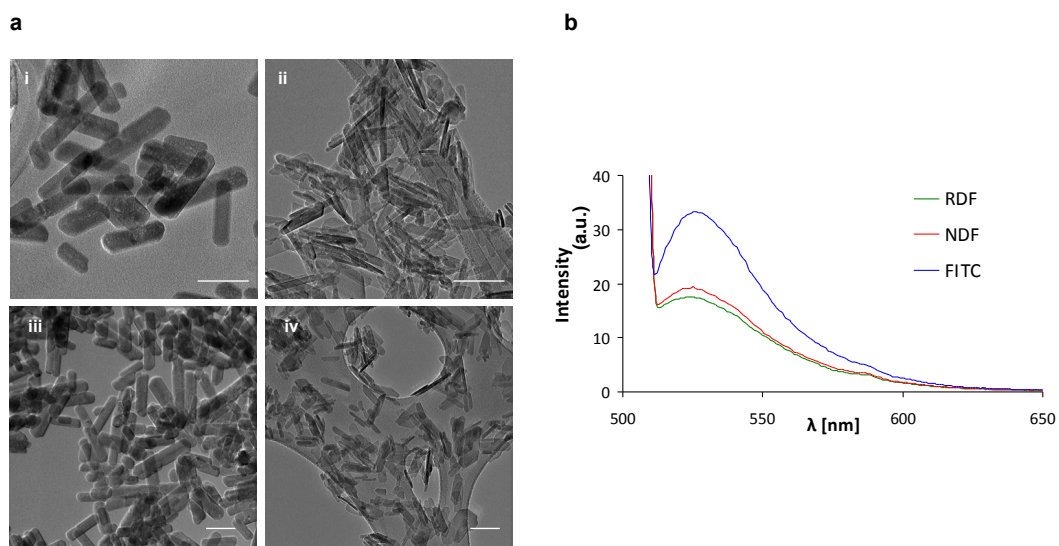
Figure 4-1. (a) Transmission electron micrographs of nanoparticles showing their size and shapes. (i) rod-shaped hydroxyapatite; (ii) needle-shaped hydroxyapatite; (iii) FITC-tagged rod-shaped hydroxyapatite; and (iv) FITC-tagged needle-shaped hydroxyapatite. Scale bars represent 100 nm. (b) Fluorescent emission spectra of FITC, RDF and NDF in ethanol with excitation wavelength at 501 nm.
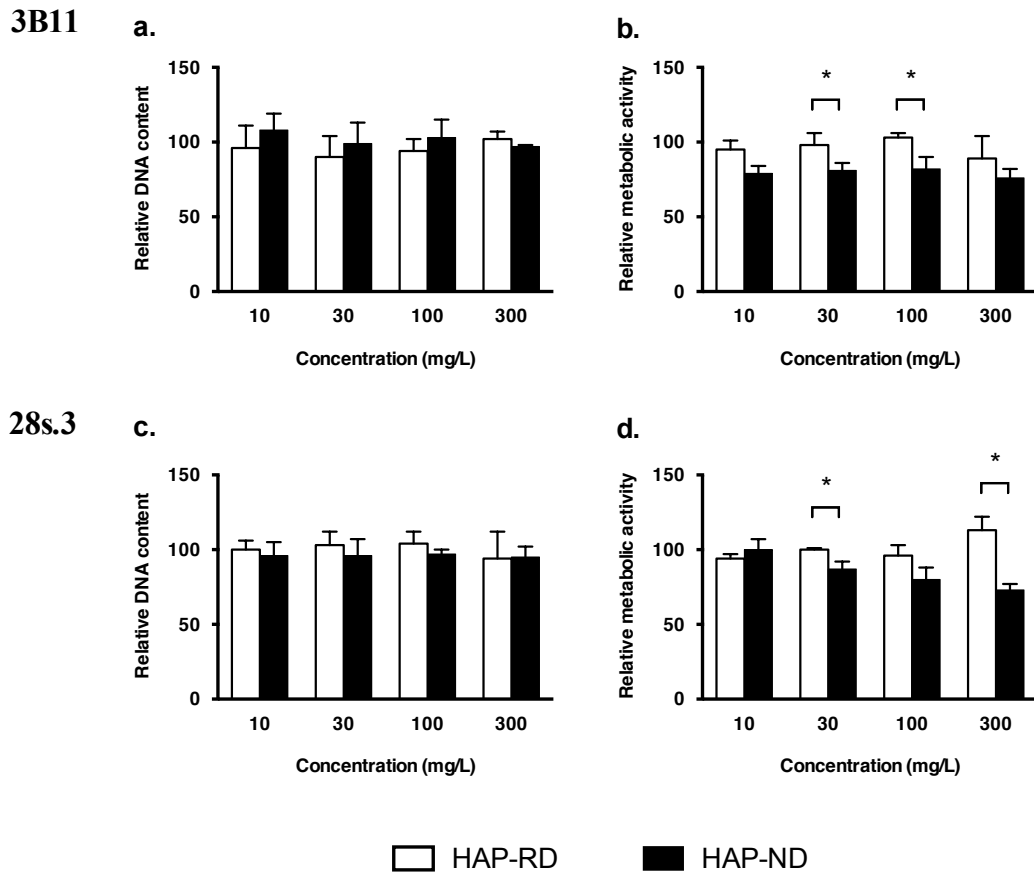
Figure 4-2. Cell viability, as quantified by the PI staining assay (a, c), and specific metabolic activity as quantified by the MTS assay and normalized to cell viability (b, d) after 24 h of 3B11 and 28.s3 cells after exposure to HAP-RD and HAP-ND at 10, 30, 100, and 300 mg/L. * indicates significant difference between HAP-RD and HAP-ND at the same concentration ($p < 0.05$).
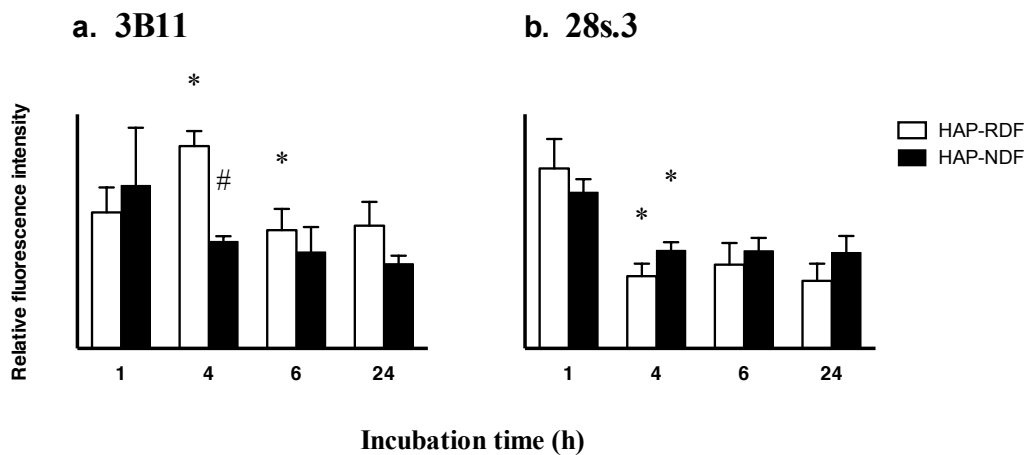
Figure 4-3. Flow cytometry data of FITC-tagged HAP-cell association. (a) 3B11 cells and (b) 28s.3 cells were incubated with 100 mg/L of RDF and NDF for 1, 4, 6 and 24 h. * indicates a significant difference in fluorescence from the preceding time point, and # indicates a significant difference between HAP-RDF and HAP-NDF at the same incubation point.
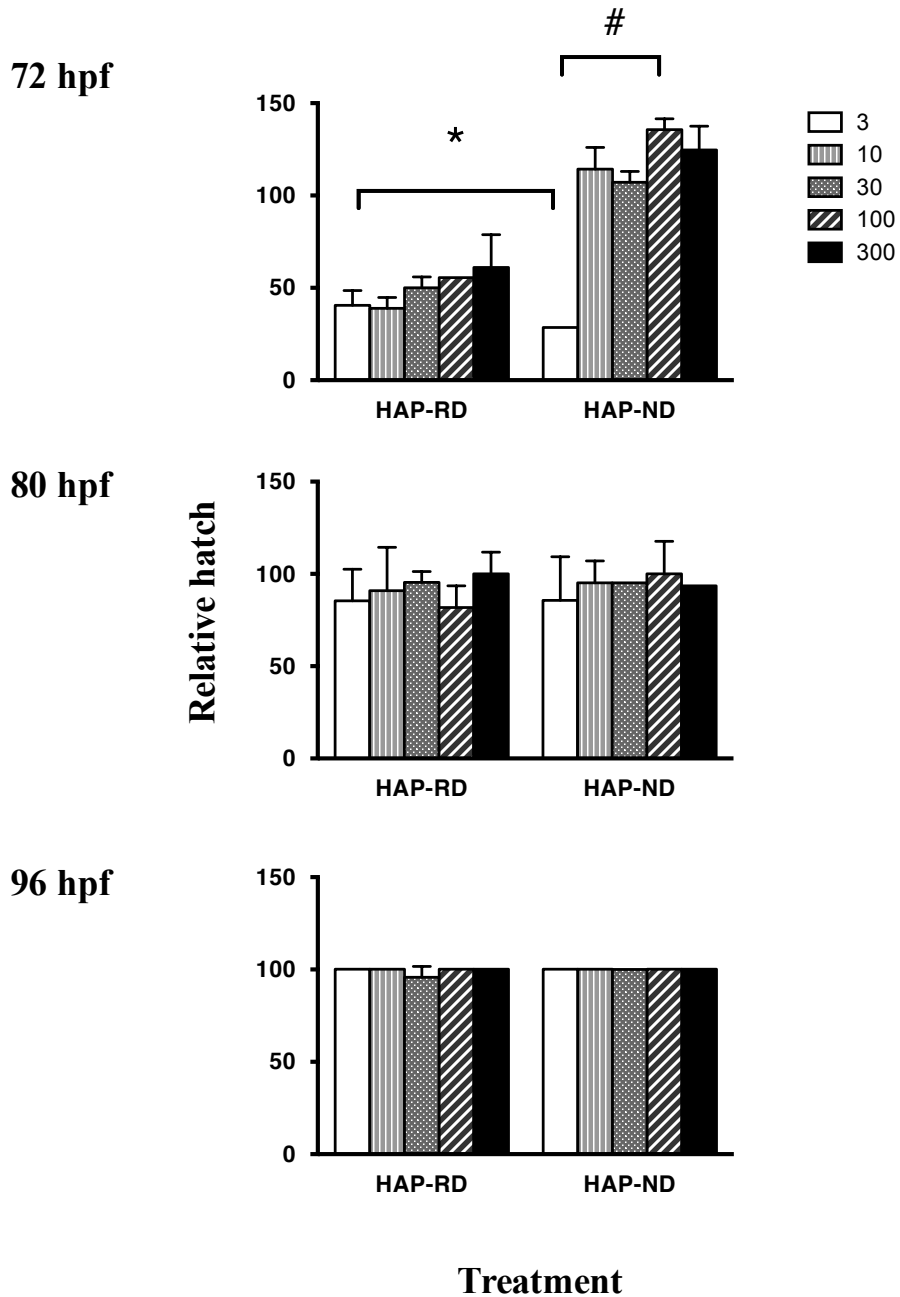
Figure 4-4. Effect of HAP-RD and HAP-ND on hatching rates of zebrafish embryos compared to control at 72 hpf, 80 hpf, and 96 hpf (n = 12). * indicates a significant difference from control. # indicates a significant difference between HAP-ND and HAP-RD particles at same concentration.

| | 72 hpf | 96 hpf | 120 hpf |
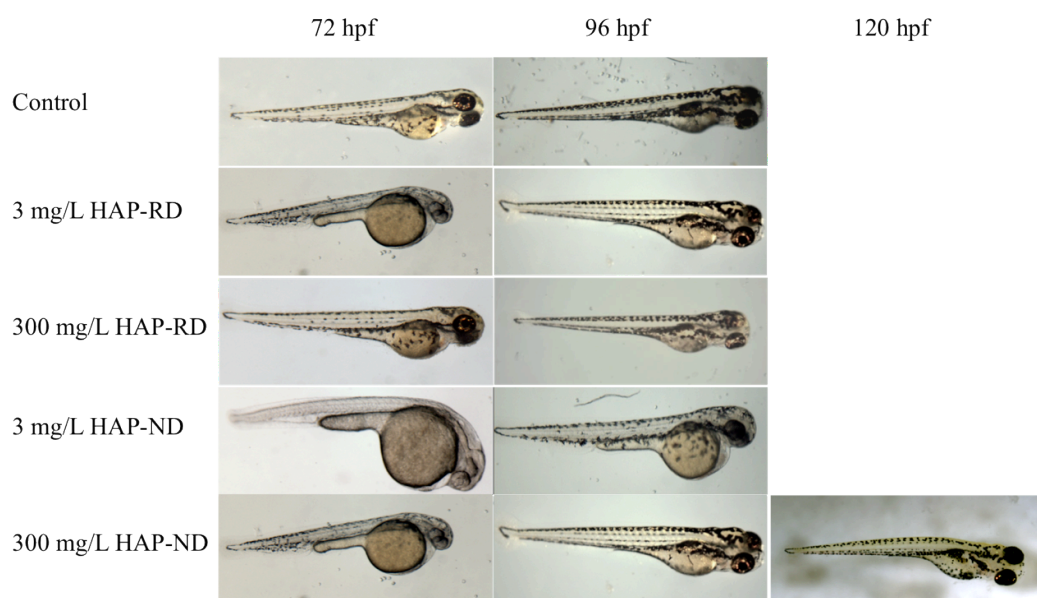
Figure 4-5. Microscopic images of embryos at 72 and 96 hpf, including representative embryo with axial curvature (bent spine) at 120 hpf upon incubation with 300 mg/L HAP-ND.

CHAPTER 5

Mechanistic insights into the effect of nanoparticles on zebrafish hatch

5.1. INTRODUCTION

The increased prevalence of nanomaterials (NMs) in consumer products as well as the rapid development of new NMs and their potential applications points to a nascent need to identify possible effects and mechanisms by which NMs can affect organisms. Likely routes of exposure of aquatic organisms will be via point source release into water, accidental spills, or injection of large amounts of NMs into groundwater for environmental remediation; all can lead to significant amounts of nanoparticle (NP) pollution (Bystrzejewska-Piotrowska *et al.* 2009). Due to the likelihood of aquatic contamination by NPs, it is vital to study the effects of NMs on aquatic organisms and determine which endpoints should be monitored.

Aquatic organisms are particularly susceptible to the effects of NPs (Scown *et al.* 2010). Many NPs are colloidal and remain suspended in the water column, facilitating entry into an aquatic organism through the skin, the gills, and the gut. Negative biological effects have been reported across all levels of aquatic life ranging from biochemical to behavioural to ecosystem effects. Observations of NPs affecting fish hatch have been reported for a number of NP formulations. For example, 5 mg/L of non-coated ZnO (Bai *et al.* 2009), 1 mg/L ZnO (George *et al.* 2011), 50 mg/L of bovine serum albumin-, starch-, or polyvinyl alcohol-capped Ag (O'Brien *et al.* 1985; Asharani *et al.* 2008), 100 µM Ag (Bar-Ilan *et al.* 2009), 15 mg/L Ag (George *et al.* 2011), 5 mg/L CdSe (George *et al.* 2011), and 120 mg/L SWCNT(Cheng *et al.* 2007) NP exposure all decrease hatching success. Studies that measure NP dissolution generally report high release of free metals. For example, 0.405 mg/L Zn^{2+} was initially released from 1 mg/L ZnO (Bai *et al.* 2009), over 25% of Zn^{2+} dissolved from 50 mg/L ZnO (Xia *et al.* 2011), and 1 mg/L dissolution from 10 mg/L ZnO (Zhu *et al.* 2009a). Limiting NP dissolution via capping or doping methods are being explored to abrogate the effects caused by free metal toxicity (Xia *et al.* 2011), as it is not clear whether delayed hatch can be attributed to the NPs or to the free metal dissolved from the NPs. Identifying the active species is of paramount importance.

Free metals affect many aquatic organisms at early stages of development (Jezierska *et al.* 2008). Delays in hatch occur with exposure to 1 µM silver in zebrafish (Powers *et al.* 2010), 1 mg/L zinc in red sea bream (Huang *et al.* 2009)(Huang et al. 2010), and 0.01 mg/L cadmium in the common carp (Witeska *et al.* 1995). Conversely, accelerated hatch has been observed in exposure to silver-exposed winter flounder (Klein-Macphee *et al.* 1984), zinc-exposed fathead minnow and herring (Brungs 1969; Somasundaram *et al.* 1984), and cadmium-exposed rainbow trout (Woodworth *et al.* 1983). Metals such as cadmium, silver, and zinc can affect ionoregulatory processes, bind sulphur groups resulting in changes in protein structure and activity, cause energy disturbances due to activation of detoxification processes, disrupt endocrine processes, inhibit DNA and protein synthesis, and result in reactive oxygen species (ROS) production (Jezierska *et al.* 2008). Disturbances in these processes can lead to morphological abnormalities and affect neurodevelopment and movement (Powers *et al.* 2010; Truong *et al.* 2012). Dissolution of metal-based NPs has been shown to induce morphological abnormalities in embryos similar to free metal induced effects such as axial curvatures and edemas, but can also result in unique consequences to exposure such as tail and yolk sac malformations (King-Heiden *et al.* 2009).

While inhibition of hatch in NP exposures has been noted, very little attention has been focused on the mechanism(s) by which NPs affect hatch. It has been suggested that NPs could delay hatch by directly affecting physiological processes, NP adsorption to the chorion resulting in a more brittle shell or creating a hypoxic environment, and/or by effects on the hatching enzyme (Cheng *et al.* 2007; Bai *et al.* 2009) but these hypotheses have not been tested. One of the important components of hatch is the release of a matrix metalloprotease enzyme from the hatching gland that weakens the chorion and allows the embryo to break free (Inohaya *et al.* 1997). Our lab has recently demonstrated that enzymes such as lactate dehydrogenase (LDH) can be inhibited directly by the presence of specific NPs (MacCormack *et al.* 2012). We hypothesize that some NPs interact with the hatching enzyme and interfere with normal hatching.

The objectives of the present study were to determine the mechanism(s) by which NPs are affecting zebrafish hatch, to elucidate if this mechanism is the same across exposures to different NMs, and to determine if these effects are due to the dissolved metals from the NPs. Using a battery of available NPs, silicon (Si), cadmium selenide (CdSe), silver (Ag), polymer capped zinc oxide (vZnO), leaf shaped uncoated zinc oxide (ZnO leaf), and spherical uncoated zinc oxide (ZnO sphere) NPs, as well as single walled carbon nanotubes (SWCNT), we tested their effects on zebrafish hatch and zebrafish hatching enzyme. These NPs represent a range of metal and non-metal materials with various coatings and of different shapes and sizes. All materials represent those either currently used in the market or are in development for wide-scale use. Importantly, we distinguished the effects of NPs themselves from their dissolved metal components. Morphological development, embryo movement, and inhibition of hatching enzyme activity were used as endpoints to elucidate the mechanism(s) of delayed hatch.

5.2. MATERIALS AND METHODS

5.2.1. Determination of free metal dissolution

To differentiate the effects of free metal from the NP itself, we instituted a dialyzation protocol using Slide-A-Lyzer dialysis cassettes (2.5K MWCO, ThermoScientific). 250 μL of 1000 mg/L of each NP was injected into a cassette and stirred at slow speed in 250 mL ddH$_2$O for 72 hours in polypropylene beakers (250 mL, Nalgene) that were soaked in 1% nitric acid overnight, and rinsed thoroughly. Before the Slide-A-Lyzers were placed in beakers, 2 mL of control water was collected and acidified with 60 μL 10M HNO$_3$ and then at 24h, 48h, and 72 h, 2 mL of water sample was collected and acidified. Dialysis of each NP was repeated three times. Ionic metal present in stock solutions and the amount of dissolution of the NPs over 72 h was measured. All water samples were tested for ionic silicon, cadmium, selenium, silver, and zinc using ICP-MS analysis (analyzed at University of Alberta, Department of Earth and Atmospheric

Sciences). Many measurements were below detectable limits, and therefore the highest concentration observed over the 72 h time period was then used as the "free metal control" in our experiments.

5.2.2. Hatch and morphology observations

Eggs in cleavage stage were rinsed three times with dTW, pipetted into 6-well polystyrene plates with 30 embryos per well, and the water was removed. 5 mL of control (dTW) or treatment solution (NP in dTW) was added to each well. Plates were only used if control embryo survival was >80%. NP treatments for hatching experiments were 1 mg/L and 10 mg/L Si and Ag, and 1 mg/L, 10 mg/L, and 100 mg/L CdSe, SWCNT, ZnO sphere, ZnO leaf, and vZnO. 100 mg/L Si NP treatments were not possible due to low stock concentration, and 100 mg/L Ag NP was not reported due to 100% mortality after 24 hpf. Paired free metal exposures were performed based on the amount of dissolved metal released from the NPs over 72 hours as determined in dialysis experiments. Free metal treatments were set at 17.5 µg/L Cd^{2+}, 76.7 µg/L Zn^{2+}, or 0.02 µg/L Ag^+ as appropriate. Embryos were exposed to 100 mg/L of capping agents (undecylenic acid, citric acid, and polymer capsule) and monitored for survival and hatch, and no differences from controls were observed. Embryos were evaluated at 24 hpf, 48 hpf, and 72 hpf and later at 96 hpf and 120 hpf if required, and dead embryos were removed. Death, hatch, and presence of physical abnormalities were recorded at each time period. Zebrafish exposures were repeated five times per treatment. Micrographs were taken on a microscope (Zeiss Observer HB050) and evaluated using digital imaging software (AxioVs40 v4.7.2). Head to tail angle and head to tail length were measured as metrics of growth and development as described by Kimmel et al. (1995) at 24, 48, and 72 hpf. Five embryos from each exposure were measured and each experiment was repeated at least three times.

5.2.3. Embryo movement study

At 48 hpf twelve embryos per session were recorded using a videocamera and subsequently analyzed using EthoVision XT software (Noldus). Embryos

were observed continuously for 30-minute intervals. Spontaneous movement was recorded and was defined as any distinguishable movement of the embryos. Fish were tested at 72 hpf to determine if touch response was affected. Any embryo not hatched from the chorion at 72 hpf was manually dechorionated and left for one hour. Fish were gently touched at the midsection with a piece of monofilament fishing line and were considered responsive if they swam any distance in response to the stimuli. Each experiment was repeated five times for each treatment and twelve embryos per replicate were tested for spontaneous movement and fifty fish per replicate were tested for touch response.

5.2.4. Protease assay

Batches of approximately 400 embryos were observed after 48 hpf and when approximately 5% of embryos had hatched they were moved to 2 mL of water. An anoxic environment was created by bubbling the water with nitrogen to induce hatch. When approximately 80% of the fish had hatched (~1-2 h), the fluid was collected and immediately frozen at -80 °C for later assessment of protease activity. Total protease activity was assessed using a G-Biosciences protease assay kit (catalogue #786-028) and performed in accordance with the manufacturer's instructions. Specifically, NPs were incubated with chorionic fluid at 28.5°C for 4 hours. Importantly, we performed controls for NP interference (*i.e.,* NP added to kit contents and monitored for optical density changes) and we found that SWCNT and 100 mg/L Ag interfered with the assay. We eliminated these NP treatments from protease activity inhibition testing. NP inhibition of protease activity in the collected chorionic fluid was determined by incubating 1, 10, or 100 mg/L NPs with chorionic fluid and comparing the protease activity to that found in the fluid without NPs. Treatments and controls were run in triplicate on each plate and values were pooled and averaged over a minimum of three separate repeats of each treatment.

5.2.5. Statistical analysis

Data was analyzed using a one-way ANOVA followed by post-hoc Tukey's Multiple Comparison Test. Results were considered statistically significant if $p \leq 0.05$. The relationship between *in vitro* NP effects on protease activity and *in vivo* NP effects on hatching was graphed and correlation coefficients (R^2) were calculated. vZnO data points were removed due to the probability that they sorbed to the chorion and had very low rates of penetrance into the chorionic space, therefore *in vitro* incubation of chorionic fluid with the vZnO would not be representative of *in vivo* interactions (see *Discussion* for further explanation). All values are reported as mean ± SEM. GraphPad Prism v.6.0 was used to perform statistical analyses and to create graphs.

5.3. RESULTS

5.3.1. Characterization of nanoparticles

Most NPs agglomerated at higher concentrations (Table 5-1). For example, at 100 mg/L, CdSe NP average hydrodynamic diameter was 703±13 nm, SWCNTs were 552±105 nm, ZnO sphere NPs were 461±27 nm, and ZnO leaf NPs were 531±27 nm. All NPs were negatively charged in dTW. Ag, SWCNT, ZnO sphere, and ZnO leaf NPs exhibited ζ-potentials between -14 to -16 mV while Si and vZnO NPs were more negatively charged with ζ-potentials at -28±3 mV and -30±5 mV, respectively. CdSe NP exhibited the highest ζ-potential at -52±2 mV.

Dialysis experiments showed low levels of dissolution in some of the NPs after 72 h (Table 5-1). Control water (dTW) had nominal amounts of tested metals (<1 μg/L). Si NP did not release detectable amounts of free metal while a maximum concentration of 0.02 μg/L Ag^+ was released from Ag NP, and 17.5 μg/L Cd^{2+} dissociated from CdSe NP, and selenium was below detectable limits. A maximum of 15.9 μg/L Zn^{2+}, 76.7 μg/L Zn^{2+}, and 0.60 μg/L Zn^{2+} dissolved from ZnO sphere, ZnO leaf, and vZnO NPs respectively. The highest

concentration of dissolved Zn^{2+} (76.7 µg/L) was used as a paired free metal concentration control for the zinc treatments.

5.3.2. Effects on hatching

The hatching rates of zebrafish embryos at 24, 48, 72, and 96 hpf are shown in Figure 5-1. At 72 hpf 91±3% of control embryos were hatched, and some NP exposure groups had significantly lower numbers of hatched embryos at this time point. 54±4% hatched embryos were observed in zebrafish exposed to 10 mg/L CdSe NP and 51±6% of embryos had hatched by 72 hpf in the 10 mg/L Ag NP treatments. However, by 96 hpf the fish in these treatments were fully hatched and were no different than control % hatch. However, in some treatments hatch was completely inhibited leading to death within the chorion by 120 hpf (Figure 5-2c). We observed this phenomenon in embryos exposed to 100 mg/L CdSe NP (39±13% at 72 hpf and 57±14% at 96 hpf), 10 mg/L ZnO sphere NP (16±6% at 72 hpf and 36±9% at 96 hpf), 10 mg/L ZnO leaf NP (6±3% at 72 hpf and 39±6% at 96 hpf). Both 100 mg/L ZnO sphere and ZnO leaf NP exposures had the most dramatic effect on hatch, and embryos in these treatments completely failed to hatch (0±0%). However, in cases where embryos did not hatch, if the chorion was manually removed at 72 hpf, 100% of the embryos survived through to 120 hpf (not shown). Si, SWCNT, and vZnO NPs at all concentrations and 1 mg/L of every NP exposure did not inhibit hatch and no free metal exposures affected the time of hatch ($p > 0.05$).

5.3.3. Effects on morphological development

Embryo head-tail angle in control embryos were 68±2° at 24 hpf, 133±2° at 48 hpf, and 158±1° at 72 hpf (Figure 5-3a). Control fish grew to 2.64±0.02 mm at 24 hpf, 2.97±0.06 mm at 48 hpf, and 3.38±0.02 mm at 72 hpf (Figure 5-3b). CdSe NP was the only treatment to affect head-tail angle (144±2°), and embryos in these exposures were more curled than controls. None of the embryos in the NP treatments or in the free metal treatments differed in length from control at any of the time points ($p > 0.05$, Figure 5-3b). No obvious morphological differences

94

such as heart edema, axial curvature, head or tail deformities, or yolk sac edema were consistently observed between any of the treatments and control embryos.

5.3.4. Effects on movement

At 48 hpf control embryos spontaneously moved within the chorion approximately 4.3±0.9 times per minute, and none of the embryos in the NP treatments nor free metal treatments significantly differed from this value. At 72 hpf, 100±0% of embryos in control, NP exposed, and free metal exposed experiments responded to the touch of the fishing line, indicating that movement was not affected by NPs (Figure 5-4).

5.3.5. Effects on protease activity

Measurements of protease activity showed that some of the NPs inhibited proteases (Figure 5-5a) and exhibited a positive correlation with *in vivo* hatch data ($R^2 = 0.76$, Figure 5-5b). Exposure to 100 mg/L CdSe and 10 mg/L Ag lowered protease activity (51±5% and 65±9%, respectively), and all ZnO NPs significantly affected protease activity. Uncoated ZnO NPs had the greatest inhibitory effect on protease activity, decreasing activity to 72±6%, 45±4%, and 23±3% for 1, 10, and 100 mg/L sphere shaped ZnO respectively and 64±10%, 39±3%, and 31±9% for the leaf shaped ZnO respectively. Despite not affecting the hatch of the embryos *in vivo*, ZnO NPs decreased protease activity at 10 and 100 mg/L to 39±6% and 13±3% of control activity, respectively. No effects were observed in the Si NP exposures or in any of the free metal treatments.

5.4. DISCUSSION

Zebrafish hatch is an essential step in development, growth, and survival. Delayed hatch can leave an organism more susceptible to predators and if hatch is completely inhibited, it can lead to eventual death within the chorion (Figure 5-2d). Zebrafish hatch is a two-step process involving the release of hatching enzyme from the hatching gland to break down the inner vitelline envelope of the

acellular chorion, and then the movement of the embryo to breach the weakened chorion (Sano *et al.* 2008). In our experiments exposure to 10 mg/L CdSe and Ag NP at 72 hpf delayed hatch, and complete inhibition of hatch was observed in embryos exposed to 10 mg/L and 100 mg/L ZnO sphere and leaf, and 100 mg/L CdSe NP (Figure 5-1). In treatments where hatch inhibition lead to mortality within the shell, embryos were manually dechorionated at 72 hpf and 100% survived, indicating that exposure to NPs was interfering with the hatching process. We determined whether these delays resulted from either slowed or stunted growth, an effect on embryo movement, or an inhibition of hatching enzyme activity.

Many NPs have been reported to affect the early development of fish. Ag, CdSe, and vZnO NPs have been shown to result in malformed heads, cardiovascular issues, stunted growth, axial malformations, and edemas (Asharani *et al.* 2008; King-Heiden *et al.* 2009; Bar-Ilan *et al.* 2009; Bai *et al.* 2009; Asharani *et al.* 2011). Smaller agglomerations of NMs may cross the chorion through the 0.5-0.7 μm chorionic pores (Rawson *et al.* 2000) and translocate across the epidermis of aquatic animals (Kashiwada 2006). NPs have been shown to adsorb to the embryos and accumulate in the retina, skin, yolk, brain, heart and blood (Lee *et al.* 2007; Asharani *et al.* 2008; Bar-Ilan *et al.* 2009; Asharani *et al.* 2011) and NPs could affect growth through production of ROS, interference with transporters such as Na^+-K^+-ATPase, or even through direct genotoxic effects (Handy, von der Kammer, *et al.* 2008a; Scown *et al.* 2010). If NPs are delaying development there could be slowed maturation of the hatching gland, resulting in a longer incubation within the chorion. The 100 mg/L CdSe NP exposed fish had a higher head-tail angle (*i.e.,* had undergone less straightening) than controls at 72 hpf (Figure 5-3a), but were not significantly different in length. These metrics indicate that these fish have either undergone slower development, resulting in a delayed hatch, and/or the CdSe exposure induced axial deformations, which could hinder movement. For the most part, delayed hatch did not seem to be attributable to slowed morphological development since every other NP exposed fish was no

different than control fish, morphologically (Figure 5-3); even the embryos that failed to hatch were normal in both length and head-tail angle at time of death.

After ruling out the possibility of NPs affecting the growth of the zebrafish, we determined if there were any effects on their ability to move to breach the weakened chorion. It has been suggested that translocation of carbon-based NMs can occur through the olfactory bulb and into the brain of largemouth bass (Oberdörster 2004) and other experiments suggest that some NPs can cross the blood-brain barrier (Kashiwada 2006; Tang *et al.* 2008; 2010) including in zebrafish embryos (Lee *et al.* 2007; Bian *et al.* 2011; Cho *et al.* 2011). Once in the brain, ROS could damage microglia (Long *et al.* 2006; Lévy *et al.* 2010), or result in death of neural cells (Liu *et al.* 2010; Shiohara *et al.* 2011). Reports of NPs affecting voltage gated channels (Zhao *et al.* 2009; Liu *et al.* 2009; Cho *et al.* 2011), neurotransmitter activity (Wang *et al.* 2009; 2013), and/or regenerative axonal growth (Zhong 2009; Di Wu *et al.* 2012; Wang *et al.* 2013) indicate that NPs have the potential to affect neuronal function. In our study, no changes in behaviour were noted; both spontaneous movement and response to touch were not affected by any of our materials (Figure 5-4). Despite the fact that no behavioural or developmental problems were documented in our study, it is possible that delays in hatch could still be attributed to neurodevelopmental effects. For example, Powers *et al.* (2010) did not observe inhibition of spontaneous movement with 0.1 μM Ag^+ exposure in zebrafish embryos, and fish responded normally to touch, but when the same fish were observed at 5 and 10 days post fertilization, it was noted that the distance swam by larval fish was lower in Ag^+ exposed fish. Further experiments studying the longer-term effects on swimming or other endpoints may provide more information on the potential for NMs to affect neurodevelopment.

In addition to assessing embryo growth and movement, we also investigated hatching enzyme activity in zebrafish embryos exposed to NPs. *Danio rerio* have two zinc-based matrix metalloprotease hatching enzyme genes (ZHE1 and ZHE2) related to the astacin family of enzymes (Sano *et al.* 2008; Clark *et al.* 2010). Gene duplication events and subsequent mutations have

resulted in very low expression of ZHE2 and non-functional for hatching (Sano *et al.* 2008; Gorham *et al.* 2012). At fertilization, the chorion hardens due to polymerization of two glycoprotein subunits and at time of hatch, ZHE1 is released and partially digests the inner vitelline membrane of the chorion with broad substrate specificity (Sano *et al.* 2008; Clark *et al.* 2010). Gene transcripts for ZHE1 can be detected as early as 10 hpf and can be observed at the anterior of the yolk sac as early as 24 hpf (Inohaya *et al.* 1997; Sano *et al.* 2008; Suresh *et al.* 2012; Perreault *et al.* 2012). In our experiments, NPs that delayed or inhibited hatch *in vivo* inhibited protease activity (Figure 5-5a), and these effects were generally well correlated (R^2=0.76, Figure 5-5b).

A large body of research has demonstrated that NPs have different affinities for proteins based on their charge, size, and surface coating (Lundqvist *et al.* 2008; Bae *et al.* 2011). While these affinities become weaker or stronger with different NP surface functionalities, some proteins appear to interact with NPs in manners not solely predictable by shape, surface coating, or agglomeration state (Limbach *et al.* 2005; Lundqvist *et al.* 2008; Deng *et al.* 2009). For example, if interaction with ZHE1 was solely based on physical characteristics such as hydrated size and ζ-potential, we would expect 100 mg/L SWCNT to also inhibit hatch due to similar characteristics as 100 mg/L ZnO sphere and leaf (Table 5-1), however it has no effect on hatch. As a result, prediction of these interactions is difficult with our current understanding. Uncoated ZnO sphere and leaf-shaped materials used in this study have similar hydrated size and ζ-potential (Table 5-1), but are of different shapes, yet had the same effect both *in vivo* and in the *in vitro* protease inhibition assay. This suggests that shape did not play a large role in the inhibition of ZHE1, in contrast to what has been shown in other studies (Kühnel *et al.* 2009; Deng *et al.* 2009; Laurent *et al.* 2012). Interestingly, the polyacrylic acid-coated vZnO NPs did not inhibit hatch *in vivo* (Figure 5-1g) but inhibited protease activity at concentrations as low as 10 mg/L *in vitro* (Figure 5-5a). We have demonstrated that NPs synthesized with the same polymer capping agent are ~38% bound to the chorion and only ~0.07% was adsorbed or absorbed to embryo itself (Felix *et al.,* unpublished data), indicating that little of this NP penetrates the

chorion *in vivo*. This would prevent interaction with ZHE1 and therefore not affect hatch. Exposing embryos to NPs with similar surface functionality does not always yield similar effects; 10 mg/L undecanoic acid functionalized Si NP did not affect hatching ability at 72 hpf (87±5% hatch, Figure 5-1a), but 10 mg/L mercaptoundecanoic functionalized CdSe NP (the same surface coating presented to the water) significantly delayed hatch (54±4% hatch; Figure 5-1b). Interactions between the hatching enzyme and the NPs could cause deformation and inactivation of the protein (Fei & Perrett 2009; Ward & Kach 2009; Casals *et al.* 2010). Structural changes in enzymes can cause inactivation or decreased selectivity for substrates. For example, LDH activity can be inhibited or abolished completely by Si, CdSe, and gold NPs (Zhu *et al.* 2009a; MacCormack *et al.* 2012) and SWCNT interaction with α-chymotrypsin abolishes activity (Rawson *et al.* 2000; Karajanagi *et al.* 2004). Negative outcomes of inhibition of enzymes *in vivo* have not been comprehensively explored, though it is clear that interactions with biologically relevant proteins could result in sub-lethal or even lethal effects. For example, binding of NPs to serum proteins such as immunoglobins or complement factors could impair immune responses (Hoo *et al.* 2008; Lundqvist *et al.* 2008; Deng *et al.* 2009). Given that NPs can inhibit a number of enzymes it is possible that aquatic species dependent on hatching enzymes could be similarly affected by exposure to NPs.

Our study was designed to distinguish NP-specific effects from the confounding effects of the free metals resulting from either dissolution or contamination. Paired free metal exposures demonstrated that inhibition of hatch is likely a NP-specific effect; none of the free metal exposures affected morphology, movement, or hatching enzyme activity. However, we realize that although we measured the free release of metal over time, there is still the possibility that our measured free metal release from the NPs is not indicative of the true free metal release with embryos present in the water. Furthermore, the mechanism of toxicity may still be from the free ions where NPs may be translocating into and dissolving within the fish (Nel *et al.* 2009; Montes-Burgos *et al.* 2009). It has been suggested that the chorion is more permeable to Zn^{2+} and

Cd^{2+} than Ag^+ (Rombough 1985; Hoo *et al.* 2008), thus if there were high dissociation rates then it would be expected that the ZnO and CdSe NP exposures yield that highest effects.

In this study we have shown NPs have effects distinct from their dissolved constituents and these effects may not be presented as direct lethality. Longer hatching duration in aquatic organisms leaves embryos susceptible to predation and to mortality via environmental factors. The inhibition of proteases correlates with the ability of zebrafish embryos to hatch, which suggests that inhibition of ZHE1 seems to be the factor driving hatch delay and inhibition. Lack of hatch is sometimes overlooked as an endpoint for toxicology studies, but our results clearly show that some NPs can cause death due to an inability to hatch. Our results show that there are nano-specific hatching effects in experimental conditions.

We have demonstrated that some NP exposures can result in an inhibition of zebrafish hatch, and in some cases lead to mortality of the embryo within the chorion. Our tests showed that this is a NP-specific effect and were independent from the effects of exposure to ionic metal equivalent to that dissolved from the NP core. Most of the NPs used did not affect growth or morphological development of the fish up to 72 hpf, but there was a strong correlation between inhibition of hatching protease activity and the inhibition of hatch *in vivo*. This study highlights the need to record and report hatch data in embryo toxicological testing and to consider the possible interactions occurring at the biochemical level as these interactions may affect an organism's fitness *in vivo*.

Table 5-1. Functionalization, production source, hydrodynamic size, ζ-potential, and concentration of free metal dissolved from NP core.

NP	Functionalization	Source	Size (nm)			ζ - potential (mV)			Free metal dissolution (µg/L)
			1 mg/L	10 mg/L	100 mg/L	1 mg/L	10 mg/L	100 mg/L	
Si	undecylenic acid	Veinot	151±2	150±1	147±2		-28±3	-43±6	0 Si
CdSe	undecylenic acid	Veinot	181±12	240±8	703±13		-47±0	-52±2	17.5 Cd^{2+}
Ag	citric acid	Veinot	80±2	90±1	96±1	-13±0	-13±0	-13±0	0.02 Ag^{+}
SWCNT	carboxylic acid	Simard	99±60	284±71	552±105	-13±1	-12±0	-12±0	N/A
ZnO sphere		Loo	96±123	146±18	461±27	-12±1	-16±0	-16±1	15.9 Zn^{2+}
ZnO leaf		Loo	169±31	147±32	531±27	-12±0	-14±0	-13±0	76.7 Zn^{2+}
vZnO	polyacrylic acid	Vive Nano	20±2	25±1	153±12		-30±5	-35±3	0.60 Zn^{2+}
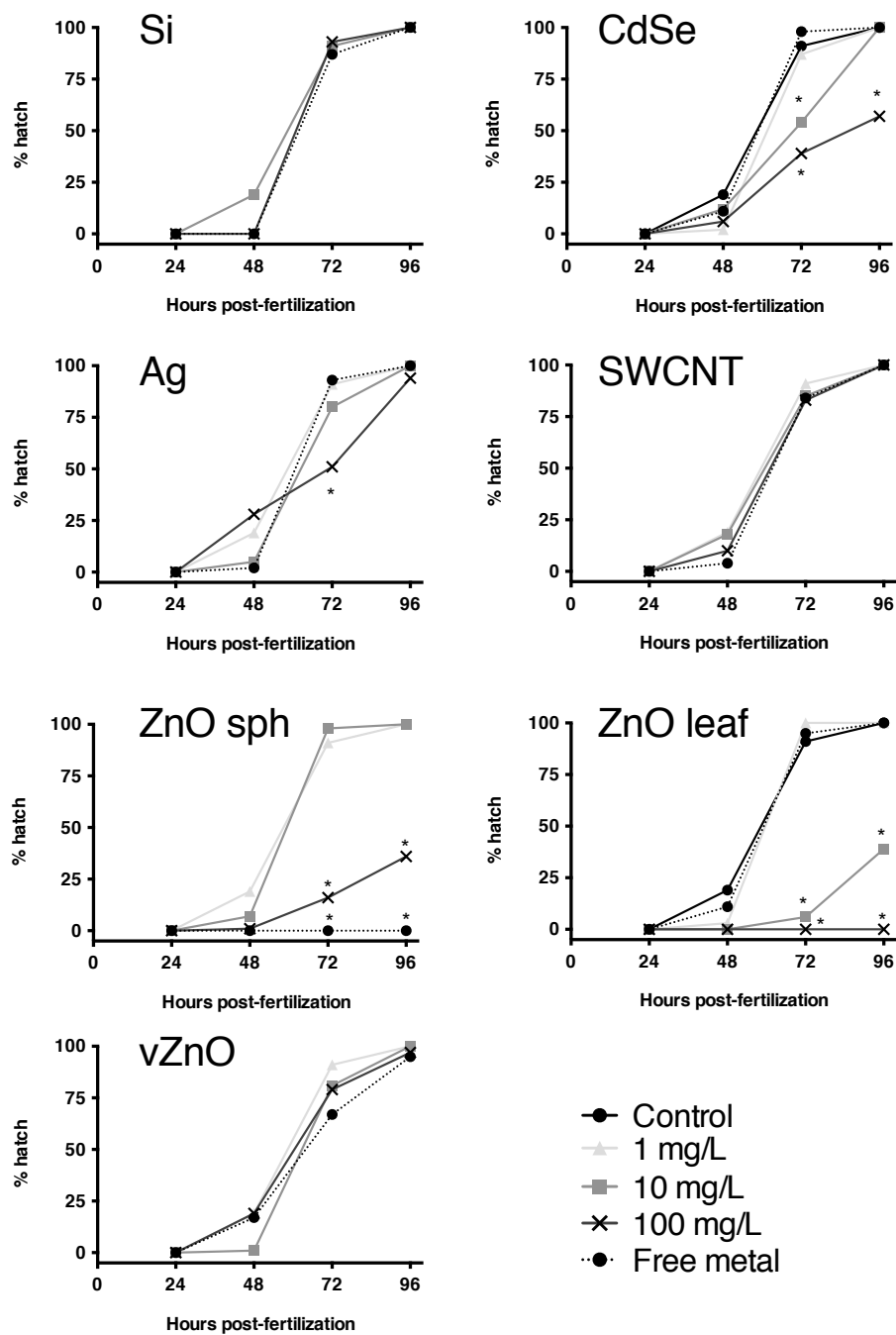
Figure 5-1. Zebrafish hatching success at 24, 48 72, and 96 hpf when exposed to undecanoic functionalized Si NPs, mercapto-undecanoic functionalized CdSe NPs; citrate-capped Ag NPs, lysine functionalized SWCNT, spherical ZnO NPs, leaf-shaped ZnO NPs and polymer coated ZnO NPs.

Figure 5-2. Representative micrographs of (a) control zebrafish embryos at 72 hpf hatched form the chorion, and zebrafish exposed to 100 mg/L CdSe NPs or 10 and 100 mg/L ZnO sphere and leaf NPs, (b) still unhatched at 72 hpf and (c) unhatched and dead within the chorion at 96 hpf.

a.

b.
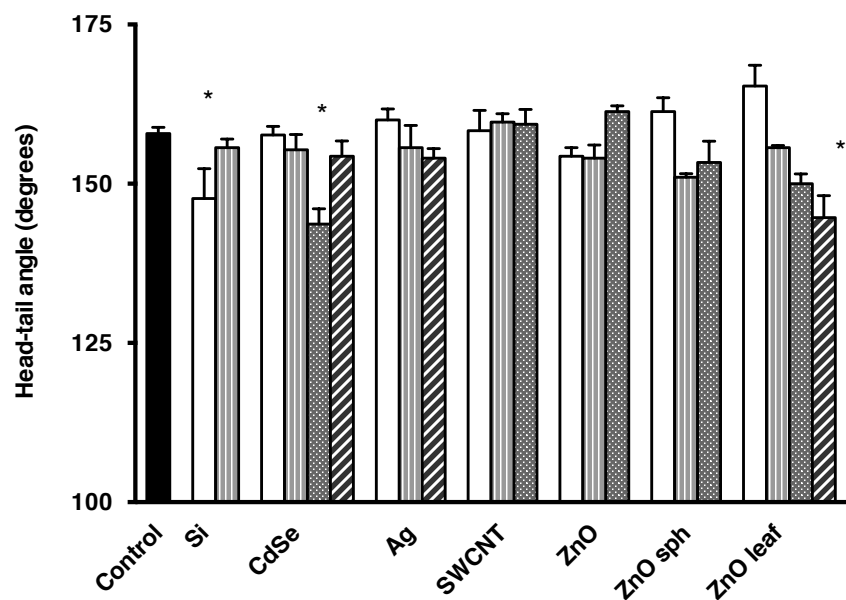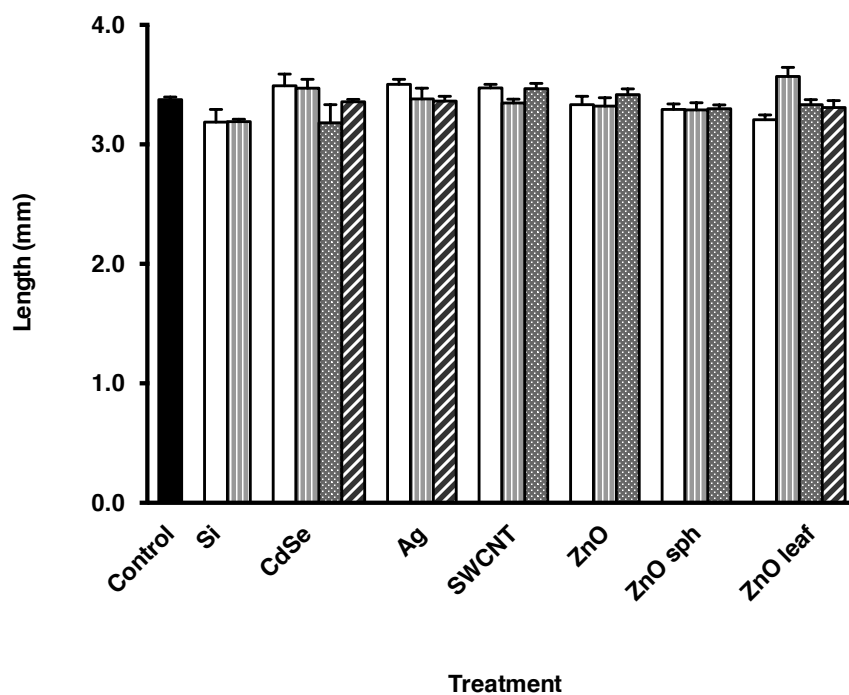
Figure 5-3. Embryo morphological delay at 72 hpf exposed to NPs and paired free metal exposures, measured as (a) head-tail angle and, (b) total body length (mm).
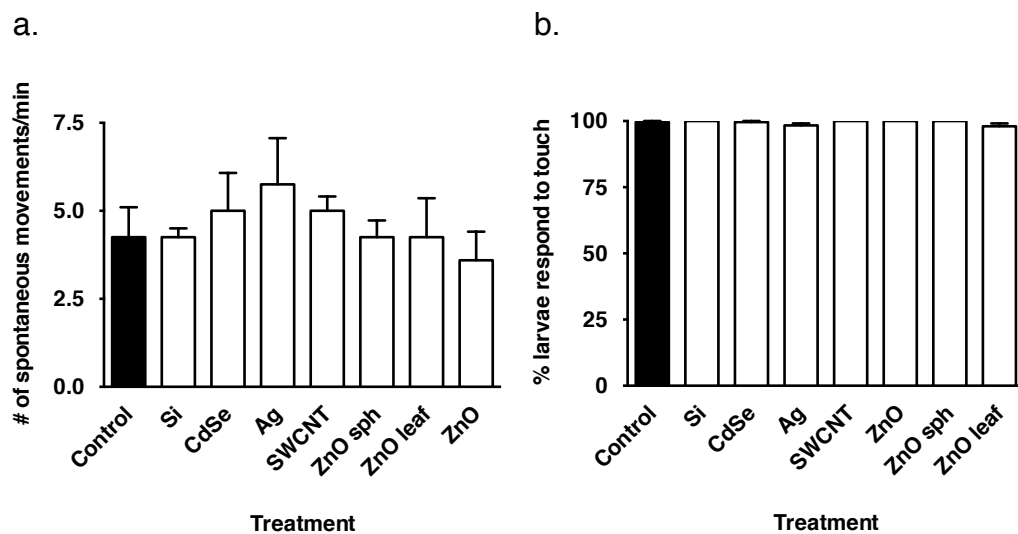
Figure 5-4. Effect of NPs on embryo movement. (a) Number of spontaneous movements/min at 48 hpf, and (b) Percentage of larvae that responded to touch at 72 hpf.

a.

b.

$$y = 1.45x - 33.25$$
$$R^2 = 0.79$$
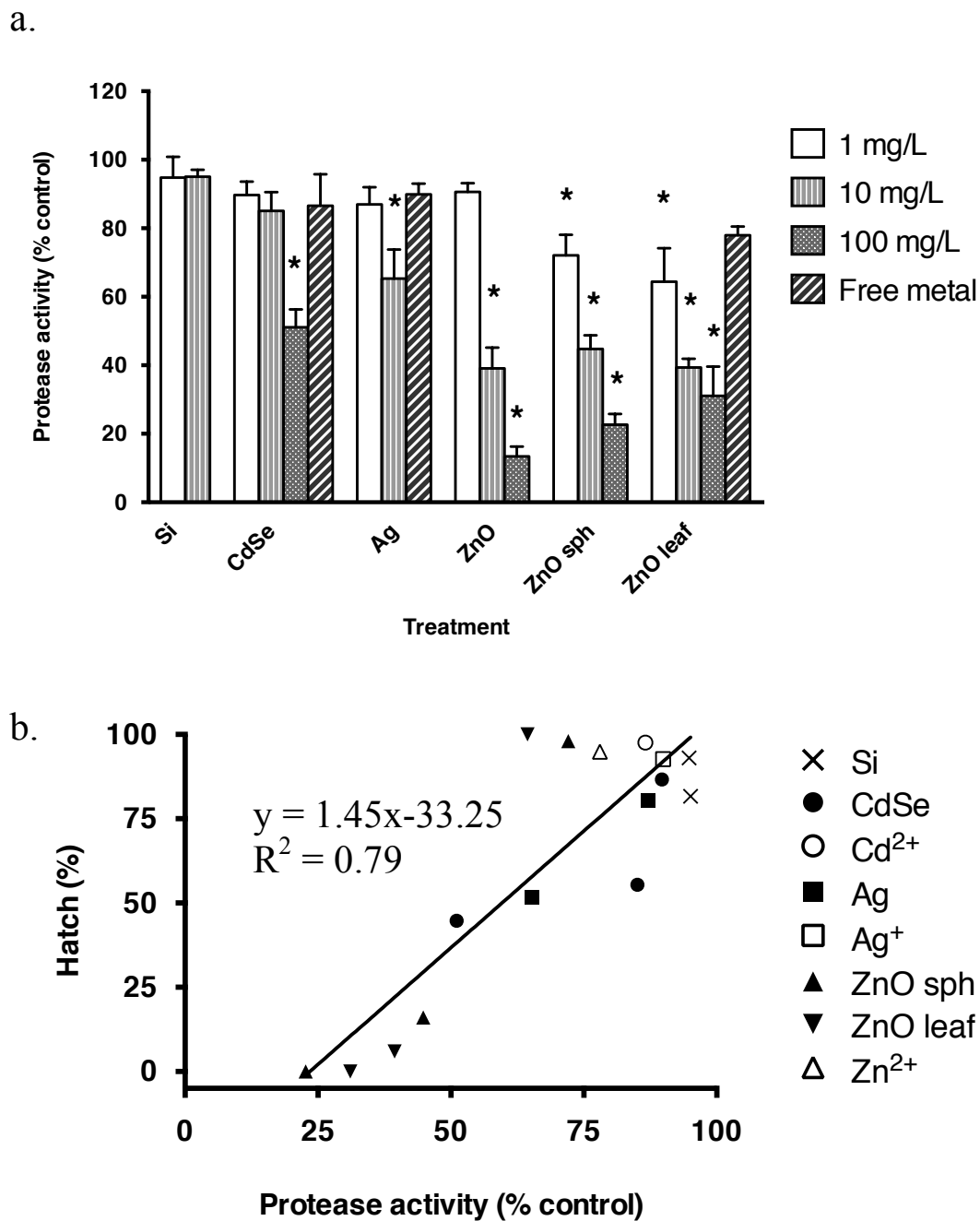
Figure 5-5. (a) Inhibition of total protease activity in the presence of NPs and free metal as compared to control. (b) Correlation between total protease activity and zebrafish hatch, excluding vZnO.

CHAPTER 6

The influence of humic acid on the aquatic effects of nanoparticles

6.1. INTRODUCTION

Nanomaterial use and production is rapidly increasing, and nanoparticles (NPs) will certainly end up in the aquatic environment. As evidence supporting NP-induced negative effects on aquatic organismal health is mounting, there is elevated concern regarding current NP regulations and testing methods. Evaluation and adjustment of NP-toxicity testing protocols to ensure accurate predictions on the consequences of aquatic release is necessary. The majority of current studies are performed in laboratory conditions, and often the pristine waters in which experiments are performed do not mimic natural conditions (Nowack & Bucheli 2007; Harush-Frenkel *et al.* 2008; Park *et al.* 2011; Nowack *et al.* 2011). Determining which environmental factors may mitigate or exacerbate NP toxicity, and establishing whether current standardized laboratory tests are representative of natural environments is essential.

Natural water sources are complex, and various environmental factors affect the physicochemical characteristics of aquatic NPs. Natural factors such as salinity, pH, ionic strength, or the presence of natural organic materials (NOM) affect NP behaviour and consequently alters availability and toxicity to aquatic organisms (Ryman-Rasmussen *et al.* 2006; Christian *et al.* 2008; Zhang & Monteiro-Riviere 2009). An important component of natural water sources are humic acids (HA) are substances that result from the decay of organic matter and are a type of NOM (MacCarthy 2001; Ryman-Rasmussen *et al.* 2006; Park *et al.* 2011). Humic substances are ubiquitous in aquatic environments and have several unique characteristics (MacCarthy 2001; Clift *et al.* 2010; George *et al.* 2011). The molecular heterogeneity of these compounds varies greatly; however, the general composition and behaviour of HAs is relatively consistent. NOMs are regularly reported to alter the severity of biological effects in a multitude of toxicants, such as organic chemicals (*e.g.,* Lee *et al.* 1993; Fabrega *et al.* 2009; Bian *et al.* 2011) and metals (*e.g.,* Bury *et al.* 1999; Jin *et al.* 2001; Meinelt *et al.* 2001; Ryan *et al.* 2004; Wiley *et al.* 2004). NOMs can alter the uptake, bioaccumulation, and toxicity of various substances , and NOMs themselves are

redox reactive (MacCarthy 2001; Chithrani & Chan 2007), and can negatively affect organisms.

A number of studies have examined the physicochemical behavior of NPs in natural aquatic systems (Chithrani & Chan 2007; Diegoli *et al.* 2008; Petosa *et al.* 2010; Meng *et al.* 2011). Fewer studies address the biological impact of NPs on fishes in the presence of HA, and have focused on TiO_2 (Shaw & Handy 2011; Yang *et al.* 2013) or carbon based materials (Borm 2005; Kim *et al.* 2012). The use of zebrafish (*Danio rerio*) embryos for acute toxicity testing is efficient, cost-effective, and well-developed (Hill 2005; Beer *et al.* 2012). They are sensitive to developmental effects of various toxicants, including heavy metals, and are indicators of aquatic hazard (Hill 2005; Jezierska *et al.* 2008; Bai *et al.* 2009). In previous studies, we found that a range of metallic and non-metallic NPs in laboratory conditions can inhibit ZF hatch, and result in death within the chorion (Ong et al. 2013; Chapter 5). In this study, we tested six different NP formulations to determine whether the presence of 10 mg/L humic acid would alter NP-toxicity, hatch, development, and movement of embryonic zebrafish.

6.2. MATERIALS AND METHODS

6.2.1. Preparation and characterization of HA solutions

Final NP exposure solutions were diluted in E3 medium (5 mM NaCl, 0.17 mM KCl, 0.33 mM $CaCl_2 \cdot 2H_2O$, 0.33mM $MgSO_4 \cdot 7H_2O$) for zebrafish embryo exposures. Suwannee River HA (International Humic Substances Society) was slowly shaken and hydrated overnight in the dark as a 1 g/L stock in E3 medium and made fresh every two weeks. Hydrodynamic diameter and ζ-potential measurements of NPs and NPs+HA were performed in E3 medium to represent exposure conditions. The hydrodynamic diameter and ζ-potential of each NP, or NPs with the addition of 10 mg/L HA (henceforth referred to as NP+HA) was acquired using a Malvern Instrument Zetasizer Nano ZS equipped with a 633 nm laser (Westborough, MA) and measured in 173º backscatter mode.

6.2.2. Hatch and morphology observations

Cleavage stage embryos were collected and rinsed in E3 medium, and then embryos from the same breeding adults were sorted into groups of 30 embryos in a 6-well polystyrene plate. Extra liquid was removed and 5 mL of treatment solution was added. Treatments were 10 mg/L CdSe, 10 mg/L Ag, 200 mg/L SWCNT, 100 mg/L ZnO, 100 mg/L ZnO sph, and 100 mg/L ZnO leaf, with and without 10 mg/L HA. Controls (E3 medium and E3 medium + HA) were run internally on each plate, and plates were only used if control survival was ≥80%. Survival and hatch were monitored at 24, 48, and 72 hours post fertilization (hpf), and dead embryos were removed at each time point. Exposures were repeated six times per treatment. The same exposure protocol was repeated for morphological measurements, and three embryos from each treatment were randomly chosen to be measured using a light microscope (Zeiss Observer HB050) and evaluated using digital imaging software (AxioVs40 v4.7.2). Head to tail angle and head to tail length were measured as metrics of growth and development as described by Kimmel *et al.* (1995) at 24, 48, and 72 hpf. Each treatment was repeated at least six times.

6.2.3. Embryo movement study

Groups of ten 48 hpf embryos was videotaped for 10 minute intervals and spontaneous movements (*i.e.,* any distinguishable movement) were manually counted. Spontaneous movement trials were repeated three times. Touch response was monitored at 72 hpf; any embryos that were still within the chorion were manually dechorionated with forceps and left for one hour. Fish were gently touched at the midsection with a piece of monofilament fishing line and if the fish responded and swam any distance, they were considered responsive. Touch response experiments were repeated three times per treatment and fifty fish per replicate were tested for touch response.

6.2.4. Protease assays

Protease activity was measured in the chorionic fluid of embryonic zebrafish with Ag, ZnO sph, and ZnO leaf to determine if addition of humic acid could alter hatching enzyme activity. After 48 hpf, embryos were observed and when approximately 5% of embryos had hatched roughly 400 embryos were collected and moved to 2 mL E3 medium. Nitrogen was bubbled into the water to create an anoxic environment to induce hatch. When approximately 80% of the fish had hatched, the fluid was filtered with fine mesh and a syringe, and immediately frozen at -80 °C. A G-Biosciences protease kit (catalogue #786-028) was used to assess activity and NPs and NPs+HA were incubated with chorionic fluid at 28.5°C for 4 hours. Control wells with chronic fluid with no NPs were run alongside each treatment. To test for NP-assay interference, we performed controls for NP interference (*i.e.,* NP added to assay contents and monitored for optical density changes without chorionic fluid) and confirmed that none of these NPs interfered with the assay. Each treatment was run in triplicate on each plate and repeated three times.

6.2.5. Statistical analysis

Data was statistically analyzed using a one-way ANOVA and if significant differences were found, a post-hoc Tukey's Multiple Comparison Test was performed. Results were considered statistically significant if $p \leq 0.05$. All values are reported as mean±standard error. GraphPad Prism v.6.0 was used to perform statistical analyses and to create graphs. Values are reported as mean ± SEM.

6.3. RESULTS & DISCUSSION

Various environmental factors influence the activity, bioavailability, and toxicity of NPs, and these conditions are often not represented in laboratory experiments. Ubiquitous in all bodies of water are HAs, and in this study we demonstrate that the presence 10 mg/L HA alters both the physical characteristics

of NPs and their developmental effects on zebrafish embryos. HA itself can induce toxic responses, notably the ability to induce oxidative stress-related damage to aquatic organisms (Steinberg *et al.* 2006; Ispas *et al.* 2009). In E3 medium, 10 mg/L HA on its own did not affect survival, hatch, morphological development, nor movement, thus allowing focus on NP-HA interactions and their biological effects.

Most of the NPs did not induce developmental effects. Only Ag exposure resulted in statistically significant length reduction in 48 h embryos, averaging 3.07±0.04 mm, compared to 3.19±0.02 mm control embryos (Figure 6-1). ZnO sph and ZnO leaf both slowed the uncurling of the embryos at 96 h (147±2° and 145±2° respectively) (Figure 6-2). In all of these cases, addition of HA abrogated this effect; average Ag+HA length was 3.12±0.04 mm (Figure 6-1), and ZnO sph and leaf+HA were restored to 153±2° and 151±2°, respectively (Figure 6-2). These results indicate that in natural environments fish embryo development may not be affected by NPs in the presence of certain HAs.

Interaction between HA and NPs, as indicated by their change in hydrodynamic diameter and decreased polydispersity (*i.e.,* more homogenous agglomerates) (Table 6-1), is thought to prevent binding of the NPs to membranes, and thus limiting NP damage (Li *et al.* 2010; Chen *et al.* 2011; Griffitt *et al.* 2011; Lin & Wiesner 2012). Membrane-NP interaction can induce injury *via* oxidative damage or reduction of membrane potential, and may also allow for uptake of NPs in embryonic fish (Nel *et al.* 2009; Johnston *et al.* 2010; Laurent *et al.* 2012; Lapresta-Fernandez *et al.* 2012). NOMs can adsorb to, and coat, carbon (Guo *et al.* 2008; Hyung & Kim 2008; Edgington *et al.* 2010) and metal (Baalousha *et al.* 2008; Guo *et al.* 2008; Diegoli *et al.* 2008; Fabrega *et al.* 2009) NPs, and may even replace the engineered capping agents (Handy *et al.* 2008b; Diegoli *et al.* 2008). As a consequence, surface properties are modified and alter NP-membrane interactions both sterically and electrostatically when incubated with NOM (Christian *et al.* 2008; Fabrega *et al.* 2009; Truong *et al.* 2012; Li *et al.* 2013; Kim *et al.* 2013). Increases in negative charge in the presence of HA, as seen with the bare ZnO sph (+2±0 to -24±0 mV) and ZnO leaf

(-13±2 to -25±1 mV) (Table 6-1), likely increase electrostatic repulsion between the NPs and negatively charged membranes (Chen *et al.* 2011; Lin *et al.* 2012). The negative ζ- potential of the polymer capped ZnO NPs without HA (-20±2 mV; Table 6-1), in addition to their stable coating, provide both electrostatic and steric repulsions, and likely account for some of the toxicity differences between capped ZnO and pristine ZnO sph and leaf. Ionic metal dissociation from NPs is often associated with negative biological effects (Diegoli *et al.* 2008; Scown *et al.* 2010), and may also contribute to toxicity. Metals are known to disturb developmental processes, including perturbations of enzyme activity and osmoregulation, increases in oxidative stress, and activation of detoxification processes, resulting in reduced energy allocation to developmental processes (Jezierska *et al.* 2008; Lynch *et al.* 2009). It is possible that HA decreased metal dissolution through capping of the surface of the ZnO sph and ZnO leaf NPs (Chithrani & Chan 2007; Fabrega *et al.* 2009), whereas the other metal NPs already had stable coatings and thus less dissociation of metals. The HA itself may also have adsorbed metal ions, removing this threat (Playle 1998; Kashiwada 2006).

Interestingly, despite the improvement in morphological development with the addition of HA, NP+HA treatments still resulted in lethal toxicity. Ag, SWCNT, CdSe, and ZnO did not affect survival over the 96 h exposure, and were not significantly different than control (88±1% survival) (Figure 3). However, exposure to ZnO sph and ZnO leaf resulted in a reduced survival of 56±13% and 30±16%, respectively (Figure 6-3). Even with addition of HA, the survival rates did not change in both ZnO sph (51±12%) and ZnO leaf (43±10%), and were still significantly lower than the HA control (91±1%) (Figure 3). In general, NOM has been shown to improve survival in NP-exposed non-vertebrate aquatic organisms (*e.g.,* Gao *et al.* 2009; Fabrega *et al.* 2009; Tang *et al.* 2010; Lee *et al.* 2011; Chen *et al.* 2011). However, addition of NOM in NP-exposed piscine studies has produced mixed results; increased survival (Kim *et al.* 2012; Lin & Wiesner 2012), no effect on survival (Kim *et al.* 2012), and decreased survival (Nel *et al.* 2009; Yang *et al.* 2013) have all been reported. In this study, mortality was only

observed at 96 h if the embryo had hatched, and embryos that were not hatched were still alive (as determine by manual dechorionation and observation of embryos) (Figure 6-4). The chorion may minimize embryo-NP interaction through adsorbing or limiting access of the NPs during early development (Kashiwada 2006; Lee *et al.* 2007; Ma *et al.* 2012b). It is unknown how NOM may affect the transport of NPs through the chorion. After hatch, the embryos are susceptible to direct contact with NPs, and the beneficial effects of HA may be diminished after the chorion has been breached.

The most apparent effect of addition of NOM was the reversal of the hatch inhibition in ZnO sph and ZnO leaf exposed embryos. Previous studies have shown that ZnO NPs inhibit zebrafish hatch (Fischer & Chan 2007; Bai *et al.* 2009). Without HA, $97\pm1\%$ of control embryos had hatched by 72 h, and $100\pm0\%$ by 96 h, whereas only $13\pm7\%$ of ZnO sph and $12\pm11\%$ of ZnO leaf exposed fish had hatched by 96 h (Figure 6-5). Hatch success was fully restored to $98\pm2\%$ in ZnO sph+HA exposed embryos, and increased to $70\pm12\%$ in ZnO leaf+HA embryos (Figure 6-5). However HA did not completely reverse effects in ZnO leaf+HA exposures; hatch success was still lower than control+HA embryos ($100\pm12\%$). Unfunctionalized ZnO sph and leaf both slowed development of the embryos (Figure 6-2), likely contributing to the delayed hatch. In addition, zebrafish hatch is dependent on both the release of zebrafish hatching enzyme and movement of the embryo (Sano *et al.* 2008). We ruled out the detrimental effect of NPs and NOMs on movement; spontaneous movement and touch response after hatch were not altered (Figure 6-6, touch response not shown as 100% of fish responded). Therefore, we surmised that inhibition of hatch was likely attributable to NP-hatch enzyme interactions (Chapter 5). We predicted that adsorption and coating of NPs by HA could sterically or electrostatically prevent this interaction from occurring. In isolated protease experiments, NPs were found to reduce enzymatic activity (Figure 6-7). Both ZnO sph and ZnO leaf reduced protease activity to 47 ± 10 % and 34 ± 10 % of control activity. However, NP-induced inhibited activity of protease was not remediated with the addition of HA, and ZnO sph+HA and ZnO leaf+HA treatments did not change protease

activity (39±9 % and 32±8 %, respectively) (Figure 6-7). While this suggests that this may not be the mechanism by which HA is abrogating hatch inhibition, many complex interactions are occurring during *in vivo* experiments (*e.g.,* adherence to chorion, settling of NPs, interaction with other proteins), and this may not be fully represented *in vitro*. In addition, HA and NPs were not incubated together prior to performing the protease assay, and sorption and interaction of HA to NPs can change over time (Baalousha *et al.* 2009), which may not be represented properly here. Further experiments exploring isolated hatching enzyme and its activity in the presence of NPs and NOMs need to be performed.

Although this study suggests that humic acid may diminish some negative developmental effects of NPs to embryonic zebrafish, ultimately, the presence of HA did not abrogate the lethality of the unfunctionalized ZnO NPs. The presence of HA can clearly affect NP toxicity, indicating that laboratory studies of NP effects in pristine solutions may not be representative of natural environments. Predictive water quality models will have to include NOM as they affect the physicochemical characteristics and behaviour of NPs. The stabilization of NPs in aquatic systems due to NOM may also be of concern due to their increased mobility (Johnson *et al.* 2009; Love *et al.* 2012)(Johnson et al. 2009). Different sources of NOM can result in different toxicity of various toxicants (Ryan *et al.* 2004; Hyung & Kim 2008; Gao *et al.* 2009; Edgington *et al.* 2010; Lee *et al.* 2011; Iversen *et al.* 2011; Tantra & Knight 2011), and different concentrations of HA can affect aggregation state and toxicity (Tieleman *et al.* 2002; Gao *et al.* 2012). Factors such as pH (Hyung & Kim 2008; Iversen *et al.* 2011; Rivolta *et al.* 2012), ionic strength (Hyung & Kim 2008; Singh *et al.* 2012; Truong *et al.* 2012), salts (Chen & Elimelech 2007; Iversen *et al.* 2011), and sunlight (Shiohara *et al.* 2011; Park *et al.* 2011; Yang *et al.* 2013) can play a role in the degree of toxicity and effects resulting from a combination of these factors will certainly be dynamic and complex (Liu *et al.* 2011; Wang *et al.* 2011). Studying the effects of NPs in a range of relevant environmental conditions is essential for accurate projection of the potential aquatic toxicity of NPs, and isolating and testing each component of natural waters is the first step towards achieving these goals.

Table 6-1. Physicochemical characteristics of NPs without (in white), and with addition of 10 mg/L Suwannee River humic acid (in gray).

	Diameter (nm)	Polydispersity	Charge (mV)
CdSe 10	39±19	1.0000	-13±0
CdSe 10 + HA	114±39	0.9268	-10±0
Ag 10	93±1	0.2327	-19±0
Ag 10 + HA	86±6	0.2740	-18±0
SWCNT 200	385±49	0.9367	-18±0
SWCNT 200 + HA	189±70	0.7527	-24±0
ZnO 100	19±0	0.1967	-20±2
ZnO 100 + HA	13±0	0.2750	-14±0
ZnO sph 100	272±41	0.9217	+ 2±0
ZnO sph 100 + HA	202±8	0.5377	-24±0
ZnO leaf 100	-	1.0000	-13±2
ZnO leaf 100 + HA	261±9	0.3523	-25±1
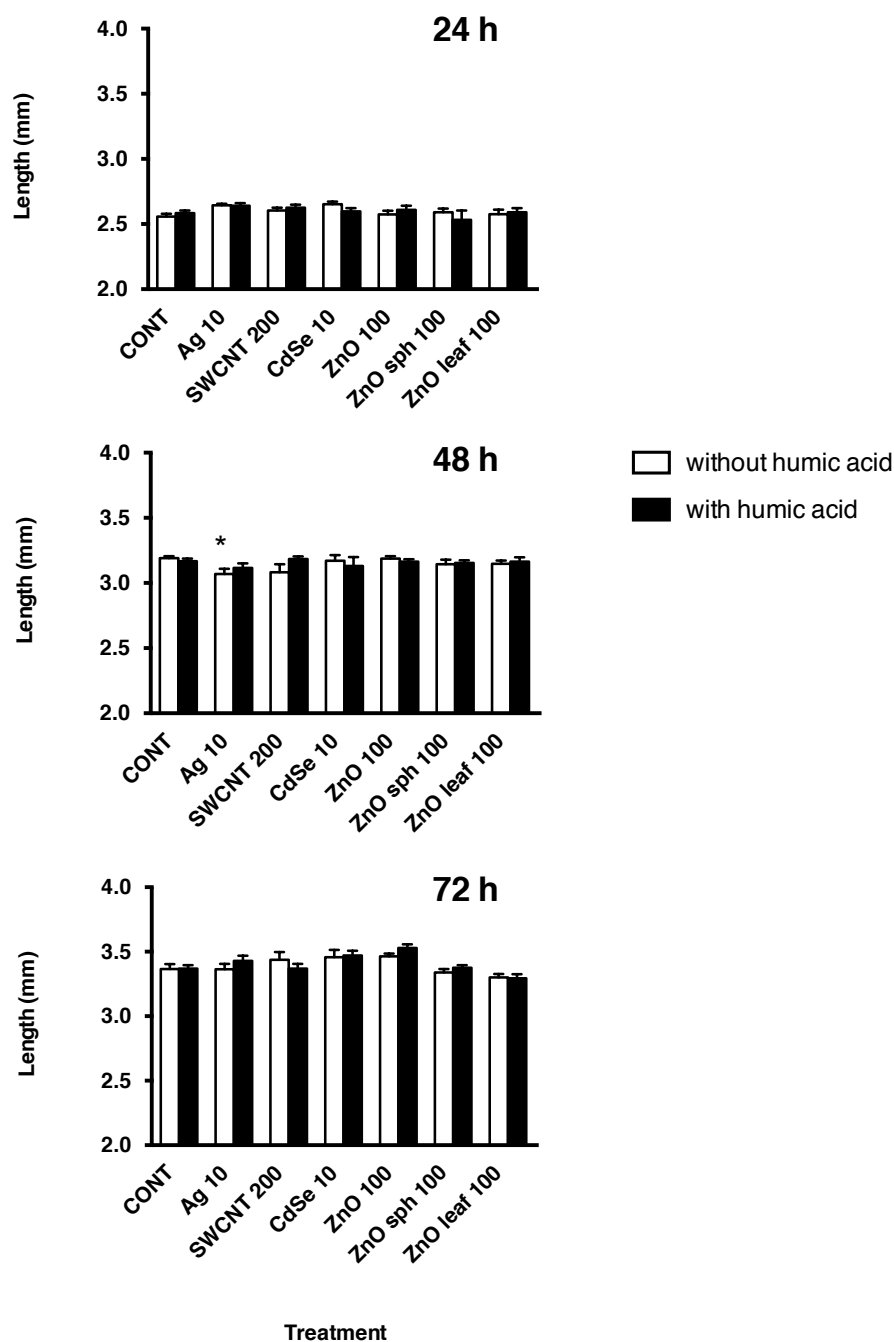
Figure 6-1. Length (mm) of zebrafish embryos at 24, 48, and 72 h after exposure to NPs with and without 10 mg/L HA. * denotes a significant difference ($p <$ 0.05) when compared to control.
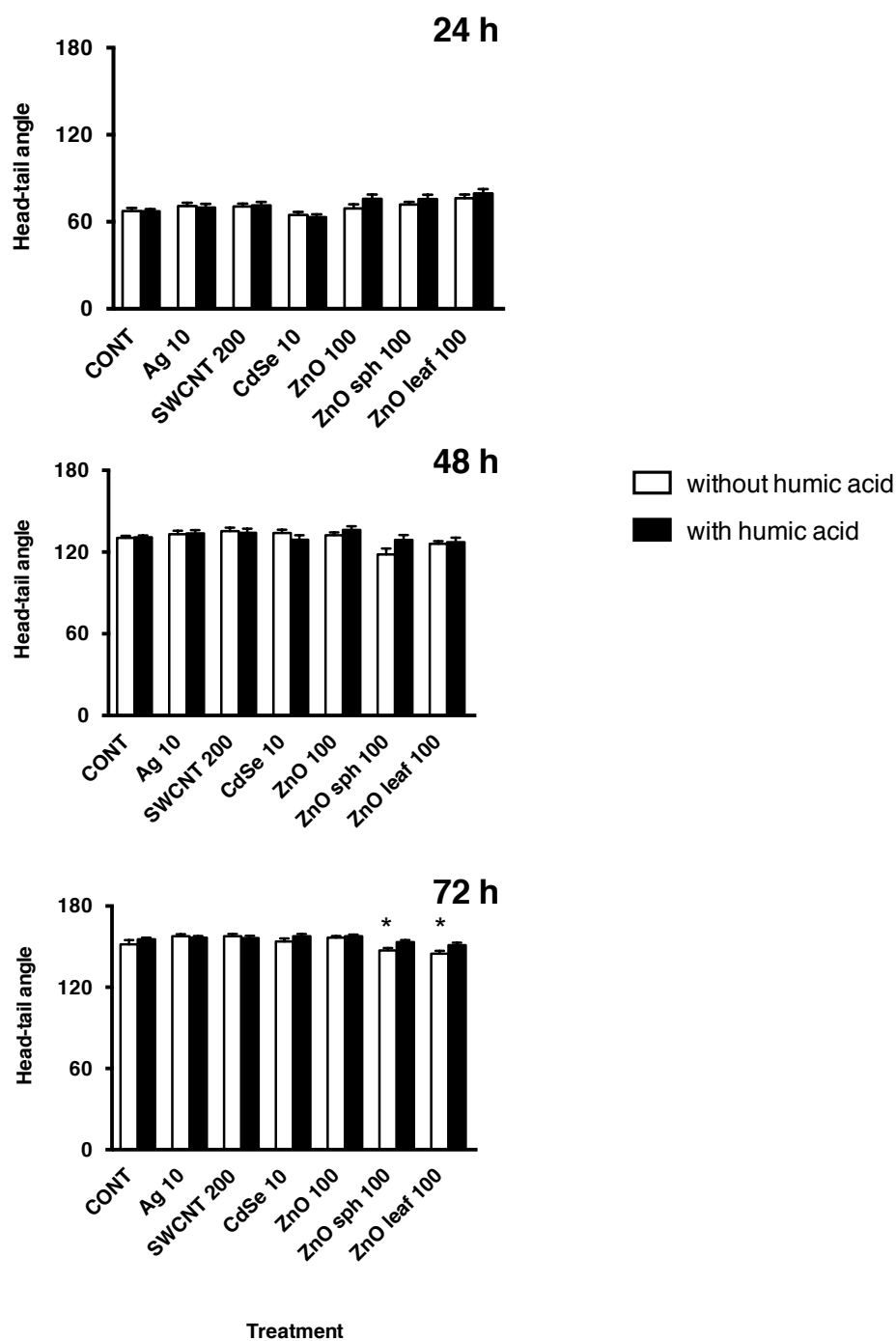
Figure 6-2. Head-tail angle of zebrafish embryos at 24, 48, and 72 h after exposure to NPs with and without 10 mg/L HA. * denotes a significant difference ($p < 0.05$) when compared to control.
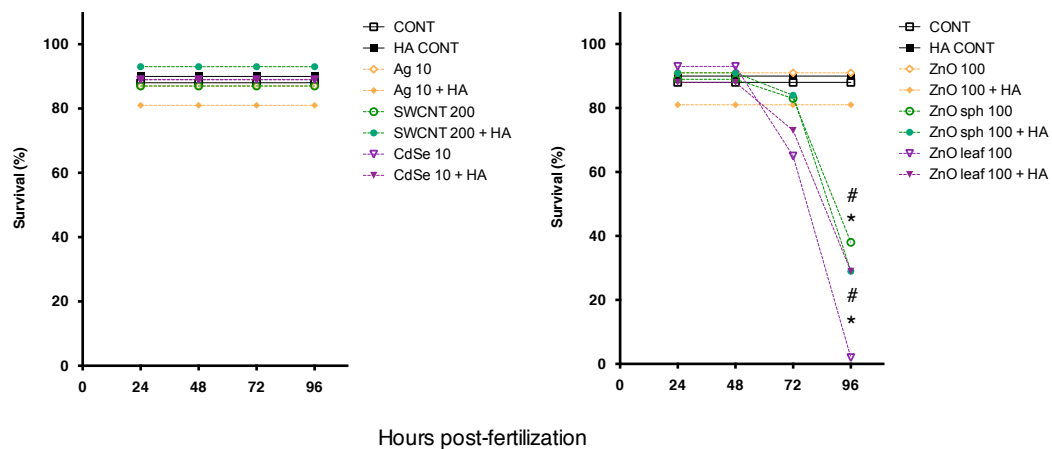
Figure 6-3. Survival (%) of zebrafish embryos at 24, 48, and 72 and 96 h after exposure to NPs without (open symbols) and with (closed symbols) 10 mg/L HA. * denotes a significant difference ($p < 0.05$) when compared to control. # denotes a significant difference ($p < 0.05$) when compared to HA control.
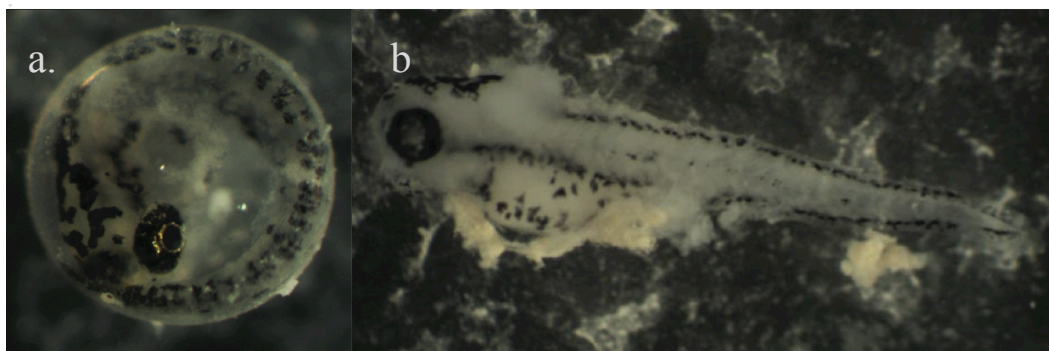
Figure 6-4. Micrographs of 96 hpf embryos exposed to ZnO sph + HA. a, Unhatched embryo still within the chorion and alive. b, Hatched embryo hatched and dead.
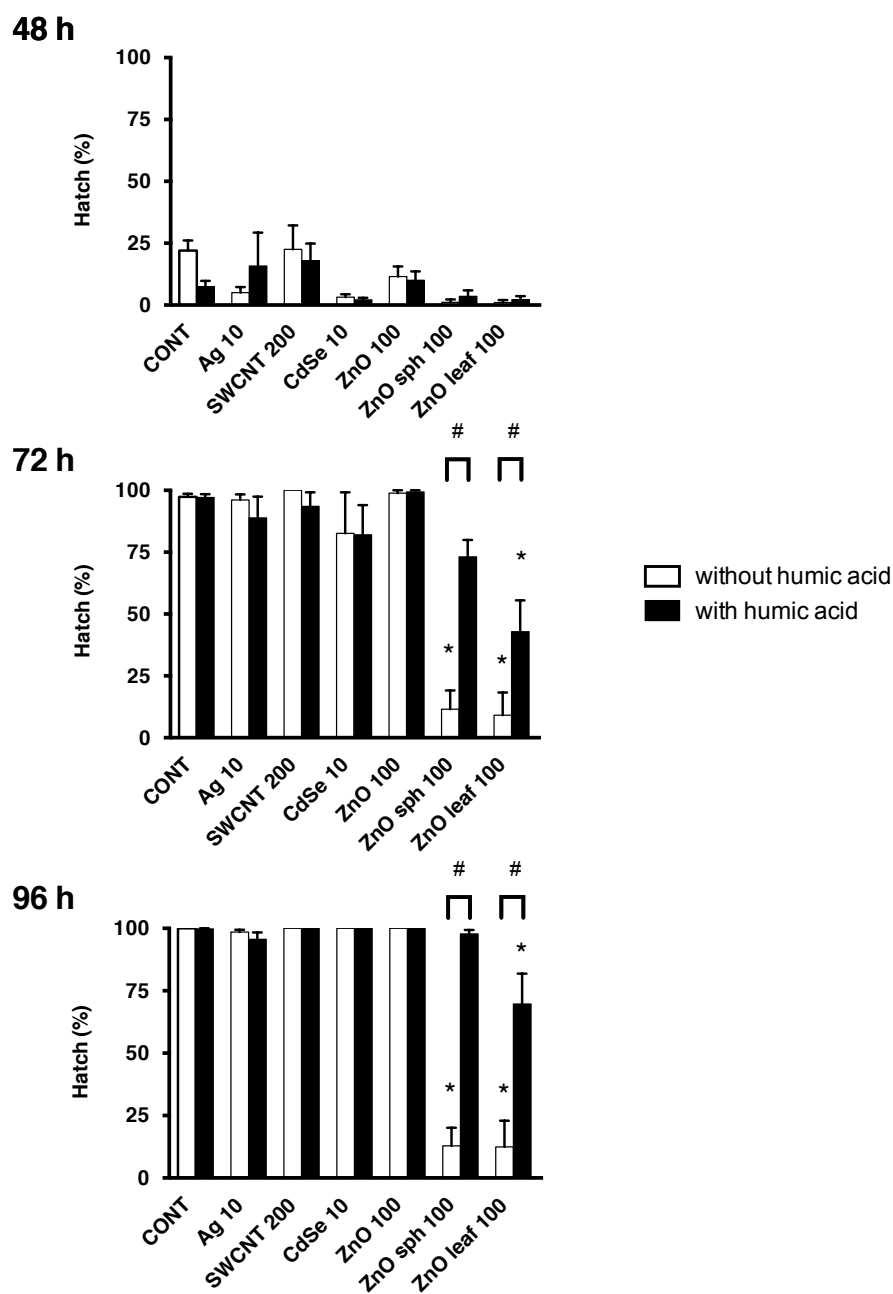
Figure 6-5. Hatch (%) at 48, 72, and 96 h of embryos exposed to nanoparticles and without (white bars), and with (black bars) 10 mg/L humic acid. * denotes a significant difference ($p < 0.05$) when compared to control. # denotes a significant difference ($p < 0.05$) when compared to HA control.
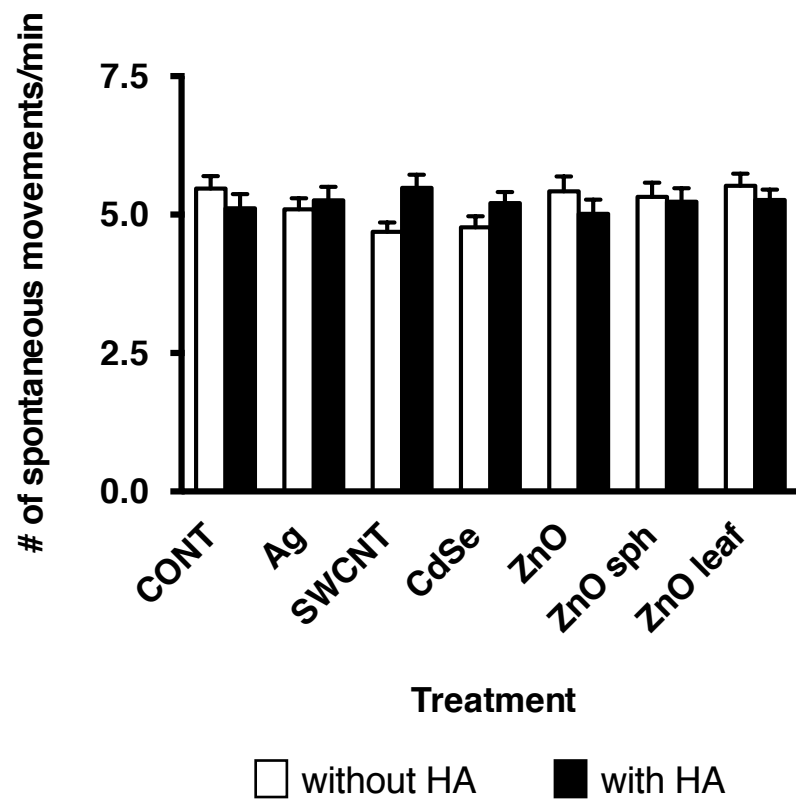
Figure 6-6. Spontaneous movements (movement/min) measured in 48 hpf embryos, measured over a ten minute period. No significant differences in movements were measured.
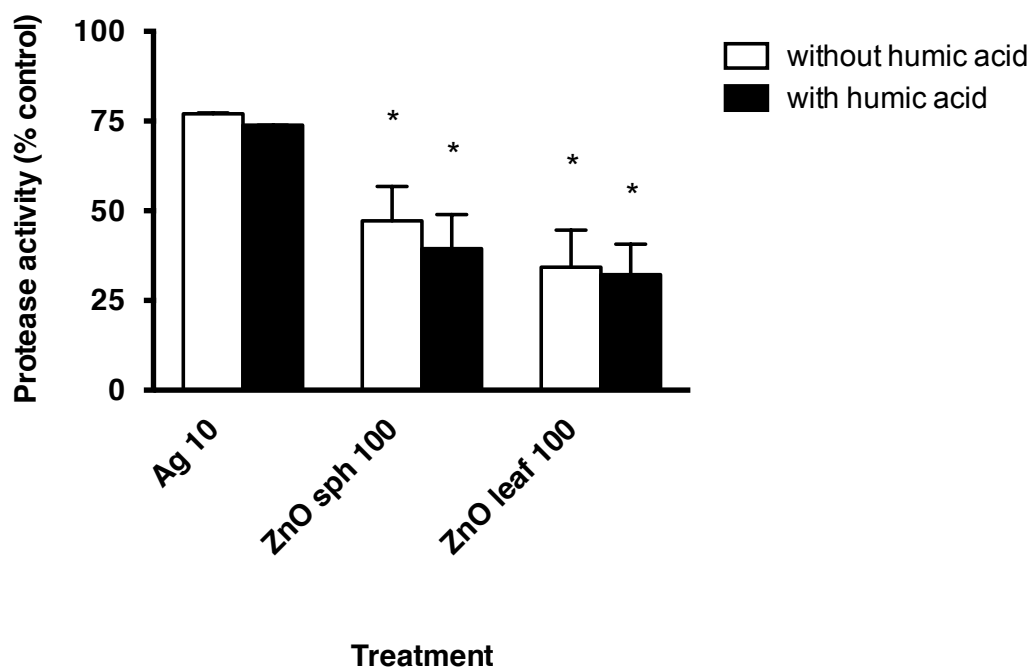
Figure 6-7. Protease activity (% control) of Ag, ZnO sph and ZnO leaf without HA (white bars) and with HA (black bars). * denotes $p < 0.05$ between treatments and control

CHAPTER 7

Inhibition of sodium uptake in silver nanoparticle-exposed juvenile trout

7.1. INTRODUCTION

Nanotechnology will enables a rapidly expanding industry due to increased production efficiency and heightened development of nanomaterials (NMs). A large number of the NMs presently used in consumer products are metal-based nanoparticles (NPs), including silver, copper, titanium, zinc, and gold cores. Silver (Ag) NPs are currently one of the most widely used NPs due to their unique physicochemical properties and bactericidal function, as well as relatively low manufacturing cost (Fabrega *et al.* 2009). The Woodrow Wilson database currently lists 313 consumer products that contain Ag NPs (as of 10 Mar 2011), including clothing, personal care products, wound dressings, teddy bears, washing machines, and air purifiers (Project on Emerging Technologies 2011).

Increased production of Ag NP-containing products will result in greater release of these particles and ionic Ag^+ into aquatic environments. Recent studies demonstrated that ionic Ag^+ and Ag NP can be released into wastewater from socks, washing machines, fabrics, facades, athletic shirts, toothpaste, as well as shampoo and detergent (Benn & Westerhoff 2008; Geranio *et al.* 2009; Benn *et al.* 2010; Kaegi *et al.* 2010; Farkas *et al.* 2011b). Estimates indicate that one household could potentially release 470 μg of ionic Ag^+ into the sewer daily from Ag NP-containing products (Benn *et al.* 2010), and, using SEM, it has been confirmed that Ag NPs are already present in wastewater.

An expansive body of research has detailed the toxic effects and bioavailability of ionic Ag^+ on aquatic organisms (Nebeker *et al.* 1983; Karen *et al.* 1998; Bianchini & Wood 2002; Bianchini *et al.* 2002; Grosell *et al.* 2009). Ag^+ may compete with Na^+ uptake across the apical membrane of the gills (Bury *et al.* 1999); however, it is unlikely that this phenomena would occur with Ag NPs as the diameter of the channels would not permit NPs to enter (Shaw & Handy 2011). A number of *in vivo* studies have demonstrated inhibition of Na^+ uptake and transporter activity in fish during exposure to ionic Ag^+ (Wood *et al.* 1996; Morgan *et al.* 1997) and it has been suggested this was attributable to inhibition of both carbonic anhydrase (CA) and Na^+,K^+-ATPase (NKA) (Morgan 2004). *In*

vitro studies have also confirmed acute ionic Ag^+ exposure in freshwater rainbow trout causes a reduction in Na^+ and Cl^- uptake across the gills by inhibiting NKA and CA activity within mitochondrial-rich cells (Wood *et al.* 2009; Goss *et al.* 2011).

Recently, studies have begun to assess the toxicity of Ag NPs to aquatic organisms and many of these studies have identified a number of biological effects on both vertebrate and invertebrate species (see review by Fabrega *et al.* 2011). In fish, Ag NPs have been reported to lower tolerance to hypoxia in Eurasian perch, *Perca fluviatilis* (Bilberg *et al.* 2010)*,* impair development in Japanese medaka embryos, *Oryzias latipes* (Wu *et al.* 2010)*,* and cause abnormal development in zebrafish, *Danio rerio* (Yeo & Kang 2008)*,* suppress the olfactory response in the Eurasian perch and crucian carp, *Carassius carassius* (Bilberg *et al.* 2011)*,* and increase stress levels, decrease plasma Na^+ concentrations, and inhibit NKA expression in juvenile Atlantic salmon, *Salmo salar* (Farmen *et al.* 2012).

Given the current interest in nanomaterials for large-scale applications and the uncertainty surrounding their toxicity, it is vitally important for regulators to determine if toxic effects are attributable to NPs themselves or ionic metal dissociating from the NPs. The aim of this study was to determine if Ag NPs affect sodium transport in juvenile trout *in vivo* and to distinguish the effects of Ag NPs from the dissolved ionic Ag^+ on unidirectional Na^+ uptake in juvenile rainbow trout (*Oncorhynchus mykiss*). In addition, we wanted to determine the potential mechanism of NP-interference of Na^+ uptake. These data will help establish whether metallic NPs require regulation that is independent of current "bulk materials" regulation due to NP-specific effects.

7.2. MATERIALS AND METHODS

7.2.1. Characterization of Ag NPs

Transmission electron microscopy (TEM) samples of Ag NPs were drop-cast from an aqueous suspension onto a carbon coated copper grid and dried

under vacuum. TEM and energy dispersive X-ray (EDX) analyses were performed using a JEOL-2010 (LaB6 filament) electron microscope with an accelerating voltage of 200 keV. X-ray Powder Diffraction (XRD) was performed using an INEL XRG 3000 X-ray diffractometer equipped with a Cu Kα radiation source ($\lambda = 1.54$ Å) and the sample was drop-coated in a silicon wafer. UV-vis spectra were recorded with a Hewlett-Packard 8453 UV-vis DAD spectrophotometer. Dynamic light scattering (DLS) and ζ-potential analyses were conducted to evaluate the Ag NPs in the same water used for the uptake experiments.

7.2.2. Animals

Juvenile rainbow trout (approximately 3 g) were maintained indoors in flow through 450 l fiberglass tanks supplied with aerated and de-chlorinated city of Edmonton tap water (hardness as $CaCO_3$: 1.6 mmol/L; alkalinity: 120 mg/L; NaCl: 0.5 mmol/L; pH 8.2; and temp 15 ˚C). Fish were fed ground dry commercial trout pellets once daily and were kept on a 14 h light:10 h dark photoperiod.

7.2.3. Dialysis experiment

Dialysis was performed to characterize the release of Ag^+ from the citrate-capped Ag NPs. Polypropylene beakers (250 ml; Nalgene) were soaked in 1% nitric acid in ddH_2O overnight to remove trace metal impurities and rinsed thoroughly with ddH_2O. 250 μl of a 1 g/L Ag NP stock was injected into Slide-A-Lyzer cassettes (2.5K MWCO, ThermoScientific, average pore size ~ 3 nm) and was slowly stirred in 250 mL of de-chlorinated city of Edmonton tap water. 2 mL water samples were collected prior to the introduction of the Slide-A-Lyzer to measure for baseline metals, and after 30 min to measure the amount of total Ag present in the stock solution. The Slide-A-Lyzer was then transferred to a fresh beaker of 250 mL water and samples were taken at 1 h, 3 h, 12 h, 24 h and 48 h, to measure the rate of dissolution of ionic Ag^+ from the NPs. Water samples were tested for total Ag using ICP-MS analysis (University of Alberta, Department of Earth and Atmospheric Sciences, detection limit 0.01 μg/L). The maximum

measured concentration of dissolved Ag (0.02 µg/L) was used in exposure experiments as a paired free metal control.

7.2.4. Trout exposures to Ag NPs

Juvenile rainbow trout were transferred to individual dark 60 ml chambers supplied with a constant flow of aerated, de-chlorinated city of Edmonton tap water that was kept at a constant temperature of 15 ˚C and fish were acclimated for 24 h. Unidirectional Na^+ flux was measured using radiolabelled ^{22}Na over a 3 h flux period according to established techniques (Goss & Wood 1990). A no-fish control was ran prior to the experiment and confirmed that there was no ^{22}Na disappearance from the flux chambers during a 3 h flux period. Water flow to chambers was stopped for the duration of flux experiments and 0.1 µCi/L of ^{22}Na was added to each chamber and allowed to mix for 5 min. To individual chambers, distilled water (0 mg/L Ag; control), 1.0 mg/L citrate-capped Ag NPs, 1.0 mg/L dialyzed citrate-capped Ag NPs or 10 µg/L and 0.02 µg/L Ag^+ (as bulk $AgNO_3$) were added and allowed to mix for 5 min. After equilibration (time 0 h) and at the end of the flux period (3 h), a 5 ml water sample was collected from each chamber and analyzed for ^{22}Na radioactivity using a Gamma counter (Packard Cobra II, Auto Gamma, Model 5010, Perkin Elmer, MA, USA) and total [Na^+] using atomic absorption spectrophotometry (Perkin Elmer, Model 3300, CT, USA). Juvenile rainbow trout were euthanized by an overdose of tricane methanesulfonate (MS-222; 1.0 g/L) buffered with $NaHCO_3^-$ at the completion of the experiment and the fish's gills were perfused with heparinized (15 mg) ice cold PBS (137 mmol/L NaCl, 2.7 mmol/L KCl, 4.3 mmol/L Na_2PO_4, 1.4 mmol/L NaH_2PO_4; pH 7.8; 290 mOsm). The left gill arch of each fish was then removed and placed in an 1.5 ml microcentrifuge tube containing SEI buffer (200 mmol/L sucrose, 20 mmol/L Na_2EDTA, 40 mmol/L imidazole) for measurement of NKA activity and the right gill arch removed and snap frozen in liquid nitrogen for measurement of CA activity and stored at -80˚C for further analysis.

7.2.5. Measurement of gill Na$^+$,K$^+$-ATPase and CA activity

Gill NKA activity was measured following the method developed by McCormick (1993). In brief, gill samples were thawed immediately prior to the assay and SEID buffer (200 mmol/L sucrose, 20 mmol/L Na$_2$EDTA, 40 mmol/L imidazole, and 0.1 % Na$^+$ deoxycholic acid; Sigma, St. Louis, MO, USA) was added to the tube. Tissue was homogenized on ice using a Polytron PT 1200 E handheld homogenizer (Kinematica A G, Switzerland) for 10 sec and centrifuged in an Eppendorf 5810R centrifuge (Eppendorf, Ontario, Canada) at 5,000 x g for 1 min. Homogenate (10 µL) from each sample was loaded into four wells on a 96-well plate and assay mixture (50 mmol/L imidazole, 2.8 mmol/L phosphoenolpyruvate, 0.22 mmol/L NADH, 0.7 mmol/L ATP, 4 U/mL lactic dehydrogenase, 5 U/mL pyruvate kinase, 47 mmol/L NaCl, 5.25 mmol/L MgCl and 10.5 mmol/L KCl) was added to the homogenate, with two replicates containing ouabain (0.5 mmol/L; Sigma). The optical density of the reaction was read at 340 nm using a kinetic assay at 10 sec intervals for a period of 10 min on a SpectraMax 340PC^{384} microplate spectrophotometer (Molecular Devices, CA, USA). Gill NKA activity was calculated by subtracting the ouabain-treated ATPase activity from the control ATPase activity and were reported as µmoles ADP mg^{-1} protein h^{-1}. Additional controls were run to determine if Ag NPs had an effect on the NKA assay. An Ag NP only control was run to examine possible false positives due to absorbance, fluorescence or luminescence of NPs. To test for potential false positives due to interactions between the Ag NPs, the assay mixture and/or the gill homogenate, a NP plus assay mixture control was run in the absence of the gill homogenate and in the presence of gill homogenate.

Carbonic anhydrase activity was measured according to Henry (1991), using the electrometric delta pH method. In brief, gill samples were homogenized in cold Tris buffer (100mM Tris base, 225mM mannitol, 75mM sucrose, adjusted to pH 7.4 with 10% phosphoric acid), centrifuged for 10 min at 13200 rpm, and supernatant was collected. 50 µL of the sample was injected into a chamber containing 6 mL of 4°C Tris buffer, and 200 µL of cooled CO$_2$-saturated distilled water was immediately injected to start the reaction. The reaction rate was

recorded for a 0.15 pH change to obtain the rate of reaction (pH units/sec) using a Radiometer GK2401 C combined pH electrode connected to a Radiometer PHM64 research pH meter and data software (Acqknowledge v3.7.3). The true net catalyzed rate was calculated by subtracting uncatalyzed rate (no sample injected) from the catalyzed rate (with sample) and buffer capacity was calculated to convert the rate to μmol CO_2 ml^{-1} min^{-1}. Each sample was measured in triplicate.

7.2.6. Statistical analysis

Data are reported as the mean ± SEM. All data sets were tested for homogeneity of variance and compared via a one-way ANOVA using SigmaPlot (version 11, Systat, Chicago, IL, USA). If significant differences ($p \leq 0.05$) were found, a post-hoc multiple comparisons Tukey test was applied to determine these differences.

7.3. RESULTS AND DISCUSSION

7.3.1. Characterization and dialysis of Ag NPs

The preparation of the citrate-capped Ag NPs was at a high concentration (>4 g/L) and used a fast reduction process through the addition of a reducing reagent ($NaBH_4$), therefore the size diameters of generated NP were not mono-distributed. DLS measurements showed most of the NPs possessed hydrodynamic diameter of 54.5 nm, indicating that some agglomeration was occurring. ζ-potential measurement of the silver NPs demonstrated NPs possessed a negative surface charge of -24.9 mV. UV-vis analysis showed the NP surface plasma absorbance peak was 428 nm for the citrate-capped silver NPs in solution (Figure 7-1a). TEM images of citrate-capped Ag NPs in the stock solution ranged in size from 5.89 – 35.37 nm (Figure 7-1b) with a mean size of 17.53 ± 9.43 nm (Figure 7-1c). X-ray powder diffraction and selected area electron diffraction (SAED) analyses confirmed the synthesized citrate-capped Ag NPs had crystalline structure (Figure 7-1d).

Citrate-capped Ag NPs used in this study were very stable with only trace amounts of ionic Ag^+ (< 0.01 µg/L) present in the stock solution. The highest concentration of Ag^+ measured during the 48 h dialysis experiment was 0.02 µg/L. This concentration was used as a paired ionic Ag^+ control in all subsequent experiments and represented the maximum concentration of ionic Ag^+ released from the Ag NPs over 48 h in the experimental media. After 2 h of dialyses, no further Ag^+ appeared to be released from the citrate-capped Ag NPs as $[Ag^+]$ were below detectable limits in samples collected at 3, 12, 24 and 48 h. The concentration of ionic Ag^+ dissociating from the NPs was less than 0.002 % of total silver, indicating that these NPs are very stable in the experimental solution and ideal for determining NP-specific effects. Other studies have reported that up to 25 - 50 % of the Ag^+ present in their Ag NP stock solution is in the form of ionic Ag^+ (Bilberg *et al.* 2011; Farmen *et al.* 2012) resulting in difficulties distinguishing between NP and free metal effects. Each NP formulation will differ in dissociation of ionic metal based on various factors, such as NP size, surface characteristics, and concentration, and also due to solution properties (Grassian 2008). To differentiate between NP and dissolved metal effects, it is important to measure ionic metal concentrations in NP stock solutions and determine ionic metal dissolution rates in the experimental media, as various metals, including Ag^+, are well known to elicit toxic effects in aquatic environments at low concentrations (Nebeker *et al.* 1983; Wendelaar Bonga & Lock 1992; Bianchini *et al.* 2002).

7.3.2. Sodium flux

We show that citrate-capped Ag NPs significantly inhibit Na^+ uptake in juvenile trout by over 60 % compared to the control and by over 50 % compared to the 0.02 µg/L ionic Ag^+ control (Figure 7-2). Sodium uptake in freshwater trout is thought to be mediated *via* a Na^+/H^+ exchanger or by an apical Na^+ channel type mechanism, and can be dependent on water chemistry (Wang 1987). It is possible the noted inhibition results from a direct effect on either (or both) of these mechanisms or via an inhibition of intracellular processes after translocation

of the NPs into the gill cells. This inhibition would explain some observed ionoregulatory and acid-base imbalances where reductions in plasma [Na^+] were noted following exposure to Ag NPs (Farmen *et al.* 2012). Ultimately, this would result in decreased physiological function and eventual death. Exposure of juvenile trout to 10 μg/L of ionic Ag^+ was used as a positive control and significantly inhibited Na^+ uptake by over 50 %. Ionic Ag^+ is well known to be an ionoregulatory toxicant in freshwater organisms and has previously been shown to significantly inhibit Na^+ uptake by over 50 % in rainbow trout (Wood *et al.* 1996), *Daphnia magna* (Bianchini & Wood 2002) and freshwater crayfish, *Cambarus diogenes* (Grosell *et al.* 2009) at this level.

Exposure of juvenile trout to 0.02 μg/L ionic Ag^+, the highest measured concentration of ionic Ag^+ dissolved from our NP stock solutions, as shown by dialysis, did not cause any significant inhibition of Na^+ uptake (Figure 7-2). This indicates the significant decrease in Na^+ uptake after exposure to Ag NPs is a "nano specific effect". To support this finding, we used Ag NPs that had been dialyzed immediately prior to the experiment and released non-detectable levels of ionic Ag^+ to measure Na^+ uptake. Dialyzed and non-dialyzed NP formulations both significantly inhibited Na^+ uptake by a similar degree compared to both the control and 0.02 μg/L ionic Ag^+ (Figure 7-2). In a recent study using juvenile Atlantic salmon, *Salmo salar*, Ag NP exposure resulted in decreased plasma [Na^+] after exposure to 100 μg/L of Ag NPs for 48 h (Farmen *et al.* 2012). However, the authors were unable to determine if the decrease was caused by the Ag NPs themselves or Ag^+ dissociating from the NPs because ionic Ag^+ or small Ag^+ complexes (<3nm in size) made up a large percentage (25 %) of the total 100 μg/L Ag NP stock solution (Farmen *et al.* 2012). In the current study, we clearly show that Ag NPs can significantly inhibit Na^+ uptake in fish in the absence of significant dissolution. This result highlights the importance of Ag NPs as an emerging aquatic toxicant and the pressing need for further studies to understand their potential impact on the environment.

7.3.3. Gill Na$^+$,K$^+$-ATPase and CA activity

In the current study, gill NKA activity in juvenile trout was significantly inhibited by ~50% after 3 hour exposure to Ag NPs (Figure 7-3). Griffitt *et al.* (2007) reported a 50 % decrease in gill NKA activity of zebrafish after they were exposed to 1.5 mg/L copper NPs and Shaw *et al.* (2012) recently demonstrated strong inhibition of gill NKA of approximately 6-fold in the gills of rainbow trout exposed to a low copper NP concentration of 100 μg/L for 10 days. Aluminum NPs have also been shown to significantly inhibit gill NKA activity in zebrafish (Griffitt *et al.* 2011) and gill NKA expression levels have been shown to be significantly down-regulated in zebrafish exposed to silver and copper NPs (Griffitt *et al.* 2008) and rainbow trout exposed to Ag NPs (Farmen *et al.* 2012).

In our study, CA was not affected by either Ag NPs or ionic Ag$^+$ (Figure 7-4), contrary to previous reports where 10 μg/L Ag$^+$ has been reported to inhibit CA activity by 28 % in rainbow trout (Morgan *et al.* 1997). However, these experiments differed both in fish size (up to 10x larger) and length of exposure (48 h fluxes versus our 3 h fluxes), suggesting that fish size and length of exposure to ionic Ag$^+$ will result in different 'snapshots' of Ag$^+$ effects. Indeed, exposure to ionic Ag$^+$ can temporally affect CA activity; trout gill CA activity was depressed by 4.3 μg/L Ag$^+$ up to 5 hours of exposure, and then returned to normal values between 5-8 hours of exposure, then depressed again after 8 hours (Morgan 2004). It is possible the fish in our study were affected at other time points, but were tested during this 'recovery' period. Very little has been reported about the potential for NPs to affect CA in fish. Some reports suggest that human CA bind to NPs (Lundqvist *et al.* 2004; Manokaran *et al.* 2010), therefore NPs may affect the function of these important enzymes. NP-interactions with proteins *in vivo* have the potential to affect the activity of proteins and change the physiological status of an organism; therefore it is important to continue examining these interactions.

7.3.4. Mechanisms of inhibition

In this study, Ag NPs significantly decrease Na^+ uptake in juvenile rainbow trout through the inhibition of gill NKA activity. Uptake of NPs has been shown to be dependent on size, charge, and surface chemistry of the particles but a firm understanding of this uptake is still unknown. It has been suggested NPs can be taken up *via* endocytic pathways (Chithrani & Chan 2007; von der Kammer *et al.* 2008a; Safi *et al.* 2011), while other studies point to receptor-mediated uptake (Chithrani & Chan 2007; Jiang *et al.* 2008). Translocation of Ag NPs into organisms has been shown *in vivo* in zebrafish embryos (Lee *et al.* 2007) and in *C. elegans* (Meyer *et al.* 2010). Similarly, adsorption to the cell membrane and uptake of Ag NPs has been demonstrated *in vitro* in lymphoblastoid cells (Safi *et al.* 2011) and in rainbow trout cells (Farkas *et al.* 2011b). Once inside the cell, there could be interaction between Ag NPs and various proteins, specifically NKA. NPs are known to interact with proteins and can affect protein activity (Fei & Perrett 2009; Casals *et al.* 2010). Biologically relevant proteins such as human carbonic anhydrase (HCAI) interact with silica NPs and disrupt the normal conformation of HCAI (Manokaran *et al.* 2010). Furthermore, this interaction with NPs, as shown in lactate dehydrogenase (LDH) and α-chymotrypsin (Karajanagi *et al.* 2004; MacCormack *et al.* 2012), can lead to an inhibition or complete elimination of activity. NP-protein interactions can be altered by physicochemical characteristics of the NPs. Charge, size, shape, and surface coating can all affect the NP-protein affinity (Lundqvist *et al.* 2008), therefore further studies will need to be performed to determine if the NPs used in this study interact directly with NKA.

While we did not find any effects of the free metal dissolved from the NPs, there is a possibility of intracellular dissociation of ionic Ag^+ from Ag NPs. If these NPs are being taken up by endocytic pathways, they may be packaged in endosomes or lysosomes, and these acidic environments could cause dissolution of the NPs (Cho *et al.* 2011; Zhao *et al.* 2011a). For example, superparamagnetic iron oxide NPs have been found to dissolve within endosomes or lysosomes into free iron, resulting in ROS increases (Laurent et al., 2012). However, much of this

ionic Ag^+ would likely be bound up by chloride or other intracellular inorganic ligands. Furthermore, NP adsorption to the mucus layer of the gills can occur (Smith *et al.* 2007), and NPs adsorbed to the gill surface may undergo higher dissolution rates than those in the water, leading to increased concentration of free metal at the gill site. Further work is needed to ascertain whether increased NP dissolution occurs *in vivo*. Regardless, there is evidence supporting that equivalent concentration of NP and ionic metal in the water can result in differential effects. Griffitt *et al.* (2008) conducted a microarray analysis of zebrafish gills after exposure to both copper and Ag NPs or ionic Cu and Ag and found very little overlap in gene expression profiles, suggesting that the mechanism of NP toxicity is different than ionic metal toxicity.

This study is the first to demonstrate specific inhibition of Na^+ uptake by NPs themselves independent of the free ion in solution resulting from dissolution of the Ag NP. Exposure to 1.0 mg/L citrate-capped Ag NP inhibits activity of NKA and results in decreased Na^+ flux. At this point we are unable to distinguish whether this inhibition is caused by Ag NPs directly binding to NKA or by ionic Ag^+ affecting NKA after being released from the NPs at the gill surface or after translocation and dissolution inside the cell. Future research will be addressing these possibilities and will ultimately aid in developing regulations for safe use of silver-based NMs.
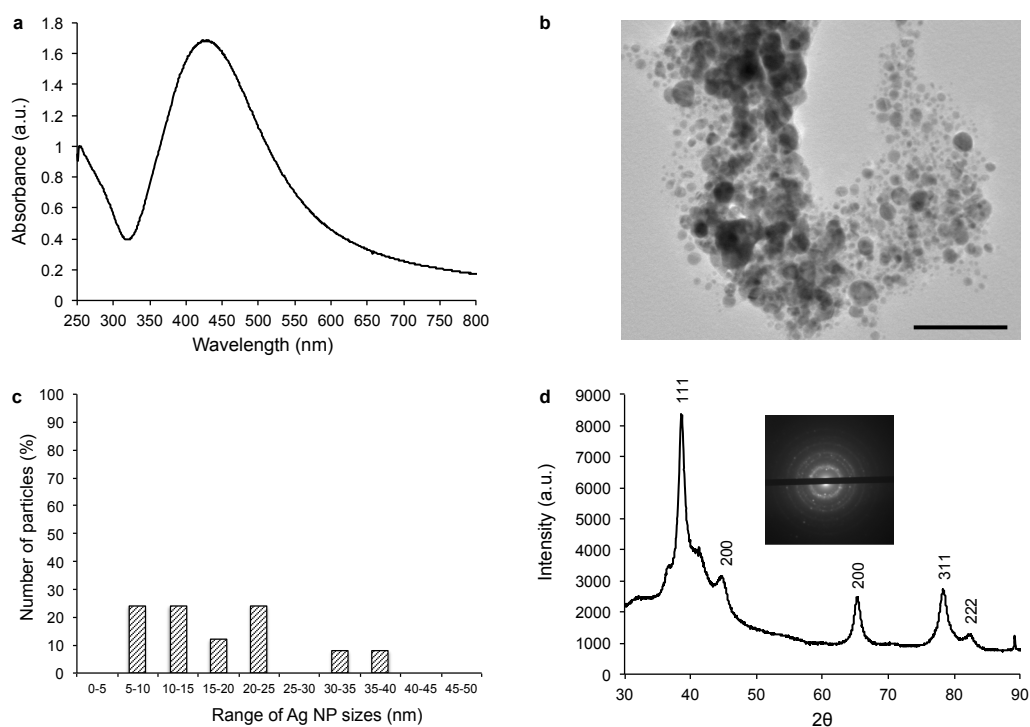
Figure 7-1. Characterization of citrate-capped silver NPs. (a) UV-vis spectrum; (b) TEM image of NPs in aqueous solution, scale bar = 100 nm; and (c) size distribution of citrate-capped silver NPs, with measurements obtained from the TEM images. Silver NPs ranged in size from 5.89 – 35.37 nm with an average size of 17.53 ± 9.43 nm. (d) X-ray powder diffraction (XRD) of citrate-capped silver NPs in solid and TEM measured EDS (embedded image).

136
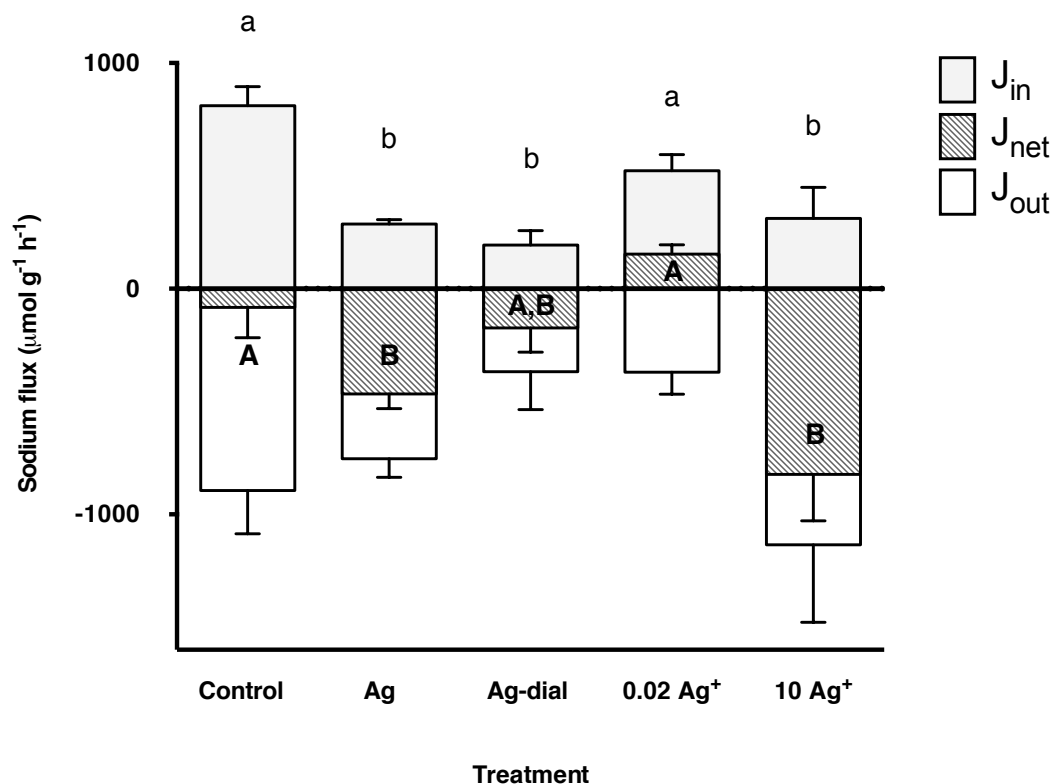
Figure 7-2. Unidirectional Na^+ fluxes in juvenile trout after exposure to 1 mg/L Ag NP (Ag), 1 mg/L dialyzed Ag NP (Ag-dial), and 0.02 and 10 µg/L ionic Ag^+ (0.02 and 10 Ag^+). Values are displayed as means ± SEM, $n = 6$. Positive values represent Na^+ uptake (J_{in}), negative values are Na^+ excretion out of fish (J_{out}) and hatched bars are net Na^+ flux (J_{net}). Groups with different lowercase or capital letters are significantly different from each other (ANOVA, $p < 0.05$). There were no significant differences between groups for Na^+ excretion.
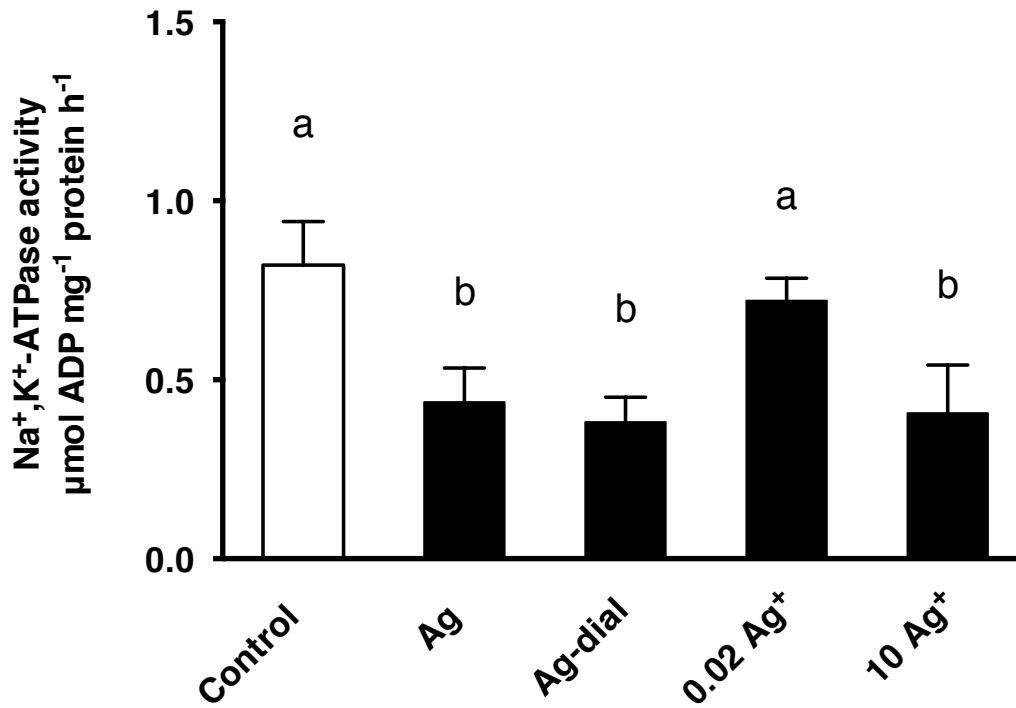
Figure 7-3. The effects of 1 mg/L Ag NP (Ag), 1 mg/L dialyzed Ag NP (Ag-dial), and 0.02 and 10 μg/L ionic Ag^+ (0.02 and 10 Ag^+) on gill NKA activity in juvenile trout. Values are means ± SEM, $n = 6$. Groups with different letters are significantly different from each other (ANOVA, $p < 0.05$).
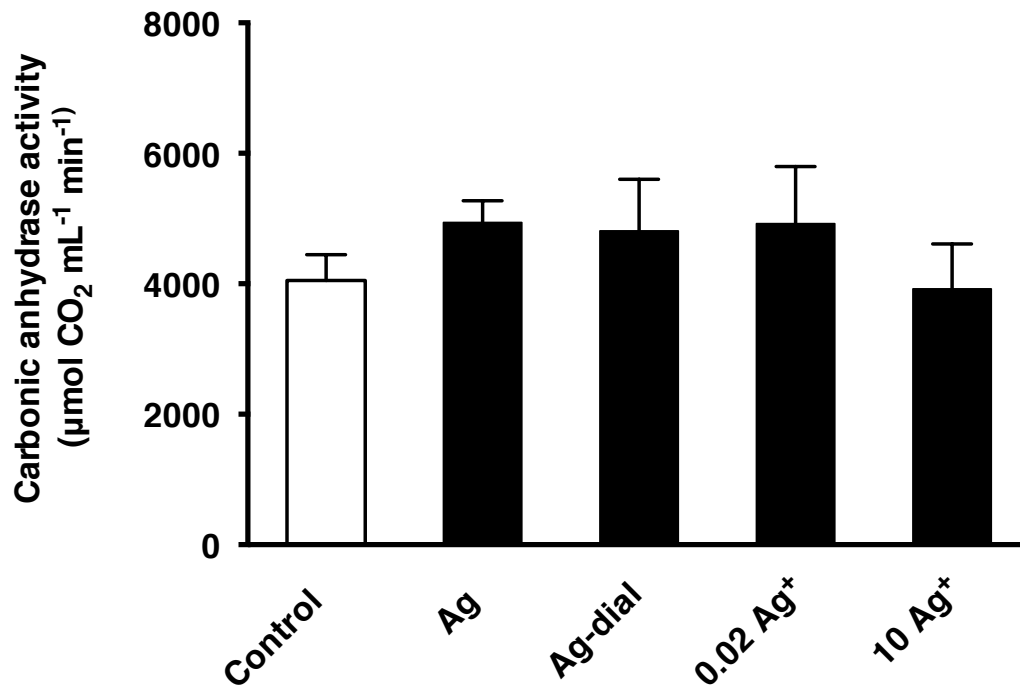
Figure 7-4. The effects of 1 mg/L Ag NP (Ag), 1 mg/L dialyzed Ag NP (Ag-dial), and 0.02 and 10 µg/L ionic Ag^+ (0.02 and 10 Ag^+) on gill CA activity in juvenile trout. Values are means ± SEM, $n = 6$. No significant differences were observed (ANOVA, $p > 0.05$).

CHAPTER 8

Conclusions and future directions

8.1. CONCLUSIONS AND FUTURE DIRECTIONS

My doctoral thesis examined the effects of NPs at the biochemical, cellular, and whole animal levels. It focused on aquatic freshwater animals, as these organisms are highly vulnerable to toxicants, and are highly likely come in contact with NP contamination. The experiments presented here were focused on addressing four main goals, as set out in the introduction: 1) To determine appropriate biochemical, *in vitro*, and *in vivo* assays for NP toxicity testing; 2) To link physicochemical characteristics with NP-toxicity; 3) To ascertain whether there is NP-specific toxicity; and 4) To elucidate mechanisms by which NP-interactions can affect biological function, with a focus on environmentally and physiologically relevant molecules.

### 8.1.1 Biochemical, *in vitro*, and *in vivo* assays

Performing experiments at the biochemical, cellular, and whole animal levels each have their own advantages and weaknesses. While *in vitro* and biochemical experiments can produce large amounts of data at low cost in a relatively short amount of time, the results do not necessary reflect those of *in vivo* studies. Exposure media changes the physicochemical properties of a NP, altering NP behavior and uptake, and therefore exposures in cell media may not represent those in freshwater media. In Chapter 3 I showed that Beas2B and HepG2 cells have different oxidative stress responses to CdSe NPs, indicating that there are differences in sensitivities between cells lines. However, laboratory cell lines may have some inherent issues; they may not accurately represent native cells lines in terms of complexity and furthermore, it has been suggested that long-term passage of these lines may alter their native characteristics (Hughes *et al.* 2007; Jones & Grainger 2009). Therefore, the use of *in vitro* lines to represent *in vivo* outcomes may not be realistic and must be treated with caution. However, solely performing *in vivo* experiments does not give enough information on the mechanism of effects. The value of using cell lines may be better employed after discoveries have been made *in vivo*. For example, we determined that sodium uptake in trout was inhibited in the presence of Ag NPs, and the mechanism by

which this occurs could be further elucidated using isolated gill cells. *In vitro* experiments could help distinguish whether NKA activity can be directly affected by NPs at the cellular or biochemical level, such as through physical interaction, or if the effects are caused by whole body responses to NPs, such as in response to decreased thyroid function in concert with lowered NKA activity (Monette *et al.* 2008).

It also necessary to include biochemical experiments to complement these data and understand the mechanisms of NP-induced damage. I used this approach in determining the effect of NPs on hatch. I hypothesized that chorionase, an enzyme essential for hatch, would be inhibited by NP interaction. Isolation of total chorionic fluid and subsequent testing of enzyme activity supported this hypothesis; however, the chorionic fluid contains a myriad of enzymes and proteins, and so it would be useful to isolate the specific hatching enzyme to confirm these results. Purification of hatching enzyme through high performance liquid chromatography, as performed by Sano *et al.* (2008), or production through cell transfection of the hatching gene could provide hatching enzyme isolates. A combination of *in vivo*, *in vitro*, and biochemical experimental techniques will help nanotoxicologists identify relevant environmental concerns, and then ascertain the mechanisms of NP effects. This will give a base for valuable data that can be used to further understand more complex systems, such as those at the community, population, and ecosystem levels.

8.1.2. Linking physicochemical characteristics with NP-effects

General conclusions made from the data presented in this thesis add to the growing literature confirming that core composition, functionalization and coatings, charge, shape, agglomerate size, and dissolution all affect NP behavior, interactions, and toxicity. However, prediction of toxicity solely based on one characteristic is often not possible; for example, in Chapter 2 I predicted that electrostatic forces should strongly dictate NP-protein interactions, but positively and negatively charged NPs often had the same effect on interference. NPs with similar core sizes and coatings, such as the quantum dot materials and the

polymer coated Vive NPs should in theory have similar surface features by which the cells or membranes recognize and process them. However, in most cases presented, interference or toxicity differs between these NPs. These differences are likely due to variances in the conditions used. For example, the media in which experiments are performed significantly change these physicochemical characteristics. Addition of humic acid changed hydrodynamic size and ζ-potential, which altered their biological effects, emphasizing the need to characterize NPs within the exposure media used. Undecylenic acid-functionalized CdSe NPs were not found to be acutely toxic in *in vitro* experiments, nor in *in vivo* exposure in E3 medium, but affected development and hatch in zebrafish embryos exposed in dTW. The higher ionic strength of the cell media and E3 medium alter the ζ-potential of the NPs and cause higher agglomeration, likely affecting NP interaction with membranes and enzymes and resulting in different outcomes. Furthermore, the NPs will undergo changes over time; UV exposure, oxidation, interactions with molecules, aging, dissolution within the organism, and so forth, will affect their physicochemical status (von der Kammer *et al.* 2012). Currently, these data are not always collected. Continuous tracking the properties of NPs during the actual exposures will provide more valuable data pertaining to their effects and how they relate to physicochemical properties.

8.1.3. Ascertaining NP-specific effects

Distinguishing the effects of NPs from their dissolved counterparts was examined throughout these series of experiments. Dialysis of the NPs in their exposure media revealed that most of the NPs used in this study were quite stable and did not release high amounts of metal. This minimized the effects of free metal and made these NPs ideal to investigate NP-specific effects. I concluded that NP-specific effects could occur at the biochemical level, interfering with developmental and physiological processes such as zebrafish hatch and trout ionoregulation. While these studies show stability of NPs in exposure media, I did not determine whether NPs dissolve within an organism or cells after uptake. Not

much is known about the physicochemical state of a NP after uptake; live-cell imaging using pH- (*e.g.,* BCECF dye) or Ca^{2+}- (*e.g.,* Fura-2AM) sensitive dyes would provide indications of whether NPs are affecting intracellular processes and use of free metal indicator dyes (*e.g.,* Fluozin for zinc), could detect dissolution of NPs. Differentiation of free metal and NP effects within an organism has proved to be difficult; measurement of NPs inside an organism are often dependent on methods that require ionization or dissolution of NPs (*e.g.,* ICP-MS). One possible method to distinguish NP from free metals effects *in vivo* could take advantage of metallothionein function. Upregulation of metallothionein is often used as an indicator of free metals effects and NP dissolution (King-Heiden *et al.* 2009; Pham *et al.* 2012). Inhibition or downregulation of this gene, such as through the production of a morpholino to block production of MT in aquatic organisms, in combination with exposure to stable, non-dissolving NPs, could provide more insight as to whether NPs are transforming within an organism and whether effects are due to dissolved metal.

8.1.4. Interactions and mechanisms of NP toxicity

The colloidal nature of NPs, its high affinity for proteins, and the ability for it to deform and inhibit enzyme activity are likely the distinguishing factors between NPs and other toxicants. I propose that NPs can bind to dyes, proteins, enzymes, transporters, and other small molecules that will affect biochemical and physiological status and create complications unique to nanotoxicity testing.

One of the main findings presented in this thesis was the discovery of extensive NP interference in a number of assays commonly used to assess toxicity. This is of concern, as a large amount of cellular and animal toxicity research employs these types of tests. Further research into the mechanism by which these assays are affected would allow for modification of existing assays, or innovation of new analyses that would be more appropriate for NP testing. Interference could be occurring through either the binding and deformation of the proteins used in the assay, or the oxidation the dyes by NPs themselves. Conformational protein changes can be studied with a number of techniques.

Fluorescence spectroscopy, a relatively straightforward technique, could give a general sense if structural changes are occurring in protein in the presence of NP. Tryptophan residues fluoresce with 295 nm excitation, and any conformation changes may expose or hide these amino acids (Shang *et al.* 2007). Therefore, shifts in fluorescence signal in protein with and without NP would indicate conformational changes. Secondary structure of proteins can be measured with circular dichroism (MacCormack *et al.* 2012). This technique employs dichroic light to detect helical structures, random coils, and beta sheets (Greenfield & Fasman 1969), and has been used to detect denatured proteins (Sreerama *et al.* 2000). Fourier Transform Infrared Spectroscopy (FTIR) can also be used to elucidate effects on secondary structure and can provide an idea of the relative changes of molecular bonds upon NP exposure (Surewicz *et al.* 1993). The use of NPs for dye degradation and oxidation is already being exploited, and techniques used to measure oxidation state of NP, such as x-ray photoelectron spectroscopy (Arabatzis 2003), could be used to elucidate whether NPs are reducing the dyes used in assays and interfering with their absorbance or fluorescence.

Interactions of NPs with environmentally relevant molecules, such as humic acid, will be essential components of well-rounded aquatic studies. In natural aquatic environments the inhibition of hatch by NP exposure may be abrogated by NP-humic acid interactions. It is unknown whether the interactions between NOM and NPs will persist over time. Physicochemical studies suggest that the agglomeration, dissolution, aging, and settling of NPs in natural environments will change over time (Nowack *et al.* 2011). Given that the physicochemical properties of a NP can significantly alter toxicity, long-term aquatic toxicity tests in environmentally relevant media are warranted.

NP-interaction with physiologically relevant molecules and the resultant effects are often not taken into account, as they are not traditional modes of toxic action. Many of these effects may be indirect. For example, the binding of nutrients or the binding of hatching enzyme does not occur within an animal, yet is crucial for viability and survival. Aquatic organisms may be particularly vulnerable to colloidal interactions due to the numerous biological surfaces over

which they will be exposed. Given that NPs have been found to collect in the digestive system of fish (Zhao *et al.* 2011a; Shaw *et al.* 2012), NPs may bind to and interfere with digestive enzyme function and resulting in decreased assimilation efficiency. Binding of NPs to the gills and skin (Johnston *et al.* 2010) could lead to interactions with proteases and lysozymes that protect fish from bacterial infection (Ellis 2001). The affinity between amino acids and NPs (Joshi *et al.* 2004) may impair the detection of these natural odorants in fish, leading to decreased predator or prey detection (Tierney *et al*. 2010). Given that every biological process involves a countless proteins and enzymes, these interactions and consequent physiological effects need to be explored.

8.2. FINAL THOUGHTS

The field of nanotechnology has rapidly developed throughout my PhD and over the past decade. As a result of this progress, nanotoxicologists have had to collaborate with scientists and engineers in all fields, consistently modify approaches, and think beyond pre-conceived notions based on classical toxicology. A need to provide extensive physicochemical characterization, perform thorough examination for NP-interference in assays, consider specific colloidal interactions, and monitor non-traditional endpoints have distinguished the field of Nanotoxicology. While the generation and publication of nanotoxicity data has advanced at an astonishing speed, perhaps this field may benefit from more careful consideration on how to proceed. Collection of nanotoxicology data solely based on the paradigms of classical toxicity testing may inundate the literature and make it very difficult to extricate beneficial data to advance our understanding of these materials. That being said, we need to continue to move forward and attempt to close the gap between development and toxicological testing of these materials. Nanotechnology can certainly provide substantial world-wide benefits, and nanotoxicologists must continue to provide reliable and relevant data to support this development.

9.1. LITERATURE CITED

Aaron JS, Greene AC, Kotula PG, Bachand GD, Timlin JA (2010) Advanced optical imaging reveals the dependence of particle geometry on interactions between CdSe quantum dots and immune cells. *Small*, **7**, 334–341.

Albrecht C, Scherbart AM, Berlo DV *et al.* (2009) Evaluation of cytotoxic effects and oxidative stress with hydroxyapatite dispersions of different physicochemical properties in rat NR8383 cells and primary macrophages. *Toxicology in Vitro*, **23**, 520–530.

An H, Jin B (2012) Prospects of nanoparticle–DNA binding and its implications in medical biotechnology. *Biotechnology Advances*, **30**, 1721–1732.

Arabatzis I (2003) Characterization and photocatalytic activity of Au/TiO2 thin films for azo-dye degradation. *Journal of Catalysis*, **220**, 127–135.

Asharani PV, Lian Wu Y, Gong Z, Valiyaveettil S (2008) Toxicity of silver nanoparticles in zebrafish models. *Nanotechnology*, **19**, 255102.

Asharani PV, lianwu Y, Gong Z, Valiyaveettil S (2011) Comparison of the toxicity of silver, gold and platinum nanoparticles in developing zebrafish embryos. *Nanotoxicology*, **5**, 43–54.

Asuri P, Bale SS, Karajanagi SS, Kane RS (2006a) The protein–nanomaterial interface. *Current Opinion in Biotechnology*, **17**, 562–568.

Asuri P, Karajanagi SS, Dordick JS, Kane RS (2006b) Directed assembly of carbon nanotubes at liquid−liquid interfaces: Nanoscale conveyors for interfacial biocatalysis. *Journal of the American Chemical Society*, **128**, 1046–1047.

Baalousha M, Manciulea A, Cumberland S, Kendall K, Lead JR (2008) Aggregation and surface properties of iron oxide nanoparticles: influence of pH and natural organic matter. *Environmental Toxicology and Chemistry*, **27**, 1875–1882.

Bae E-J, Park H-J, Park J-S *et al.* (2011) Effect of chemical stabilizers in silver nanoparticle suspensions on nanotoxicity. *Bulletin of the Korean Chemical Society*, **32**, 613–619.

Bai W, Zhang Z, Tian W *et al.* (2009) Toxicity of zinc oxide nanoparticles to zebrafish embryo: a physicochemical study of toxicity mechanism. *Journal of Nanoparticle Research*, **12**, 1645–1654.

Bailey RE, Nie S (2003) Alloyed semiconductor quantum dots: Tuning the optical properties without changing the particle size. *Journal of the American Chemical Society*, **125**, 7100–7106.

Bar-Ilan O, Albrecht RM, Fako VE, Furgeson DY (2009) Toxicity assessments of multisized gold and silver nanoparticles in zebrafish embryos. *Small*, **5**, 1897–1910.

Batley GE, Kirby JK, McLaughlin MJ (2012) Fate and risks of nanomaterials in aquatic and terrestrial environments. *Accounts of Chemical Research*,

Beer C, Foldbjerg R, Hayashi Y, Sutherland DS, Autrup H (2012) Toxicity of silver nanoparticles—Nanoparticle or silver ion? *Toxicology Letters*, **208**, 286–292.

Belyaeva EA, Dymkowska D, Więckowski MR, Wojtczak L (2008) Mitochondria as an important target in heavy metal toxicity in rat hepatoma AS-30D cells. *Toxicology and Applied Pharmacology*, **231**, 34–42.

Benn TM, Westerhoff P (2008) Nanoparticle silver released into water from commercially available sock fabrics. *Environmental Science & Technology*, **42**, 4133–4139.

Benn T, Cavanagh B, Hristovski K, Posner JD, Westerhoff P (2010) The release of nanosilver from consumer products used in the home. *Journal of Environment Quality*, **39**, 1875.

Berridge MV, Herst PM, Tan AS (2005) Tetrazolium dyes as tools in cell biology: new insights into their cellular reduction. *Biotechnology Annual Review*, **11**, 127–1252.

Bian S-W, Mudunkotuwa IA, Rupasinghe T, Grassian VH (2011) Aggregation and dissolution of 4 nm ZnO nanoparticles in aqueous environments: Influence of pH, ionic strength, size, and adsorption of humic acid. *Langmuir*, **27**, 6059–6068.

Bianchini A, Wood CM (2002) Physiological effects of chronic silver exposure in

Daphnia magna. Comparative Biochemistry and Physiology, Part C, **133**, 137–145.

Bianchini A, Grosell M, Gregory SM, Wood CM (2002) Acute silver toxicity in aquatic animals is a function of sodium uptake rate. *Environmental Science & Technology*, **36**, 1763–1766.

Bilberg K, Døving KB, Beedholm K, Baatrup E (2011) Silver nanoparticles disrupt olfaction in Crucian carp (Carassius carassius) and Eurasian perch (*Perca fluviatilis*). *Aquatic Toxicology*, **104**, 145–152.

Bilberg K, Malte H, Wang T, Baatrup E (2010) Silver nanoparticles and silver nitrate cause respiratory stress in Eurasian perch (*Perca fluviatilis*). *Aquatic Toxicology*, **96**, 159–165.

Borm P (2005) Research strategies for safety evaluation of nanomaterials, part v: Role of dissolution in biological fate and effects of nanoscale particles. *Toxicological Sciences*, **90**, 23–32.

Braunbeck T, Lammer E (2006) Background paper on fish embryo toxicity assays. German Federal Environmental Agency.

Brungs WA (1969) Chronic toxicity of zinc to the fathead minnow, *Pimephales promelas* Rafinesque. *Transactions of the American Fisheries Society*, **98**, 272–280.

Burleson D, Driessen M, Penn RL (2005) On the characterization of environmental nanoparticles. *Journal of Environmental Science and Health, Part A*, **39**, 2707–2753.

Bury NR, Galvez F, Wood CM (1999) Effects of chloride, calcium, and dissolved organic carbon on silver toxicity: Comparison between rainbow trout and fathead minnows. *Environmental Toxicology and Chemistry*, **18**, 56–62.

Bystrzejewska-Piotrowska G, Golimowski J, Urban PL (2009) Nanoparticles: Their potential toxicity, waste and environmental management. *Waste Management*, 1–9.

Casals E, Pfaller T, Duschl A, Oostingh GJ, Puntes V (2010) Time evolution of the nanoparticle protein corona. *ACS Nano*, **4**, 3623–3632.

Casey A, Herzog E, Davoren M *et al.* (2007) Spectroscopic analysis confirms the

interactions between single walled carbon nanotubes and various dyes commonly used to assess cytotoxicity. *Carbon*, **45**, 1425–1432.

Castaño A, Gómez-Lechón MJ (2005) Comparison of basal cytotoxicity data between mammalian and fish cell lines: A literature survey. *Toxicology in Vitro*, **19**, 695–705.

CEPA (2007) Proposed regulatory framework for nanomaterials under the Canadian Environmental Protection Act, 1999. Webpage: http://www.ec.gc.ca/subsnouvelles-newsubs/default.asp?lang=En&n=FD117B60-1#s3

Chan W-H, Shiao N-H, Lu P-Z (2006) CdSe quantum dots induce apoptosis in human neuroblastoma cells via mitochondrial-dependent pathways and inhibition of survival signals. *Toxicology Letters*, **167**, 191–200.

Chapman PM, Wang F (2000) Issues in ecological risk assessment of inorganic metals and metalloids. *Human and Ecological Risk Assessment: An International Journal*, **6**, 965–988.

Chen J, Xiu Z, Lowry GV, Alvarez PJJ (2011) Effect of natural organic matter on toxicity and reactivity of nano-scale zero-valent iron. *Water Research*, **45**, 1995–2001.

Chen KL, Elimelech M (2007) Influence of humic acid on the aggregation kinetics of fullerene (C60) nanoparticles in monovalent and divalent electrolyte solutions. *Journal of Colloid and Interface Science*, **309**, 126–134.

Chen N, He Y, Su Y *et al.* (2012) The cytotoxicity of cadmium-based quantum dots. *Biomaterials*, **33**, 1238–1244.

Cheng J, Flahaut E, Cheng SH (2007) Effect of carbon nanotubes on developing zebrafish (*Danio rerio*) embryos. *Enironmental Toxicology amd Chemistry*, **26**, 708–716.

Chithrani BD, Chan WCW (2007) Elucidating the mechanism of cellular uptake and removal of protein-coated gold nanoparticles of different sizes and shapes. *Nano Letters*, **7**, 1542–1550.

Cho SJ, Maysinger D, Jain M *et al.* (2007) Long-term exposure to cdte quantum dots causes functional impairments in live cells. *Langmuir*, **23**, 1974–1980.

Cho W-S, Duffin R, Howie SE *et al.* (2011) Progressive severe lung injury by zinc oxide nanoparticles; the role of Zn^{2+} dissolution inside lysosomes. *Particle and Fibre Toxicology*, **8**, 27.

Choi J, Zhang Q, Reipa V *et al.* (2009) Comparison of cytotoxic and inflammatory responses of photoluminescent silicon nanoparticles with silicon micron-sized particles in RAW 264.7 macrophages. *Journal of Applied Toxicology*, **29**, 52–60.

Chow ESH, Cheng SH (2003) Cadmium affects muscle type development and axon growth in zebrafish embryonic somitogenesis. *Toxicological Sciences*, **73**, 149–159.

Christian P, von der Kammer F, Baalousha M, Hofmann T (2008) Nanoparticles: structure, properties, preparation and behaviour in environmental media. *Ecotoxicology*, **17**, 326–343.

Clark RJ, Dang MKM, Veinot JGC (2010) Exploration of organic acid chain length on water-soluble silicon quantum dot surfaces. *Langmuir*, **26**, 15657–15664.

Clift MJD (2012) Quantum dots: An insight and perspective of their biological interaction and how this relates to their relevance for clinical use. *Theranostics*, **2**, 668–680.

Clift MJD, Boyles MSP, Brown DM, Stone V (2010) An investigation into the potential for different surface-coated quantum dots to cause oxidative stress and affect macrophage cell signalling *in vitro*. *Nanotoxicology*, **4**, 139–149.

Clift MJD, Varet J, Hankin SM *et al.* (2011) Quantum dot cytotoxicity *in vitro*: An investigation into the cytotoxic effects of a series of different surface chemistries and their core/shell materials. *Nanotoxicology*, **5**, 664–674.

Cormode DP, Skajaa T, Fayad ZA, Mulder WJM (2009) Nanotechnology in medical imaging: Probe design and applications. *Arteriosclerosis, Thrombosis, and Vascular Biology*, **29**, 992–1000.

Cross SE, Innes B, Roberts MS *et al.* (2007) Human skin penetration of sunscreen nanoparticles: *in-vitro* assessment of a novel micronized zinc oxide formulation. *Skin Pharmacology and Physiology*, **20**, 148–154.

Cundy AB, Hopkinson L, Whitby RLD (2008) Use of iron-based technologies in contaminated land and groundwater remediation: A review. *Science of The Total Environment*, **400**, 42–51.

Daniel M-C, Astruc D (2004) Gold nanoparticles: assembly, supramolecular chemistry, quantum-size-related properties, and applications toward biology, catalysis, and nanotechnology. *Chemical Reviews-Columbus*, **104**, 293.

Deng ZJ, Mortimer G, Schiller T *et al.* (2009) Differential plasma protein binding to metal oxide nanoparticles. *Nanotechnology*, **20**, 455101.

Derfus AM, Chan WCW, Bhatia SN (2004) Probing the cytotoxicity of semiconductor quantum dots. *Nano Letters*, **4**, 11–18.

Di Wu, Pak ES, Wingard CJ, Murashov AK (2012) Multi-walled carbon nanotubes inhibit regenerative axon growth of dorsal root ganglia neurons of mice. *Neuroscience Letters*, **507**, 72–77.

Diegoli S, Manciulea AL, Begum S *et al.* (2008) Interaction between manufactured gold nanoparticles and naturally occurring organic macromolecules. *Science of The Total Environment*, **402**, 51–61.

Dobrovolskaia MA, Clogston JD, Neun BW *et al.* (2008) Method for analysis of nanoparticle hemolytic properties *in vitro*. *Nano Letters*, **8**, 2180–2187.

Drexler E (1986) Engines of creation: The coming era of nanotechnology. Anchor Books, New York, NY, USA.

Edgington AJ, Roberts AP, Taylor LM *et al.* (2010) The influence of natural organic matter on the toxicity of multiwalled carbon nanotubes. *Environmental Toxicology and Chemistry*, **29**, 2511–2518.

Ellis AE (2001) Innate host defense mechanisms of fish against viruses and bacteria. *Developmental & Comparative Immunology*, **25**, 827–839.

Elsaesser A, Taylor A, de Yanés GS *et al.* (2010) Quantification of nanoparticle uptake by cells using microscopical and analytical techniques. *Nanomedicine*, **5**, 1447–1457.

Elzey S, Grassian VH (2009) Agglomeration, isolation and dissolution of commercially manufactured silver nanoparticles in aqueous environments. *Journal of Nanoparticle Research*, **12**, 1945–1958.

Erogbogbo F, Yong K-T, Roy I *et al.* (2011) *In vivo* targeted cancer imaging, sentinel lymph node mapping and multi-channel imaging with biocompatible silicon nanocrystals. *ACS Nano*, **5**, 413–423.

Evans DH (2005) The multifunctional fish gill: Dominant site of gas exchange, osmoregulation, acid-base regulation, and excretion of nitrogenous waste. *Physiological Reviews*, **85**, 97–177.

Fabrega J, Fawcett SR, Renshaw JC, Lead JR (2009) Silver nanoparticle impact on bacterial growth: Effect of pH, concentration, and organic matter. *Environmental Science & Technology*, **43**, 7285–7290.

Fabrega J, Luoma SN, Tyler CR, Galloway TS, Lead JR (2011) Silver nanoparticles: Behaviour and effects in the aquatic environment. *Environment International*, **37**, 517–531.

Farkas J, Christian P, Gallego-Urrea JA *et al.* (2011a) Uptake and effects of manufactured silver nanoparticles in rainbow trout (*Oncorhynchus mykiss*) gill cells. *Aquatic Toxicology*, **101**, 117–125.

Farkas J, Peter H, Christian P *et al.* (2011b) Characterization of the effluent from a nanosilver producing washing machine. *Environment International*, **37**, 1057–1062.

Farmen E, Mikkelsen HN, Evensen Ø *et al.* (2012) Acute and sub-lethal effects in juvenile Atlantic salmon exposed to low μg/L concentrations of Ag nanoparticles. *Aquatic Toxicology*, **108**, 78–84.

Farré M, Gajda-Schrantz K, Kantiani L, Barceló D (2008) Ecotoxicity and analysis of nanomaterials in the aquatic environment. *Analytical and Bioanalytical Chemistry*, **393**, 81–95.

Federici G, Shaw B, Handy R (2007) Toxicity of titanium dioxide nanoparticles to rainbow trout (*Oncorhynchus mykiss*): Gill injury, oxidative stress, and other physiological effects. *Aquatic Toxicology*, **84**, 415–430.

Fei L, Perrett S (2009) Effect of nanoparticles on protein folding and fibrillogenesis. *International Journal of Molecular Sciences*, **10**, 646–655.

Fenniri H, Deng B-L, Ribbe AE *et al.* (2002) Entropically driven self-assembly of multichannel rosette nanotubes. *Proceedings of the National Academy of*

Science, **99**, 6487–6492.

Fernández-Cruz ML, Lammel T, Connolly M *et al.* (2012) Comparative cytotoxicity induced by bulk and nanoparticulated ZnO in the fish and human hepatoma cell lines PLHC-1 and Hep G2. *Nanotoxicology*, 1–18.

Feynman, R (1960) There's plenty of room at the bottom. *Caltech Engineering and Science*, **23**, 22-36.

Filipe V, Hawe A, Jiskoot W (2010) Critical evaluation of nanoparticle tracking analysis (NTA) by NanoSight for the measurement of nanoparticles and protein aggregates. *Pharmaceutical Research*, **27**, 796–810.

Fischer HC, Chan WC (2007) Nanotoxicity: the growing need for *in vivo* study. *Current Opinion in Biotechnology*, **18**, 565–571.

Fujioka K, Hiruoka M, Sato K *et al.* (2008) Luminescent passive-oxidized silicon quantum dots as biological staining labels and their cytotoxicity effects at high concentration. *Nanotechnology*, **19**, 415102.

Gao J, Powers K, Wang Y *et al.* (2012) Influence of Suwannee River humic acid on particle properties and toxicity of silver nanoparticles. *Chemosphere*, **89**, 96–101.

Gao J, Youn S, Hovsepyan A *et al.* (2009) Dispersion and toxicity of selected manufactured nanomaterials in natural river water samples: Effects of water chemical composition. *Environmental Science & Technology*, **43**, 3322–3328.

George S, Xia T, Rallo R *et al.* (2011) Use of a high-throughput screening approach coupled with *in vivo* zebrafish embryo screening to develop hazard ranking for engineered nanomaterials. *ACS Nano*, **5**, 1805–1817.

Geranio L, Heuberger M, Nowack B (2009) The Behavior of Silver Nanotextiles during Washing. *Environmental Science & Technology*, **43**, 8113–8118.

Gorham JM, MacCuspie RI, Klein KL, Fairbrother DH, Holbrook RD (2012) UV-induced photochemical transformations of citrate-capped silver nanoparticle suspensions. *Journal of Nanoparticle Research*, **14**, 1139.

Goss GG, Wood CM (1990) Na+ and Cl− Uptake kinetics, diffusive effluxes and acidic equivalent fluxes across the gills of rainbow trout: II. Responses to bicarbonate infusion. *Journal of Experimental Biology*, **152**, 549–571.

Goss G, Gilmour K, Hawkings G *et al.* (2011) Mechanism of sodium uptake in PNA negative MR cells from rainbow trout, *Oncorhynchus mykiss* as revealed by silver and copper inhibition. *Comparative Biochemistry and Physiology, Part A*, **159**, 234–241.

Grassian VH (2008) When size really matters: Size-dependent properties and surface chemistry of metal and metal oxide nanoparticles in gas and liquid phase environments. *Journal of Physical Chemistry C*, **0**, 0–0.

Greenfield NJ, Fasman GD (1969) Computed circular dichroism spectra for the evaluation of protein conformation. *Biochemistry*, **8**, 4108–4116.

Griffitt RJ, Brown-Peterson NJ, Savin DA *et al.* (2011) Effects of chronic nanoparticulate silver exposure to adult and juvenile sheepshead minnows (Cyprinodon variegatus) (SJ Klaine, Ed,). *Environmental Toxicology and Chemistry*, **31**, 160–167.

Griffitt RJ, Hyndman K, Denslow ND, Barber DS (2008) Comparison of molecular and histological changes in zebrafish gills exposed to metallic nanoparticles. *Toxicological Sciences*, **107**, 404–415.

Griffitt RJ, Weil R, Hyndman KA *et al.* (2007) Exposure to copper nanoparticles causes gill injury and acute lethality in zebrafish (*Danio rerio*). *Environmental Science & Technology*, **41**, 8178–8186.

Grosell M, Brauner CJ, Kelly SP *et al.* (2009) Physiological responses to acute silver exposure in the freshwater crayfish (Cambarus diogenes diogenes)—a model invertebrate? *Environmental Toxicology and Chemistry*, **21**, 369–374.

Guo L, Bussche Von Dem A, Buechner M *et al.* (2008) Adsorption of essential micronutrients by carbon nanotubes and the implications for nanotoxicity testing. *Small*, **4**, 721–727.

Gülden M, Mörchel S, Seibert H (2005) Comparison of mammalian and fish cell line cytotoxicity: impact of endpoint and exposure duration. *Aquatic Toxicology*, **71**, 229–236.

Hall JB, Dobrovolskaia MA, Patri AK, McNeil SE (2007) Characterization of nanoparticles for therapeutics. *Nanomedicine*, **2**, 789–803.

Han X, Gelein R, Corson N *et al.* (2011) Validation of an LDH assay for

assing nanoparticle toxicity. *Toxicology*, **287**, 99–104.

Han YJ, Loo SCJ, Phung NT, Boey F, Ma J (2008) Controlled size and morphology of EDTMP-doped hydroxyapatite nanoparticles as model for 153Samarium-EDTMP doping. *Journal of Materials Science: Materials in Medicine*, **19**, 2993–3003.

Hanada S, Fujioka K, Futamura Y *et al.* (2013) Evaluation of anti-inflammatory drug-conjugated silicon quantum dots: Their cytotoxicity and biological effect. *International Journal of Molecular Sciences*, **14**, 1323–1334.

Handy RD, von der Kammer F, Lead JR *et al.* (2008a) The ecotoxicology and chemistry of manufactured nanoparticles. *Ecotoxicology*, **17**, 287–314.

Handy RD, Owen R, Valsami-Jones E (2008b) The ecotoxicology of nanoparticles and nanomaterials: current status, knowledge gaps, challenges, and future needs. *Ecotoxicology*, **17**, 315–325.

Hankin S, Boraschi D, Duschl A, Lehr C-M, Lichtenbeld H (2011) Towards nanotechnology regulation–Publish the unpublishable. *Nano Today*, **6**, 228–231.

Harada Y, Wang JT, Doppalapudi VA *et al.* (1998) Differential effects of different forms of hydroxyapatite and hydroxyapatite/tricalcium phosphate particulates on human monocyte/macrophages *in vitro*. *Journal of Biomedical Materials Research*, **31**, 19–26.

Harush-Frenkel O, Rozentur E, Benita S, Altschuler Y (2008) Surface charge of nanoparticles determines their endocytic and transcytotic pathway in polarized MDCK cells. *Biomacromolecules*, **9**, 435–443.

Hassellöv M, Readman JW, Ranville JF, Tiede K (2008) Nanoparticle analysis and characterization methodologies in environmental risk assessment of engineered nanoparticles. *Ecotoxicology*, **17**, 344–361.

Health Canada (2011) Policy Statement on Health Canada's working definition for nanomaterials. http://www.hc-sc.gc.ca/sr-sr/pubs/nano/pol-eng.php

Hedderman TG, Keogh SM, Chambers G, Byrne HJ (2004) Solubilization of SWNTs with organic dye molecules. *The Journal of Physical Chemistry B*, **108**, 18860–18865.

Hendren CO, Mesnard X, Dröge J, Wiesner MR (2011) Estimating production data for five engineered nanomaterials as a basis for exposure assessment. *Environmental Science & Technology*, **45**, 2562–2569.

Heng BC, Zhao X, Tan EC *et al.* (2011) Evaluation of the cytotoxic and inflammatory potential of differentially shaped zinc oxide nanoparticles. *Archives of Toxicology*, **85**, 1517–1528.

Henry RP (1991) Techniques for measuring carbonic anhydrase activity *in vitro*. *Carbonic Anhydrases: Cellular Physiology and Molecular Genetics. Plenum, New York*, 119–131.

Henry TB, Petersen EJ, Compton RN (2011) Aqueous fullerene aggregates (nC60) generate minimal reactive oxygen species and are of low toxicity in fish: a revision of previous reports. *Current Opinion in Biotechnology*, **22**, 533–537.

Hertog den J (2005) Chemical genetics: drug screens in zebrafish. *Bioscience Reports*, **25**, 289–297.

Hessel CM, Henderson EJ, Veinot JGC (2007) An investigation of the formation and growth of oxide-embedded silicon nanocrystals in hydrogen silsesquioxane-derived nanocomposites. *Journal of Physical Chemistry C*, **111**, 6956–6961.

Hikosaka K, Kim J, Kajita M, Kanayama A, Miyamoto Y (2008) Platinum nanoparticles have an activity similar to mitochondrial NADH:ubiquinone oxidoreductase. *Colloids and Surfaces B: Biointerfaces*, **66**, 195–200.

Hill AJ (2005) Zebrafish as a model vertebrate for investigating chemical toxicity. *Toxicological Sciences*, **86**, 6–19.

Holder AL, Goth-Goldstein R, Lucas D, Koshland CP (2012) Particle-induced artifacts in the MTT and LDH viability assays. *Chemical Research in Toxicology*, **25**, 1885–1892.

Holsapple MP (2005) Research strategies for safety evaluation of nanomaterials, part ii: Toxicological and safety evaluation of nanomaterials, current challenges and data needs. *Toxicological Sciences*, **88**, 12–17.

Hoo CM, Starostin N, West P, Mecartney ML (2008) A comparison of atomic

force microscopy (AFM) and dynamic light scattering (DLS) methods to characterize nanoparticle size distributions. *Journal of Nanoparticle Research*, **10**, 89–96.

Hoshino A, Fujioka K, Oku T *et al.* (2004) Physicochemical properties and cellular toxicity of nanocrystal quantum dots depend on their surface modification. *Nano Letters*, **4**, 2163–2169.

Huang W, Cao L, Shan X *et al.* (2009) Toxic effects of zinc on the development, growth, and survival of Red Sea Bream *Pagrus major* embryos and larvae. *Archives of Environmental Contamination and Toxicology*, **58**, 140–150.

Huang X, El-Sayed IH, Yi X, El-Sayed MA (2005) Gold nanoparticles: Catalyst for the oxidation of NADH to NAD. *Journal of Photochemistry and Photobiology B: Biology*, **81**, 76–83.

Hughes P, Marshall D, Reid Y, Parkes H, Gelber C (2007) The costs of using unauthenticated, over-passaged cell lines: how much more data do we need? *BioTechniques*, **43**, 575–586.

Hyung H, Kim J-H (2008) Natural organic matter (NOM) adsorption to multi-walled carbon nanotubes: Effect of nom characteristics and water quality parameters. *Environmental Science & Technology*, **42**, 4416–4421.

Inohaya K, Yasumasu S, Araki K *et al.* (1997) Species-dependent migration of fish hatching gland cells that commonly express astacin-like proteases in common. *Development, Growth & Differentiation*, **39**, 191–197.

Irizar J, Dinglasan J, Goh JB *et al.* (2008) Raman spectroscopy of nanoparticles using hollow-core photonic crystal fibers. *IEEE Journal of Selected Topics in Quantum Electronics*, **14**, 1214–1222.

Ispas C, Andreescu D, Patel A *et al.* (2009) Toxicity and developmental defects of different sizes and shape nickel nanoparticles in zebrafish. *Environmental Science & Technology*, **43**, 6349–6356.

Iversen T-G, Skotland T, Sandvig K (2011) Endocytosis and intracellular transport of nanoparticles: Present knowledge and need for future studies. *Nano Today*, **6**, 176–185.

Jezierska B, Ługowska K, Witeska M (2008) The effects of heavy metals on

embryonic development of fish (a review). *Fish Physiology and Biochemistry*, **35**, 625–640.

Jiang W, Kim BYS, Rutka JT, Chan WCW (2008) Nanoparticle-mediated cellular response is size-dependent. *Nature Nanotechnology*, **3**, 145–150.

Jin R, Cao Y, Mirkin CA *et al.* (2001) Photoinduced conversion of silver nanospheres to nanoprisms. *Science*, **294**, 1901–1903.

Johnson RL, Johnson GO, Nurmi JT, Tratnyek PG (2009) Natural organic matter enhanced mobility of nano zerovalent iron. *Environmental Science & Technology*, **43**, 5455–5460.

Johnston BD, Scown TM, Moger J *et al.* (2010) Bioavailability of nanoscale metal oxides TiO_2, CeO_2, and ZnO to fish. *Environmental Science & Technology*, **44**, 1144–1151.

Jones CF, Grainger DW (2009) *In vitro* assessments of nanomaterial toxicity. *Advanced Drug Delivery Reviews*, **61**, 438–456.

Joshi H, Shirude, PS, Bansal, V *et al*. (2004) Isothermal titration calorimetry studies on the binding of amino acids to gold nanoparticles. *The Journal of Physical Chemistry B*, **108**, 11535-11540.

Jovanović B, Anastasova L, Rowe EW *et al.* (2010) Effects of nanosized titanium dioxide on innate immune system of fathead minnow (*Pimephales promelas* Rafinesque, 1820). *Ecotoxicology and Environmental Safety*, 1–9.

Kaegi R, Sinnet B, Zuleeg S *et al.* (2010) Release of silver nanoparticles from outdoor facades. *Environmental Pollution*, **158**, 2900–2905.

Kaegi R, Ulrich A, Sinnet B *et al.* (2008) Synthetic TiO_2 nanoparticle emission from exterior facades into the aquatic environment. *Environmental Pollution*, **156**, 233–239.

Kane RS, Stroock AD (2007) Nanobiotechnology: Protein-nanomaterial interactions. *Biotechnology Progress*, **23**, 316–319.

Karajanagi SS, Vertegel AA, Kane RS, Dordick JS (2004) Structure and function of enzymes adsorbed onto single-walled carbon nanotubes. *Langmuir*, **20**, 11594–11599.

Karen DJ, Ownby DR, Forsythe BL *et al.* (1998) Influence of water quality on

silver toxicity to rainbow trout (*Oncorhynchus mykiss*), fathead minnows (*Pimephales promelas*), and water fleas (*Daphnia magna*). *Environmental Toxicology & Chemistry*. **18**, 63-70.

Kashiwada S (2006) Distribution of nanoparticles in the See-through medaka (*Oryzias latipes*). *Environmental Health Perspectives*. **114**, 1697-1702.

Kelly KL, Coronado E, Zhao LL, Schatz GC (2003) The optical properties of metal nanoparticles: The influence of size, shape, and dielectric environment. *The Journal of Physical Chemistry B*, **107**, 668–677.

Keynes R (2005) J.Z. and the discovery of squid giant nerve fibres. *Journal of Experimental Biology*, **208**, 179–180.

Kim KS, Cota-Sanchez G, Kingston CT *et al.* (2007) Large-scale production of single-walled carbon nanotubes by induction thermal plasma. *Journal of Physics D: Applied Physics*, **40**, 2375–2387.

Kim KT, Jang M-H, Kim J-Y *et al.* (2012) Embryonic toxicity changes of organic nanomaterials in the presence of natural organic matter. *Science of The Total Environment*, **426**, 423–429.

Kim KT, Truong L, Wehmas L, Tanguay RL (2013) Silver nanoparticle toxicity in the embryonic zebrafish is governed by particle dispersion and ionic environment. *Nanotechnology*, **24**, 115101.

Kim T-G, Park B (2005) Synthesis and growth mechanisms of one-dimensional strontium hydroxyapatite nanostructures. *Inorganic Chemistry*, **44**, 9895–9901.

King-Heiden TC, Wiecinski PN, Mangham AN *et al.* (2009) Quantum dot nanotoxicity assessment using the zebrafish embryo. *Environmental Science & Technology*, **43**, 1605–1611.

Kirchner C, Liedl T, Kudera S *et al.* (2005) Cytotoxicity of colloidal cdse and CdSe/ZnS nanoparticles. *Nano Letters*, **5**, 331–338.

Klaine SJ, Alvarez PJJ, Batley GE *et al.* (2008) Nanomaterials in the environment: Behaviour, fate, bioavailability, and effects. *Environmental Science & Technology*, **27**, 1825-1851.

Klein-Macphee G, Cardin JA, Berry WJ (1984) Effects of silver on eggs and

larvae of the winter flounder. *Transactions of the American Fisheries Society*, **113**, 247–251.

Kroll A, Pillukat MH, Hahn D, Schnekenburger J (2012) Interference of engineered nanoparticles with *in vitro* toxicity assays. *Archives of Toxicology*, **86**, 1123–1136.

Kühnel D, Busch W, Meißner T *et al.* (2009) Agglomeration of tungsten carbide nanoparticles in exposure medium does not prevent uptake and toxicity toward a rainbow trout gill cell line. *Aquatic Toxicology*, **93**, 91–99.

Lapresta-Fernandez A, Fernández A, Blasco J (2012) Nanoecotoxicity effects of engineered silver and gold nanoparticles in aquatic organisms. *Trends in Analytical Chemistry*, **32**, 40–59.

Laurent S, Burtea C, Thirifays C, Häfeli UO, Mahmoudi M (2012) Crucial ignored parameters on nanotoxicology: The importance of toxicity assay modifications and "cell vision" (W-C Chin, Ed,). *PLoS ONE*, **7**, e29997.

Lee KJ, Nallathamby PD, Browning LM, Osgood CJ, Xu X-HN (2007) *In vivo* imaging of transport and biocompatibility of single silver nanoparticles in early development of zebrafish embryos. *ACS Nano*, **1**, 133–143.

Lee SK, Freitag D, Steinberg C, Kettrup A, Kim YH (1993) Effects of dissolved humic materials on acute toxicity of some organic chemicals to aquatic organisms. *Water Research*, **27**, 199–204.

Lee S, Kim K, Shon HK, Kim SD, Cho J (2011) Biotoxicity of nanoparticles: effect of natural organic matter. *Journal of Nanoparticle Research*, **13**, 3051–3061.

Lévy M, Lagarde F, Maraloiu V-A *et al.* (2010) Degradability of superparamagnetic nanoparticles in a model of intracellular environment: follow-up of magnetic, structural and chemical properties. *Nanotechnology*, **21**, 395103.

Li, Rothberg LJ (2004) Label-free colorimetric detection of specific sequences in genomic DNA amplified by the polymerase chain reaction. *Journal of the American Chemical Society*, **126**, 10958–10961.

Li B, Guo B, Fan H, Zhang X (2008) Preparation of nano-hydroxyapatite particles

with different morphology and their response to highly malignant melanoma cells *in vitro*. *Applied Surface Science*, **255**, 357–360.

Li M, Lin D, Zhu L (2013) Effects of water chemistry on the dissolution of ZnO nanoparticles and their toxicity to Escherichia coli. *Environmental Pollution*, **173**, 97–102.

Li ZY, Lam WM, Yang C *et al.* (2007) Chemical composition, crystal size and lattice structural changes after incorporation of strontium into biomimetic apatite. *Biomaterials*, **28**, 1452–1460.

Li Z, Greden K, Alvarez PJJ, Gregory KB, Lowry GV (2010) Adsorbed polymer and nom limits adhesion and toxicity of nano scale zerovalent iron to e. coli. *Environmental Science & Technology*, **44**, 3462–3467.

Lim SI, Zhong C-J (2009) Molecularly mediated processing and assembly of nanoparticles: Exploring the interparticle interactions and structures. *Accounts of Chemical Research*, **42**, 798–808.

Limbach LK, Li Y, Grass RN *et al.* (2005) Oxide nanoparticle uptake in human lung fibroblasts: Effects of particle size, agglomeration, and diffusion at low concentrations. *Environmental Science & Technology*, **39**, 9370–9376.

Lin S, Wiesner MR (2012) Deposition of aggregated nanoparticles — A theoretical and experimental study on the effect of aggregation state on the affinity between nanoparticles and a collector surface. *Environmental Science & Technology*, **46**, 13270–13277.

Lin Y-S, Wu S-H, Hung Y *et al.* (2006) Multifunctional composite nanoparticles: magnetic, luminescent, and mesoporous. *Chemistry of Materials*, **18**, 5170–5172.

Liu S, Xu L, Zhang T, Ren G, Yang Z (2010) Oxidative stress and apoptosis induced by nanosized titanium dioxide in PC12 cells. *Toxicology*, **267**, 172–177.

Liu X, Wazne M, Chou T, Xiao R, Xu S (2011) Influence of Ca^{2+} and Suwannee River Humic Acid on aggregation of silicon nanoparticles in aqueous media. *Water Research*, **45**, 105–112.

Liu Z, Ren G, Zhang T, Yang Z (2009) Action potential changes associated with

the inhibitory effects on voltage-gated sodium current of hippocampal CA1 neurons by silver nanoparticles. *Toxicology*, **264**, 179–184.

Lo LY, Li Y, Yeung KW, Yuen C (2007) Indicating the development stage of nanotechnology in the textile and clothing industry. *International Journal of Nanotechnology*, **4**, 667–679.

Long TC, Saleh N, Tilton RD, Lowry GV, Veronesi B (2006) Titanium dioxide (P25) produces reactive oxygen species in immortalized brain microglia (BV2): Implications for nanoparticle neurotoxicity. *Environmental Science & Technology*, **40**, 4346–4352.

Loo SCJ, Siew YE, Ho S, Boey FYC, Ma J (2008) Synthesis and hydrothermal treatment of nanostructured hydroxyapatite of controllable sizes. *Journal of Materials Science: Materials in Medicine*, **19**, 1389–1397.

Lord MS, Foss M, Besenbacher F (2010) Influence of nanoscale surface topography on protein adsorption and cellular response. *Nano Today*, **5**, 66–78.

Love SA, Maurer-Jones MA, Thompson JW, Lin Y-S, Haynes CL (2012) Assessing nanoparticle toxicity. *Annual Review of Analytical Chemistry*, **5**, 181–205.

Lovrić J, Bazzi HS, Cuie Y *et al.* (2005) Differences in subcellular distribution and toxicity of green and red emitting CdTe quantum dots. *Journal of Molecular Medicine*, **83**, 377–385.

Lundqvist M, Stigler J, Elia G *et al.* (2008) Nanoparticle size and surface properties determine the protein corona with possible implications for biological impacts. *Proceedings of the National Academy of Science*, **105**, 14265–14270.

Lynch I, Dawson KA (2008) Protein-nanoparticle interactions. *Nano Today*, **3**, 40–47.

Lynch I, Salvati A, Dawson KA (2009) Protein-nanoparticle interactions: What does the cell see? *Nature Nanotechnology*, **4**, 546–547.

Ma H, Brennan A, Diamond SA (2012a) Phototoxicity of TiO_2 nanoparticles under solar radiation to two aquatic species: *Daphnia magna* and Japanese

medaka. *Environmental Toxicology and Chemistry*, **31**, 1621–1629.

Ma H, Brennan A, Diamond SA (2012b) Photocatalytic reactive oxygen species production and phototoxicity of titanium dioxide nanoparticles are dependent on the solar ultraviolet radiation spectrum. *Environmental Toxicology and Chemistry*, **31**, 2099–2107.

Ma S, Lin D (2012) The biophysicochemical interactions at the interfaces between nanoparticles and aquatic organisms: Adsorption and internalization. *Environmental Science: Processess and Impacts*, **15**, 145.

MacCarthy P (2001) The principles of humic substances. *Soil Science*, **166**, 738–751.

MacCormack TJ, Clark RJ, Dang MKM *et al.* (2012) Inhibition of enzyme activity by nanomaterials: Potential mechanisms and implications for nanotoxicity testing. *Nanotoxicology*, **6**, 514–525.

Mallick K, Witcomb M, Scurrell M (2006) Silver nanoparticle catalysed redox reaction: An electron relay effect. *Materials Chemistry and Physics*, **97**, 283–287.

Manokaran S, Zhang X, Chen W, Srivastava DK (2010) Differential modulation of the active site environment of human carbonic anhydrase XII by cationic quantum dots and polylysine. *BBA - Proteins and Proteomics*, **1804**, 1376–1384.

Marquis BJ, Love SA, Braun KL, Haynes CL (2009) Analytical methods to assess nanoparticle toxicity. *The Analyst*, **134**, 425.

McCormick SD (1993) Methods for nonlethal gill biopsy and measurement of Na^+, K+-ATPase activity. *Journal of the Fisheries Board of Canada*, **50**, 656–658.

McKim JM (1977) Evaluation of tests with early life stages of fish for predicting long-term toxicity. *Journal of the Fisheries Board of Canada*, **34**, 1148–1154.

Meinelt T, Playle RC, Pietrock M *et al.* (2001) Interaction of cadmium toxicity in embryos and larvae of zebrafish (*Danio rerio*) with calcium and humic substances. *Aquatic Toxicology*, **54**, 205–215.

Meng H, Yang S, Li Z *et al.* (2011) Aspect ratio determines the quantity of

mesoporous silica nanoparticle uptake by a small GTPase-dependent macropinocytosis mechanism. *ACS Nano*, **5**, 4434–4447.

Meyer JN, Lord CA, Yang XY *et al.* (2010) Intracellular uptake and associated toxicity of silver nanoparticles in *Caenorhabditis elegans*. *Aquatic Toxicology*, **100**, 140–150.

Monette MY, Björnsson BT, McCormick SD (2008) Effects of short-term acid and aluminum exposure on the parr-smolt transformation in Atlantic salmon (Salmo salar): Disruption of seawater tolerance and endocrine status. *General and Comparative Endocrinology*, **158**, 122–130.

Monteiro-Riviere NA, Inman AO (2006) Challenges for assessing carbon nanomaterial toxicity to the skin. *Carbon*, **44**, 1070–1078.

Monteiro-Riviere NA, Inman AO, Zhang LW (2009) Limitations and relative utility of screening assays to assess engineered nanoparticle toxicity in a human cell line. *Toxicology and Applied Pharmacology*, **234**, 222–235.

Montes-Burgos I, Walczyk D, Hole P *et al.* (2009) Characterisation of nanoparticle size and state prior to nanotoxicological studies. *Journal of Nanoparticle Research*, **12**, 47–53.

Morgan IJ, Henry RP, Wood CM (1997) The mechanism of acute silver nitrate toxicity in freshwater rainbow trout (*Oncorhynchus mykiss*) is inhibition of gill Na^+ and $Cl-$ 1 transport. *Aquatic Toxicology*, **38**, 145–163.

Morgan TP (2004) Time course analysis of the mechanism by which silver inhibits active Na^+ and Cl- uptake in gills of rainbow trout. *AJP: Regulatory, Integrative and Comparative Physiology*, **287**, R234–R242.

Motskin M, Wright DM, Muller K *et al.* (2009) Hydroxyapatite nano and microparticles: Correlation of particle properties with cytotoxicity and biostability. *Biomaterials*, **30**, 3307–3317.

Müller RH, Radtke M, Wissing SA (2002) Solid lipid nanoparticles (SLN) and nanostructured lipid carriers (NLC) in cosmetic and dermatological preparations. *Advanced Drug Delivery Reviews*, **54**, S131–S155.

Nebeker AV, McAuliffe CK, Mshar R, Stevens DG (1983) Toxicity of silver to steelhead and rainbow trout, fathead minnows and *Daphnia magna*.

Environmental Toxicology and Chemistry, **2**, 95–104.

Nel AE, Mädler L, Velegol D *et al.* (2009) Understanding biophysicochemical interactions at the nano–bio interface. *Nature Publishing Group*, **8**, 543–557.

Nel A, Xia T, Mädler L, Li N (2006) Toxic potential of materials at the nanolevel. *Science*, **311**, 622–627.

Nghiem THL, La TH, Vu XH *et al.* (2010) Synthesis, capping and binding of colloidal gold nanoparticles to proteins. *Advances in Natural Sciences: Nanoscience and Nanotechnology*, **1**, 025009.

Nowack B, Bucheli T (2007) Occurrence, behavior and effects of nanoparticles in the environment. *Environmental Pollution*, **150**, 5–22.

Nowack B, Ranville JF, Diamond S *et al.* (2011) Potential scenarios for nanomaterial release and subsequent alteration in the environment. *Environmental Toxicology and Chemistry*, **31**, 50–59.

Oberdörster E (2004) Manufactured Nanomaterials (Fullerenes, C60) Induce oxidative stress in the brain of juvenile largemouth bass. *Environmental Health Perspectives*, **112**, 1058–1062.

Oberdörster G, Oberdörster E, Oberdörster J (2005) Nanotoxicology: An emerging discipline evolving from studies of ultrafine particles. *Environmental Health Perspectives*, **113**, 823–839.

OBrien HKJHS, Curl RF, Smalley RE (1985) C60 buckminsterfulleren. *Nature*, **318**, 162163.

Okuda-Shimazaki J, Takaku S, Kanehira K, Sonezaki S, Taniguchi A (2010) Effects of titanium dioxide nanoparticle aggregate size on gene expression. *International Journal of Molecular Sciences*, **11**, 2383–2392.

Ong HT, Loo JSC, Boey FYC *et al.* (2007) Exploiting the high-affinity phosphonate–hydroxyapatite nanoparticle interaction for delivery of radiation and drugs. *Journal of Nanoparticle Research*, **10**, 141–150.

Osborne OJ, Johnston BD, Moger J *et al.* (2012) Effects of particle size and coating on nanoscale Ag and TiO_2 exposure in zebrafish (*Danio rerio*) embryos. *Nanotoxicology*, 1–10.

Palazzo B, Sidoti MC, Roveri N *et al.* (2005) Controlled drug delivery from

porous hydroxyapatite grafts: An experimental and theoretical approach. *Materials Science and Engineering: C*, **25**, 207–213.

Park H, Grassian VH (2010) Commercially manufactured engineered nanomaterials for environmental and health studies: Important insights provided by independent characterization. *Environmental Toxicology and Chemistry*, **29**, 715–721.

Park J, Nam J, Won N *et al.* (2011) Compact and stable quantum dots with positive, negative, or zwitterionic surface: Specific cell interactions and non-specific adsorptions by the surface charges. *Advanced Functional Materials*, **21**, 1558–1566.

Park J-H, Gu L, Maltzahn von G *et al.* (2009) Biodegradable luminescent porous silicon nanoparticles for *in vivo* applications. *Nature Publishing Group*, **8**, 331–336.

Parng C (2005) *In vivo* zebrafish assays for toxicity testing. *Current Opinions in Drug Discovery and Development*, **8**, 100–106.

Paul W, Sharma CP (1999) Development of porous spherical hydroxyapatitegranules: application towards protein delivery. *Journal of Materials Science: Materials in Medicine*, **10**, 383–388.

Perreault F, Oukarroum A, Melegari SP, Matias WG, Popovic R (2012) Polymer coating of copper oxide nanoparticles increases nanoparticles uptake and toxicity in the green alga Chlamydomonas reinhardtii. *Chemosphere*, **87**, 1388–1394.

Petosa AR, Jaisi DP, Quevedo IR, Elimelech M, Tufenkji N (2010) Aggregation and deposition of engineered nanomaterials in aquatic environments: Role of physicochemical interactions. *Environmental Science & Technology*, **44**, 6532–6549.

Pezzatini S, Solito R, Morbidelli L *et al.* (2005) The effect of hydroxyapatite nanocrystals on microvascular endothelial cell viability and functions. *Journal of Biomedical Materials Research Part A*, **76**, 656–663.

Pfaller T, Colognato R, Nelissen I *et al.* (2010) The suitability of different cellular *in vitro* immunotoxicity and genotoxicity methods for the analysis of

nanoparticle-induced events. *Nanotoxicology*, **4**, 52–72.

Pham CH, Yi J, Gu MB (2012) Biomarker gene response in male medaka (*Oryzias latipes*) chronically exposed to silver nanoparticle. *Ecotoxicology and Environmental Safety*, **78**, 239–245.

Playle RC (1998) Modelling metal interactions at fish gills. *Science of The Total Environment*, **219**, 147–163.

Porter AL, Youtie J (2009) Where does nanotechnology belong in the map of science? *Nature Nanotechnology*, **4**, 534-536.

Powers CM, Yen J, Linney EA, Seidler FJ, Slotkin TA (2010) Silver exposure in developing zebrafish (*Danio rerio*): Persistent effects on larval behavior and survival. *Neurotoxicology and Teratology*, **32**, 391–397.

Price BK, Lomeda JR, Tour JM (2009) Aggressively oxidized ultra-short single-walled carbon nanotubes having oxidized sidewalls. *Chemistry of Materials*, **21**, 3917–3923.

Project on Emerging Nanotechnologies (2011). Woodrow Wilson International Centre for Scholars and Pew Charitable Trusts. http://www.nanotechproject.org/inventories/consumer/analysis_draft/

Pyati UJ, Look AT, Hammerschmidt M (2007) Zebrafish as a powerful vertebrate model system for *in vivo* studies of cell death. *Seminars in Cancer Biology*, **17**, 154–165.

Raisuddin S, Jha AN (2004) Relative sensitivity of fish and mammalian cells to sodium arsenate and arsenite as determined by alkaline single-cell gel electrophoresis and cytokinesis-block micronucleus assay. *Environmental and Molecular Mutagenesis*, **44**, 83–89.

Ramakrishna G, Ghosh HN (2001) Emission from the charge transfer state of xanthene dye-sensitized TiO_2 nanoparticles: A new approach to determining back electron transfer rate and verifying the marcus inverted regime. *The Journal of Physical Chemistry B*, **105**, 7000–7008.

Ramesh R, Kavitha P, Kanipandian N *et al.* (2012) Alteration of antioxidant enzymes and impairment of DNA in the SiO2 nanoparticles exposed zebra fish (*Danio rerio*). *Environmental Monitoring and Assessment*.

Rawson DM, Zhang T, Kolicharan D, Jonbloed WL (2000) Field emission scanning electron microscopy and transmission electron microscopy studies of the chorion, plasma membrane and syncytial layers of the gastrula-stage embryo of the zebrafish *Brachydanio rerio*: a consideration of the structural and functional relationships with respect to cryoprotectant penetration. *Aquaculture Research*, **31**, 325–336.

Rivera-Gil P, Jimenez De Aberasturi D, Wulf V *et al.* (2012) The challenge to relate the physicochemical properties of colloidal nanoparticles to their cytotoxicity. *Accounts of Chemical Research*, 120711074456007.

Rivolta I, Panariti, Miserocchi (2012) The effect of nanoparticle uptake on cellular behavior: disrupting or enabling functions? *Nanotechnology, Science and Applications*, 87.

Rombough PJ (1985) The influence of the zona radiata on the toxicities of zinc, lead, mercury, copper and silver ions to embryos of steelhead trout sAlmo gairdneri. *Comparative Biochemistry and Physiology Part C: Comparative Pharmacology*, **82**, 115–117.

Ruizendaal L, Bhattacharjee S, Pournazari K *et al.* (2009) Synthesis and cytotoxicity of silicon nanoparticles with covalently attached organic monolayers. *Nanotoxicology*, **3**, 339–347.

Ryan AC, van Genderen EJ, Tomasso JR, Klaine, SJ (2004) Influence of natural organic matter source on copper toxicity to larval fathead minnows (*Pimephales promelas*): Implications for the biotic ligand model. *Environmental Toxicology & Chemistry*, **23**, 1567-1574.

Ryman-Rasmussen JP, Riviere JE, Monteiro-Riviere NA (2006) Surface coatings determine cytotoxicity and irritation potential of quantum dot nanoparticles in epidermal keratinocytes. *Journal of Investigative Dermatology*, **127**, 143–153.

Safi M, Courtois J, Seigneuret M, Conjeaud H, Berret JF (2011) The effects of aggregation and protein corona on the cellular internalization of iron oxide nanoparticles. *Biomaterials*, **32**, 9353–9363.

Sanchez A, Recillas S, Font X *et al.* (2011) Ecotoxicity of, and remediation with, engineered inorganic nanoparticles in the environment. *Trends in Analytical*

Chemistry, **30**, 507–516.

Sano K, Inohaya K, Kawaguchi M *et al.* (2008) Purification and characterization of zebrafish hatching enzyme - an evolutionary aspect of the mechanism of egg envelope digestion. *FEBS Journal*, **275**, 5934–5946.

Scheel J, Weimans S, Thiemann A, Heisler E, Hermann M (2009) Exposure of the murine RAW 264.7 macrophage cell line to hydroxyapatite dispersions of various composition and morphology: Assessment of cytotoxicity, activation and stress response. *Toxicology in Vitro*, **23**, 531–538.

Schultz AC (2007) Nanotechnology: Industrial revolution or emerging hazard? *Environmental Claims Journal*, **19**, 199–205.

Scown TM, van Aerle R, Tyler CR (2010) Review: Do engineered nanoparticles pose a significant threat to the aquatic environment? *Critical Reviews in Toxicology*, **40**, 653–670.

Shang L, Wang Y, Jiang J, Dong S (2007) pH-dependent protein conformational changes in albumin:gold nanoparticle bioconjugates: A spectroscopic study. *Langmuir*, **23**, 2714–2721.

Shaw BJ, Handy RD (2011) Physiological effects of nanoparticles on fish: A comparison of nanometals versus metal ions. *Environment International*, **37**, 1083–1097.

Shaw BJ, Al-Bairuty G, Handy RD (2012) Effects of waterborne copper nanoparticles and copper sulphate on rainbow trout, (*Oncorhynchus mykiss*): Physiology and accumulation. *Aquatic Toxicology*, 1–46.

Shew A (2008) Nanotech's History: An interesting, interdisciplinary, ideological split. *Bulletin of Science, Technology & Society*, **28**, 390–399.

Shiohara A, Hoshino A, Hanaki K-I, Suzuki K, Yamamoto K (2004) On the cyto-toxicity caused by quantum dots. *Microbiology and Immunology*, **48**, 669–675.

Shiohara A, Prabakar S, Faramus A *et al.* (2011) Sized controlled synthesis, purification, and cell studies with silicon quantum dots. *Nanoscale*, **3**, 3364.

Singh MP, Atkins TM, Muthuswamy E *et al.* (2012) Development of iron-doped silicon nanoparticles as bimodal imaging agents. *ACS Nano*, **6**, 5596–5604.

Singh S, D'Britto V, Prabhune AA *et al.* (2010) Cytotoxic and genotoxic assessment of glycolipid-reduced and -capped gold and silver nanoparticles. *New Journal of Chemistry*, **34**, 294.

Smith C, Shaw B, Handy R (2007) Toxicity of single walled carbon nanotubes to rainbow trout, (*Oncorhynchus mykiss*): Respiratory toxicity, organ pathologies, and other physiological effects. *Aquatic Toxicology*, **82**, 94–109.

Somasundaram B, King PE, Shackley SE (1984) Some morphological effects of zinc upon the yolk-sac larvae of Clupea harengus L. *Journal of Fish Biology*, **25**, 333–343.

Spitsbergen J, Kent M (2003) The state of the art of the zebrafish model for toxicology and toxicologic pathology research - advantages and current limitations. *Toxicologic Pathology*, **31**, 62–87.

Sreerama N, Venyaminov SY, Woody RW (2000) Estimation of protein secondary structure from circular dichroism spectra: Inclusion of denatured proteins with native proteins in the analysis. *Analytical Biochemistry*, **287**, 243–251.

Steinberg CE, Kamara S, Prokhotskaya VY *et al.* (2006) Dissolved humic substances - ecological driving forces from the individual to the ecosystem level? *Freshwater Biology*, **51**, 1189–1210.

Stone V, Johnston H, Schins RPF (2009) Development of *in vitro* systems for nanotoxicology: methodological considerations. *Critical Reviews in Toxicology*, **39**, 613–626.

Sun H, Zhang X, Niu Q, Chen Y, Crittenden JC (2006) Enhanced accumulation of arsenate in carp in the presence of titanium dioxide nanoparticles. *Water, Air, and Soil Pollution*, **178**, 245–254.

Suresh AK, Pelletier DA, Wang W *et al.* (2012) Cytotoxicity induced by engineered silver nanocrystallites is dependent on surface coatings and cell types. *Langmuir*, **28**, 2727–2735.

Surewicz WK, Mastach HH, Chapman D (1993) Determination of protein secondary structure by Fourier Transform Infrared Spectroscopy: A critical assessment. *Perspectives in Biochemistry*, **32**, 389–394.

Takeda H, Seki Y, Nakamura S, Yamashita K (2002) Evaluation of electrical polarizability and *in vitro* bioactivity of apatite Sr5(PO4)3OH dense ceramics. *Journal of Materials Chemistry*, **12**, 2490–2495.

Tan F, Wang M, Wang W, Lu Y (2008) Comparative evaluation of the cytotoxicity sensitivity of six fish cell lines to four heavy metals *in vitro*. *Toxicology in Vitro*, **22**, 164–170.

Tang J, Xiong L, Wang S *et al.* (2008) Influence of silver nanoparticles on neurons and blood-brain barrier via subcutaneous injection in rats. *Applied Surface Science*, **255**, 502–504.

Tang L, Han B, Persson K *et al.* (2010) Electrochemical stability of nanometer-scale pt particles in acidic environments. *Journal of the American Chemical Society*, **132**, 596–600.

Tantra R, Knight A (2011) Cellular uptake and intracellular fate of engineered nanoparticles: A review on the application of imaging techniques. *Nanotoxicology*, **5**, 381–392.

Teraoka H, Dong W, Hiraga T (2008) Zebrafish as a novel experimental model for developmental toxicology. *Congenital Anomalies*, **43**, 123–132.

Tieleman DP, C Biggin P, R Smith G, S P Sansom M (2002) Simulation approaches to ion channel structure–function relationships. *Quarterly Reviews of Biophysics*, **34**.

Tierney KB, Baldwin DH, Hara TJ *et al*. (2010) Olfactory toxicity in fishes. *Aquatic Toxicology*, **96**, 2-26.

Truong L, Zaikova T, Richman EK, Hutchison JE, Tanguay RL (2012) Media ionic strength impacts embryonic responses to engineered nanoparticle exposure. *Nanotoxicology*, **6**, 691–699.

Verma A, Stellacci F (2010) Effect of surface properties on nanoparticle-cell interactions. *Small*, **6**, 12–21.

Volkmer A (2005) Vibrational imaging and microspectroscopies based on coherent anti-Stokes Raman scattering microscopy. *Journal of Physics D: Applied Physics*, **38**, R59–R81.

von der Kammer F, Ferguson PL, Holden PA *et al.* (2012) Analysis of engineered

nanomaterials in complex matrices (environment and biota): General considerations and conceptual case studies (SJ Klaine, Ed). *Environmental Toxicology and Chemistry*, **31**, 32–49.

Walling MA, Novak JA, Shepard JRE (2009) Quantum dots for live cell and *in vivo* imaging. *International Journal of Molecular Sciences*, **10**, 441–491.

Wang B, Wang Z, Feng W *et al.* (2010) New methods for nanotoxicology: synchrotron radiation-based techniques. *Analytical and Bioanalytical Chemistry*, **398**, 667–676.

Wang L, Liu Y, Li W *et al.* (2011) Selective targeting of gold nanorods at the mitochondria of cancer cells: Implications for cancer therapy. *Nano Letters*, **11**, 772–780.

Wang Q, Bao Y, Zhang X *et al.* (2012) Uptake and toxicity studies of poly-acrylic acid functionalized silicon nanoparticles in cultured mammalian cells. *Advanced Healthcare Materials*, **1**, 189–198.

Wang W (1987) Factors affecting metal toxicity to (and accumulation by) aquatic organisms—Overview. *Environment International*, **13**, 437–457.

Wang W, Shi D, Lian J *et al.* (2006) Luminescent hydroxylapatite nanoparticles by surface functionalization. *Applied Physics Letters*, **89**, 183106.

Wang Y, Hu R, Lin G, Roy I, Yong K-T (2013) Functionalized quantum dots for biosensing and bioimaging and concerns on toxicity. *ACS Applied Materials & Interfaces*, 130221140111005.

Wang Z, Zhao J, Li F, Gao D, Xing B (2009) Adsorption and inhibition of acetylcholinesterase by different nanoparticles. *Chemosphere*, **77**, 67–73.

Ward JE, Kach DJ (2009) Marine aggregates facilitate ingestion of nanoparticles by suspension-feeding bivalves. *Marine Environmental Research*, **68**, 137–142.

Wassell DTH, Hall RC, Embery G (1995) Adsorption of bovine serum albumin onto hydroxyapatite. *Biomaterials*, **16**, 697–702.

Wendelaar Bonga SE, Lock R (1992) Toxicants and osmoregulations in fish. *Netherlands Journal of Zoology*, **42**.

Wiley B, Herricks T, Sun Y, Xia Y (2004) Polyol synthesis of silver

nanoparticles: Use of chloride and oxygen to promote the formation of single-crystal, truncated cubes and tetrahedrons. *Nano Letters*, **4**, 1733–1739.

Winnik FM, Maysinger D (2012) Quantum dot cytotoxicity and ways to reduce it. *Accounts of Chemical Research*, doi:10.1021/ar3000585.

Witeska M, Jezierska B, Chaber J (1995) The influence of cadmium on common carp embryos and larvae. *Aquaculture*, **129**, 129–132.

Wood CM (2011) An introduction to metals in fish physiology and toxicology: Basic principles. In: *Fish Physiology: Homeostasis and Toxicology of Essential Metals*, pp. 1–65. Elsevier.

Wood CM, Hogstrand C, Galvez F, Munger RS (1996) The physiology of waterborne silver toxicity in freshwater rainbow trout (*Oncorhynchus mykiss*) 1. The effects of ionic Ag. *Aquatic Toxicology*, **35**, 93–109.

Wood CM, Playle RC, Hogstrand C (2009) Physiology and modeling of mechanisms of silver uptake and toxicity in fish. *Environmental Toxicology and Chemistry*, **18**, 71–83.

Woodworth J, Evans A, Pascoe D (1983) The production of cadmium-binding protein in three species of freshwater fish. *Toxicology Letters*, **15**, 289–295.

Wörle-Knirsch JM, Pulskamp K, Krug HF (2006) Oops they did it again! Carbon nanotubes hoax scientists in viability assays. *Nano Letters*, **6**, 1261–1268.

Wright DA, Welbourn PM (1994) Cadmium in the aquatic environment: a review of ecological, physiological, and toxicological effects on biota. *Environmental Reviews*, **2**, 187–214.

Wu Y, Zhou Q, Li H *et al.* (2010) Effects of silver nanoparticles on the development and histopathology biomarkers of Japanese medaka (*Oryzias latipes*) using the partial-life test. *Aquatic Toxicology*, **100**, 160–167.

Xia T, Kovochich M, Brant J *et al.* (2006) Comparison of the abilities of ambient and manufactured nanoparticles to induce cellular toxicity according to an oxidative stress paradigm. *Nano Letters*, **6**, 1794–1807.

Xia T, Zhao Y, Sager T *et al.* (2011) Decreased dissolution of ZnO by iron doping yields nanoparticles with reduced toxicity in the rodent lung and zebrafish embryos. *ACS Nano*, **5**, 1223–1235.

Yang P, Quan Z, Li C *et al.* (2008) Bioactive, luminescent and mesoporous europium-doped hydroxyapatite as a drug carrier. *Biomaterials*, **29**, 4341–4347.

Yang S, Bar-Ilan O, Peterson RE *et al.* (2013) Influence of humic acid on titanium dioxide nanoparticle toxicity to developing zebrafish. *Environmental Science & Technology*, 130124114801005.

Yang S, Cai W, Liu G, Zeng H, Liu P (2009) Optical study of redox behavior of silicon nanoparticles induced by laser ablation in liquid. *Journal of Physical Chemistry C*, **113**, 6480–6484.

Yeo M, Kang M (2008) Effects of nanometer sized silver materials on biological toxicity during zebrafish embryogenesis. *Bulletin of the Korean Chemical Society*, **29**, 1179.

Yong K-T, Law W-C, Hu R *et al.* (2013) Nanotoxicity assessment of quantum dots: from cellular to primate studies. *Chemical Society Reviews*, **42**, 1236.

Yu L-P, Fang T, Xiong D-W, Zhu W-T, Sima X-F (2011) Comparative toxicity of nano-ZnO and bulk ZnO suspensions to zebrafish and the effects of sedimentation, ˙OH production and particle dissolution in distilled water. *Journal of Environmental Monitoring*, **13**, 1975.

Zhang DH, Liu XH, Wang X (2011) Monodispersed protein stabilized silver nanoprisms: synthesis, optical properties and surface-enhanced raman scattering application. *Materials Science Forum*, **688**, 162–167.

Zhang LW, Monteiro-Riviere NA (2009) Mechanisms of quantum dot nanoparticle cellular uptake. *Toxicological Sciences*, **110**, 138–155.

Zhao C-M, Wang W-X (2013) Regulation of sodium and calcium in *Daphnia magna* exposed to silver nanoparticles. *Environmental Toxicology and Chemistry*, n/a–n/a.

Zhao J, Wang Z, Liu X *et al.* (2011a) Distribution of CuO nanoparticles in juvenile carp (Cyprinus carpio) and their potential toxicity. *Journal of Hazardous Materials*, **197**, 304–310.

Zhao J, Xu L, Zhang T, Ren G, Yang Z (2009) Influences of nanoparticle zinc oxide on acutely isolated rat hippocampal CA3 pyramidal neurons.

NeuroToxicology, **30**, 220–230.

Zhao X, Heng BC, Xiong S *et al.* (2011b) *In vitro* assessment of cellular responses to rod-shaped hydroxyapatite nanoparticles of varying lengths and surface areas. *Nanotoxicology*, **5**, 182–194.

Zhong P, Yu Y, Wu J *et al.* (2006) Preparation and application of functionalized nanoparticles of CdSe capped with 11-mercaptoundecanoic acid as a fluorescence probe. *Talanta*, **70**, 902–906.

Zhong W (2009) Nanomaterials in fluorescence-based biosensing. *Analytical and Bioanalytical Chemistry*, **394**, 47–59.

Zhu M, Nie G, Meng H *et al.* (2012a) Physicochemical properties determine nanomaterial cellular uptake, transport, and fate. *Accounts of Chemical Research*, 120814132947009.

Zhu S, Oberdörster E, Haasch ML (2006) Toxicity of an engineered nanoparticle (fullerene, C60) in two aquatic species, Daphnia and fathead minnow. *Marine Environmental Research*, **62**, S5–S9.

Zhu X, Wang J, Zhang X, Chang Y, Chen Y (2009a) The impact of ZnO nanoparticle aggregates on the embryonic development of zebrafish (*Danio rerio*). *Nanotechnology*, **20**, 195103.

Zhu X, Zhu L, Duan Z *et al.* (2008) Comparative toxicity of several metal oxide nanoparticle aqueous suspensions to Zebrafish (*Danio rerio*) early developmental stage. *Journal of Environmental Science and Health, Part A*, **43**, 278–284.

Zhu Y, Li W, Li Q *et al.* (2009b) Effects of serum proteins on intracellular uptake and cytotoxicity of carbon nanoparticles. *Carbon*, **47**, 1351–1358.

Zhu Y, Zhang X, Zhu J *et al.* (2012b) Cytotoxicity of phenol red in toxicity assays for carbon nanoparticles. *International Journal of Molecular Sciences*, **13**, 12336–12348.

Zolnik BS, Gonzalez-Fernandez A, Sadrieh N, Dobrovolskaia MA (2010) Minireview: Nanoparticles and the immune system. *Endocrinology*, **151**, 458–465.

Zon LI, Peterson RT (2005) *In vivo* drug discovery in the zebrafish. *Nature*

Reviews Drug Discovery, **4**, 35–44.

10.1. APPENDICES

10.1.1. APPENDIX I: Methods of nanoparticle synthesis

A wide-range of NPs that represent those used in industry were chosen to allow for comparisons between differing characteristics such as metal vs. non-metal cores, surface coatings, size, etc.

Si NPs were synthesized in house (Veinot Lab, Department of Chemistry, University of Alberta), and functionalized with undecanoic acid were synthesized and suspended in double distilled water according to Clark *et al.* (2010). In brief, silicon NPs were prepared from high temperature annealing of hydrogen silsesquoine and covalently functionalized with undecanoic acid in ethanol, dialyzed and suspended in ddH_2O, as based on Zhong *et al.* (2006), then dialyzed overnight to remove trace metal contaminants, and stored under argon to prevent oxidation.

CdSe NPs were created in house (Veinot Lab, Department of Chemistry, University of Alberta). NPs were functionalized with mercaptoundecanoic acid and prepared in ddH_2O as described by Zhong *et al.* (2006). 0.0228 g of $CdCl_2 \cdot 2.5H_2O$ was dissolved in 125 ml of water, and 0.0524 g of 11-mercaptoundecanoic acid, dissolved in NaOH solution, was added. The solution was stirred and adjusted to pH 11 by dropwise addition of 1.0 mol/L NaOH, and then de-aerated by N_2 bubbling for 30 min. While stirring, 100 µl of freshly prepared oxygen-free NaHSe solution (0.50 mol/L) was added to the solution. NaHSe was generated by reaction of Se powder with $NaBH_4$. The molar ratio of Cd^{2+}:HSe^-:11-mercaptoundecanoic acid was 1:0.5:2.4. The resulting mixture was then refluxed at 96°C for 2 h to promote growth of NCs. Resulting solutions were then purified by dialysis in dialysis tubing (MWCO 8000 daltons) for 2 days, which water changed at 6 hour intervals.

HAP RD and HAP ND were synthesized in the Loo lab (School of Materials Science and Engineering, Nanyang University) according to Loo *et al.* (2008). Briefly, NPs were prepared using a wet chemical precipitation technique followed by hydrothermal treatment, and HAP ND were specifically synthesized

through precipitation with cetyl trimethylammonium bromide as a surfactant. NPs were tagged with FITC by condensation reaction with 3-aminopropyltriethoxysilane (APTES), and then 0.05 g FITC was added and stirred overnight at 74 °C.

Polyacrylic acid-capped ZnO and TiO_2 were provided by Vive Crop Protection (formerly Vive Nano; Toronto, Canada), and received as 10 g/L stock solutions in distilled water. In brief, oppositely charged metal salts and polymer acrylic acid were mixed in solution, then stabilized with UV radiation to cross-link the polymer chains. Then, NaOH was added, followed by hydrolysis to form NPs. The NPs are then purified by precipitation with multiple ethanol washes, then redispersed into deionized water. Further details can be found in Irizar *et al.* (2008).

RNT, organic nanotubes that undergo entropy driven self-assembly, were conjugated to lysine and synthesized and suspended in ddH_2O in house (Fenniri lab, Department of Chemistry, University of Alberta). Full details of production can be found in Supplementary Information in Fenniri *et al.* (2002).

Unfunctionalized ZnO sphere and ZnO leaf materials were prepared as described in Heng *et al.* (2011) in the Loo lab (School of Materials Science and Engineering, Nanyang University). In short, zinc nitrite and cetyl trimethylammonium bromide were stirred in water and NaOH was added drop-wise. Then, the solution was heated for 4 h, then centrifuged and washed with ethanol, then distilled water, then freeze-dried. This powder was prepared fresh in experiment-appropriate media directly before use.

SWCNT were synthesized by induction thermal plasma technology (Kim *et al.* 2007). The diameter of the SWCNT bundles range from approximately 10 to 20 nm in the as-produced material. The exact lengths of the bundles were difficult to measure because of the amorphous carbon content but most were observed to extend to a couple of μm. The as-produced SWCNT were oxidized in a HNO_3/H_2SO_4 mixture for 2 hours at 30 °C as previously reported (Price *et al.* 2009).

Citrate-capped silver NPs were synthesized in house (Veinot lab, Department of Chemistry, University of Alberta) by dissolving 0.21 g citric acid, 0.01 g BSA, and 0.0314 g $AgNO_3$ in 5 ml distilled water and were fully characterized in our lab. Directly after the BSA had completely dissolved and a clear homogeneous solution generated, 0.01 g of $NaBH_4$ was added and the solution was stirred for three hours. The solution was then centrifuged at 17000 g for 10 min, and the top clear solution was removed and the dark-red silver NPs at the bottom were re-suspended/dissolved in 5 ml of distilled water and sonicated (Fisher Scientific Ultrasonic FS60 bath, 100W, 42 kHz) for 5 min in a glass container.

**10.1.2. APPENDIX II**: Methods of nanoparticle characterization

The shape and size of NPs were determined with transmission electron microscopy analysis. The hydrodynamic diameter and zeta (ζ) potential of NPs in the media used in individual experiments and were assessed with a Malvern Instruments (Westborough, MA) Zetasizer Nano ZS equipped with a 633 nm laser. Disposable cuvettes were cleaned with filtered water immediately before use, filled with NP suspension, and then capped. Hydrodynamic diameter measurements were acquired in 173° backscattering mode and reported as the peak value of >99% intensity. All ζ-potential and hydrodynamic diameter measurements were reported as the mean of minimum three measurements plus or minus one standard deviation about the mean. Concentrations lower than 1 mg/L in all NPs resulted in erroneous readings on the Zetasizer, and thus were not reported. Large standard errors were observed in the RNTs. This is possibly the result of polydispersity in the sample or it may relate to the assumption of diameter calculations that the particles were spherical; the tubular shape of the RNTs likely renders the DLS measurements inaccurate for this particle.

10.1.3. APPENDIX III: Adult zebrafish maintenance and embryo collection

Zebrafish embryos were collected from breeding pairs of wildtype AB adult zebrafish (*Danio rerio*) in the Aquatic Facility at the University of Alberta. Adults were raised in tanks with continuous water flow (1350±100 µS/cm, pH of 7.7±0.2, 28.5±0.7°C, general water hardness of 100 ppm, carbonate hardness of 10 ppm, salinity 0.5 ppt) at 28.5°C on a 14h light/10h dark cycle. On nights prior to exposure treatments, five adult zebrafish (male-to-female ratio of 2:3) were placed in 1 L breeding tanks with fresh water. Within ten minutes of the lights turning on in the morning, the water was changed, and a 2 mm mesh at the bottom of the tank allowed for collection of embryos approximately 30 min after the start of the light cycle. Animal protocols were approved by the University of Alberta Animal Care and Use Committee for Biological Sciences.

10.1.4. APPENDIX IV. Transmission electron micrographs of nanoparticles. Nanoparticle cores range from 3-9 nm. **(**a) High-resolution TEM of silicon nanoparticles functionalized with undecylenic acid, arrow points to Si crystalline structure; (b) Cadmium selenide nanoparticles functionalized with undecylenic acid; (c) Titanium dioxide nanoparticles functionalized with polyacrylic acid; (d) Zinc oxide nanoparticles functionalized with polyacrylic acid; (e) Helical rosette nanotubes functionalized with lysine.
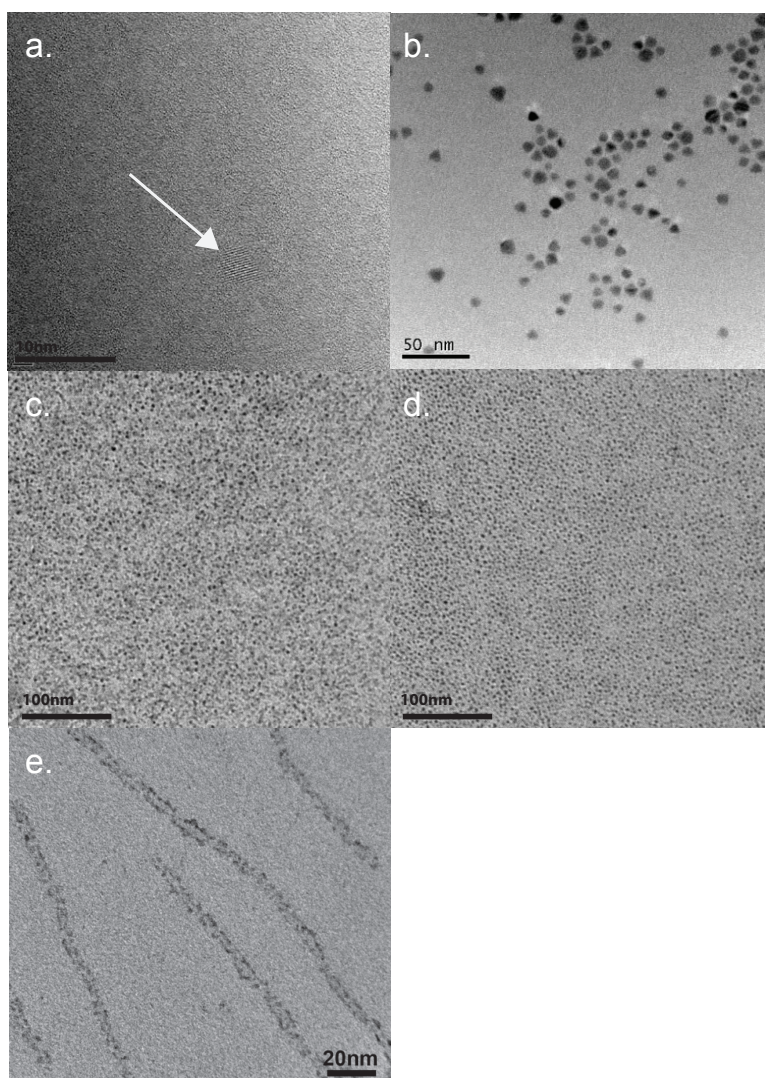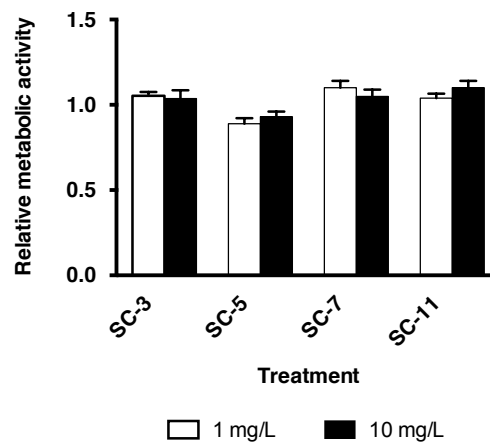
10.1.5. APPENDIX V. Side chain controls of the effects of propionic acid (SC-3), pentanoic acid (Si-5), heptanoic acid (SC-7), and undecanoic acid (SC-11) to determine the effect of 24 h exposure on (a) Beas2B and (b) HepG2 cells. No significant differences ($p > 0.05$) were observed.
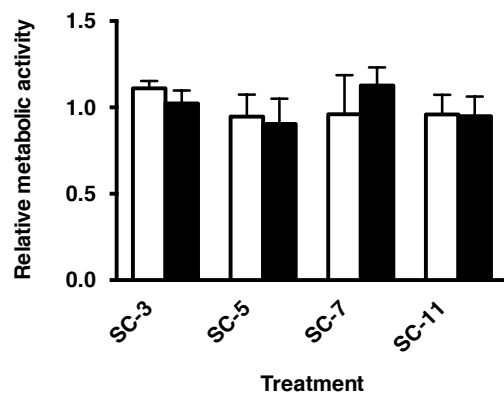
10.1.6. APPENDIX VI. Confocal images (excitation 488 nm) of zebrafish embryos showing autofluorescence throughout the whole body and yolk sac, masking any potential fluorescent signal silicon nanoparticles.